THE AMERICAN JOURNAL OF PATHOLOGY

VOLUME XXXIX JULY, 1961 NUMBER 1

EARLY EFFECTS OF X-IRRADIATION ON CARTILAGE AND BONE

P. L. MELANOTTE, M.D.,* AND R. H. FOLLIS, JR., M.D.

From the Veterans Administration Central Laboratory for Anatomical Pathology and Research, Armed Forces Institute of Pathology, Washington, D.C.

Over 50 years ago, Perthes described stunting of growth in chickens which had been exposed to roentgen rays. Since then numerous reports dealing with the effects of irradiaton on cartilage cells and osteoblasts have appeared. It is unnecessary to review an extensive literature, which Gall, Lingley and Hilcken[3] and Heller[4] have summarized. Pertinent aspects which relate to the observations to be detailed here will be commented upon later. It suffices only to indicate now that all studies so far reported have relied on conventional staining methods; moreover, most observers have not given detailed attention to early postirradiation sequences. Hence, it was felt that the application of certain histochemical procedures which have been of help in certain studies already reported might reveal data of interest. In addition, since alterations in cartilage and bone become so dramatic a week or more after irradiation, the early sequences appeared to be worthy of careful investigation. This report is concerned with observations on cartilage and bone during the first week after the application of x-rays of different intensities to a single extremity of growing rats.

A portion of the material herein reported was supported by a grant-in-aid from the American Cancer Society to the Committee on Growth, National Research Council. Presented in part at the Fifty-fourth Annual Meeting of the American Association of Pathologists and Bacteriologists, Washington, D.C., April 12, 1957.[1]

Accepted for publication, February 16, 1961.

* Damon Runyon Fellow, 1955–1957. Present address: Clinica Ortopedica, Universita, Padova, Italy.

Material and Methods

Sixty albino rats (Wistar), weighing approximately 50 gm., were used. They were maintained on a commercial chow in stainless steel cages with screen bottoms over cedar wood shavings. Prior to irradiation, each animal was anesthetized with Nembutal® administered intraperitoneally. They were then placed in a device which consisted of a circular wall of lead (2 mm.) sheet, 4.5 cm. in width and 17 cm. in diameter, in which rectangular 20 by 10 mm. holes had been cut at equal distances. The animals lay on a 4 mm. sheet of lead outside this lead partition, while a second 4 mm. sheet was placed over them. Naturally, both upper and lower lead shields had holes cut in them to conform with the circumference of the circular wall, through the holes of which the right leg of each animal was passed and fixed in position by a rubber band. Hence, only this portion of the body received radiation.

A Westinghouse constant potential dual tube x-ray machine was employed as the source of radiation. It had the following characteristics: 200 kv.; 15 ma.; distance, 54 cm.; filtration, 0.25 mm. copper, 0.55 mm. aluminum; total intensity, 120.9 r per minute. Groups of rats were given a single dose of 400, 600, 800, 1,200, and 1,800 r.

Animals were sacrificed by a blow on the head 24 hours after the irradiation and on each successive day thereafter for 9 days. After disarticulation, the right tibia was split longitudinally and fixed in neutral formalin or alcohol. Specimens, without decalcification, were embedded in paraffin, cut and stained by methods which have been described elsewhere.[5]

Results

Any study of the developing skeleton is concerned with the activity of two entirely different types of tissue: cartilage and bone. Since the dissociation of growth and metabolism of these cells in health and disease is well recognized, each will be taken up in turn. Alterations resulted from all of the intensities of radiation employed. The differences among the 5 dosage levels were only those of time of appearance and degree of severity; hence, an over-all description of the development of the changes is deemed sufficient.

Cartilage

Epiphysial cartilage cells have one main function: to provide a matrix framework which becomes calcified and upon which bone may be deposited. The principal activities of these cells are therefore to multiply and to elaborate a matrix, consisting for the most part of collagen fibrils and chondroitin sulfuric acid-protein complex. As is well known,[6,7] the cells of the upper epiphysial cartilage of the tibia of the young rat complete their life cycles at a rapid rate. The cycle—cell division, enlargement, and death—takes a relatively short time, approximately 48 to 60 hours in the animals of the age utilized here. Such growth activities lead to the characteristic histologic picture at the epiphysial plate, where 5 distinct areas are found from above downwards: (a) primitive cells; (b) cell multiplication zone with beginning column formation; (c) region of hypertrophic cells; (d) zone of calcification of cartilage ma-

trix, merging with (e) zone of cartilage cell death and capillary invasion (Fig. 1).

The alterations which were noted during the one week period of observation following irradiation may be epitomized as follows: suppression of cell multiplication, atrophy at all stages of development, loss of columnar arrangement and evidence of biochemical abnormalities. The end result was an epiphysial plate which was narrowed and disorganized, both anatomically and biochemically (Figs. 2 to 11).

The earliest change, which was found after 24 hours, consisted of failure of the cells in the proliferative zone to reach their maximal size. The number of cells in a given column was decreased as well. The cells appeared closer together, and the matrix about them seemed looser; that is, the fibrils were separated one from another. No changes were found in the nuclei of the cells. Hypertrophic cells, some of which were in process of dying at the time of irradiation, appeared to have persisted; this might have indicated that invasion by blood vessels was retarded. No decrease in calcification of the intercellular matrix could be made out during the first few days. By the third or fourth day the above changes had become more marked. In general, the cells were definitely smaller in size, though here and there structures larger than normal were found. In addition, the arrangement of the columns was disorganized, so that precise row formation was lacking in many areas. The cartilage plate was definitely reduced in width. At this time decrease in the size of cells and disorganization of row formation, as well as separation of the poorly formed rows by a seemingly swollen matrix, were well marked. As time went on—that is, up to the eighth day—such alterations became more prominent, so that at the end of the period of observation a narrowed plate which had completely lost its normal organization was found. The cartilage cells varied in size and shape. At this time, too, defects in calcification at the cartilage shaft junction were noted. Capillary invasion appeared to have ceased entirely.

Stains for glycogen and alkaline phosphatase activity indicated that in the period of observation biochemical alterations had also occurred. Normally, glycogen is found in the region of the zone of hyperplastic cells, just above the area where calcification will occur. In the irradiated animals, glycogen, as detected by staining, was soon deficient in some of the cells in this region. Moreover, glycogen persisted in certain cells close to the usual zone of capillary invasion. More abnormal still was the presence of glycogen in the cells high up in the cartilage, in areas where this material was never seen normally.

The pattern of alkaline phosphatase activity was also altered. Normally, enzymatic activity is found in the late hypertrophic and dying

cells and in the matrix about them. Following irradiation, activity soon began to decrease in this area. However, staining appeared in scattered single cells higher up in the plate where ordinarily evidences of enzyme activity were not found.

Osteoblasts

In the diaphysis the most prominent change following irradiation was seen in the osteoblasts and, as a result, in their product, osteoid. Such alterations appeared after 24 hours and were found at the lowest dosage (400 r) employed. Even at this time cells had begun to proliferate and increase in size, becoming more rounded. The basophilia of their cytoplasm increased. During the ensuing days, depending on the dosage level, the osteoblasts continued to increase in number and size; mitotic figures were easily detected. Even after one day an excess of fine argyrophilic and PAS-positive fibrils appeared between the cells. This cellular proliferation with new matrix production occurred most prominently along the inner surfaces of the cortex. However, when the metaphysis was examined after 24 hours, an increased number of cells was found on the spicules of cartilaginous matrix or along the thin borders of osteoid and true bone which had already coated some of the lattice of calcified cartilaginous matrix. Similar proliferation of cells and new matrix formation were noted about trabeculae, as well.

The argyrophilic fibers soon coalesced to form true osteoid matrix in which inorganic material then deposited. Hence, in many areas the cortex was lined by a rather loose trabeculated bone of a metaplastic type. The osteocytes which were enclosed in such calcified matrix were normal in appearance. Evidences of osteoblastic proliferation began to decrease after the first 6 to 7 days, particularly at the higher dose levels. Hence, at the end of the observation period, the tenth day, although in many areas more bone than normal was present, new proliferation was no longer taking place.

As might be expected, in association with the evidences of cellular activity, increased phosphatase staining was also found. The cytoplasm of the osteoblast displayed a positive reaction; the fibers themselves were blackened as well. Hence, the normal distribution of phosphatase activity in the shaft was greatly accentuated, and the layers of osteoblasts and fibers presented a dense blackened zone with the technique employed. A similar intensity of phosphatase activity was seen in the region of the metaphysis, for here, in the areas where cellular proliferation had taken place, phosphatase activity was excessive because of the increased number of cells.

Discussion

During the first week following x-irradiation, profound alterations take place in epiphysial cartilage. This might have been expected from the studies of the later sequences which have already been reported.[3,4,6] The present observations have added to our knowledge of this early period. The response of cartilage cells to irradiation is immediate and marked. Cell multiplication as evidenced by growth of the cartilage is affected; moreover, the normal pattern of cell maturation and column arrangement is impaired. This leads to a disorganization of the epiphysial cartilage plate which, in our experience, is unique. Growth of cartilage can be affected by any number of experimental procedures, particularly those resulting from a deficiency of specific nutrients or hormones which influence the metabolic activity of these cells.[8] However, following such procedures, though growth is decreased, the anatomic pattern is an organized one. The cartilage columns retain their orderly arrangement; the sizes and shapes of the cells are a miniature of the normal. We are aware of no other experimental procedures which lead to the disorganized pattern in cartilage observed during the first week following irradiation. The abnormality in glycogen content of the cells and in phosphatase activity clearly indicate marked alterations in metabolism of the cartilage cells. As a result of inanition or other deficient states, glycogen content of cells and phosphatase activity may decrease[9]; however, these changes are of an orderly nature and conform with the cessation of growth of the chondrocytes. They do not resemble the changes seen in the irradiated epiphyses.

It is of interest to note that Henrichsen[10] has recently pointed out that the appearance of alkaline phosphatase activity may be associated with damage or death of the cartilage cell. Our observations on the appearance of activity high up in the plate would tend to provide support for this thesis.

Cartilage cells appear to be concerned with the formation of the two principal constituents of the matrix which surrounds them: collagen and chondroitin sulfuric acid-protein complex. Stains employed for these materials are not specific enough to demonstrate any precise alterations. The looseness of the matrix and its seemingly more fibrous nature may be related to the decrease in the number of cell columns, with perhaps some swelling of the intercolumnar substance. Whether specific alterations take place in the collagen fibrils themselves or in the polysaccharide constituents will have to await detailed studies by electron microscopy, chemical determination, or autoradiographic techniques which have been applied in investigations of later stages.[11]

The most prominent alteration with respect to the osteoblast is evidence of increased activity of this cell. This evidence is based on an increase in size of the cell and basophilia of its cytoplasm, more mitotic figures, and an increase in the total number of cells. The presence of new and excessive matrix, which is in evidence 24 hours after irradiation, further indicates that these cells are overactive. The precise stimulus to such proliferative activity is, of course, not clear. No prominence in the vascular supply to the area can be made out. Increased activity is followed by a depression, a reaction which has been described to occur if the bone is not examined during the early days following irradiation. Increased osteoblastic activity is associated with histochemical evidences of phosphatase activity. This does not conform to the observations of Woodard and Laughlin,[12] yet samples studied by the latter investigators were whole bone containing marrow elements, assayed at later periods following radiation.

These experiments confirm an important observation made by Gall and co-workers that "despite the arrest of cartilaginous function, little or no interference with osteoblastic activity was detected."[8] The observations recorded herein indicate a stimulation of osteoblastic activity in the irradiated bone. These findings only re-emphasize the well-known dissociation of growth and metabolic activities between cartilage and bone in health and disease.

Summary

A study has been made of the epiphysial cartilage and osteoblasts of the tibia in rats having a single exposure of x-irradiation of increasing intensities from 400 to 1,800 r administered from 1 to 10 days before sacrifice. Prompt damage to the cartilage was evidenced by cessation of growth and alterations in certain histochemical reactions. In contrast, stimulation of osteoblastic activity, i.e., proliferation with excessive matrix production, was found.

References

1. Melanotte, P. L., and Follis, R. H., Jr. Histochemical studies on x-irradiated cartilage and bone. (Abstract) *Am. J. Path.*, 1957, 33, 607–608.
2. Perthes, G. Ueber den Einfluss den Röntgenstrahlen auf epitheliale Gewebe, insbesondere auf das Carcinom. *Arch. klin. Chir.*, 1903, 71, 955–1000.
3. Gall, E. A.; Lingley, J. R., and Hilcken, J. A. Comparative experimental studies of 200 kilovolt and 1000 kilovolt roentgen rays. I. The biological effects on the epiphysis of the albino rat. *Am. J. Path.*, 1940, 16, 605–618.
4. Heller, M. Bone. In: Histopathology of Irradiation from External and Internal Sources. Bloom, W. (ed.). McGraw-Hill Book Co., Inc., New York, 1948, pp. 70–161.
5. Follis, R. H. Jr., and Berthrong, M. Histochemical studies on cartilage and

bone. I. The normal pattern. *Bull. Johns Hopkins Hosp.*, 1949, **85**, 281–298.

6. Eeg-Larsen, N. An experimental study on growth and glycolysis in the epiphyseal cartilage of rats. *Acta physiol. scandinav.*, 1956, **38**, Suppl. 128, pp. 1–77.
7. Sissons, H. A. Experimental Study of the Effect of Local Irradiation on Bone Growth. In: Progress in Radiobiology; Proceedings of the fourth conference held in Cambridge, 14th–17th August, 1955. International Conference on Radiobiology. Oliver & Boyd, London, 1956, p. 436.
8. Follis, R. H., Jr. Nutrition and bone disease. *J. Mt. Sinai Hosp.*, 1949, **16**, 1–13.
9. Follis, R. H., Jr. Unpublished observations.
10. Henrichsen, E. Alkaline Phosphatase and Calcification; Histochemical Investigations on the Relationship Between Alkaline Phosphatase and Calcification. Cowan, H. (transl.). E. Munksgaard, Copenhagen, 1958, 85 pp.
11. Dziewiatkowski, D. D., and Woodard, H. Q. Effect of irradiation with x-rays on the uptake of S^{35} sulfate by the epiphyseal cartilage of mice. *Lab. Invest.*, 1959, **8**, 205–212.
12. Woodard, H. Q., and Laughlin, J. S. The effect of x-rays of different qualities on the alkaline phosphatase activity of living mouse bone. II. Effects of 22.5-Mevp. x-rays. *Radiation Res.*, 1957, **7**, 236–252.

We would like to thank Mr. Henry L. Meyer of the Radiation Branch, National Institutes of Health, for his kindness in irradiating the animals used in this investigation.

[*Illustrations follow*]

Legends for Figures

Except where indicated, photographs were made from sections stained with hematoxylin and eosin.

Fig. 1. Epiphysial cartilage, normal rat. × 165.

Fig. 2. Epiphysial cartilage from a rat which had received 1,200 r 3 days earlier. × 165.

Fig. 3. Epiphysial cartilage from an animal which had received 1,800 r 4 days earlier. × 165.

Fig. 4. Epiphysial cartilage from a rat which had received 1,800 r 6 days earlier. × 165.

Fig. 5. Epiphysial cartilage from a rat which had received 1,800 r 5 days earlier. × 165.

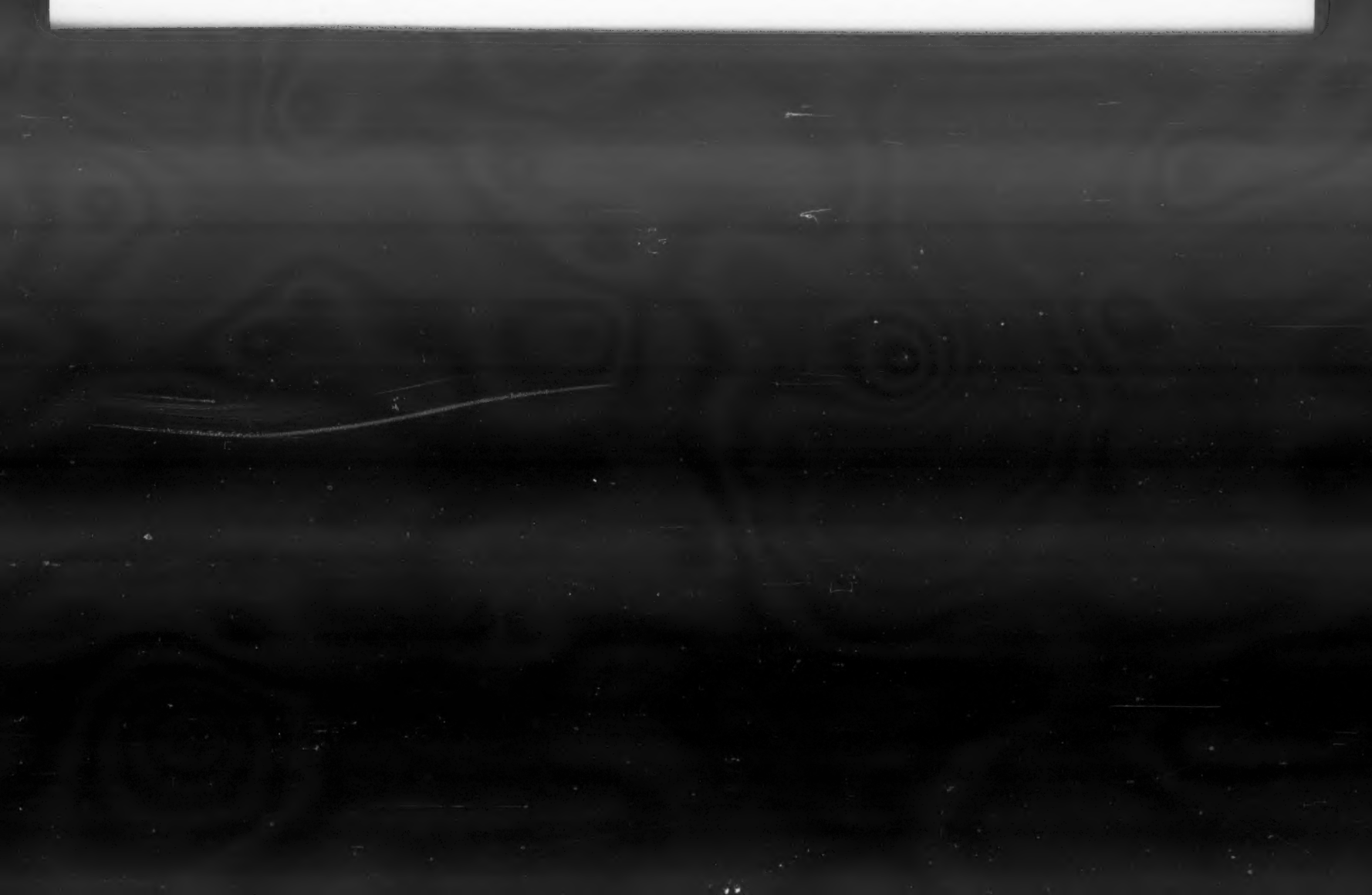

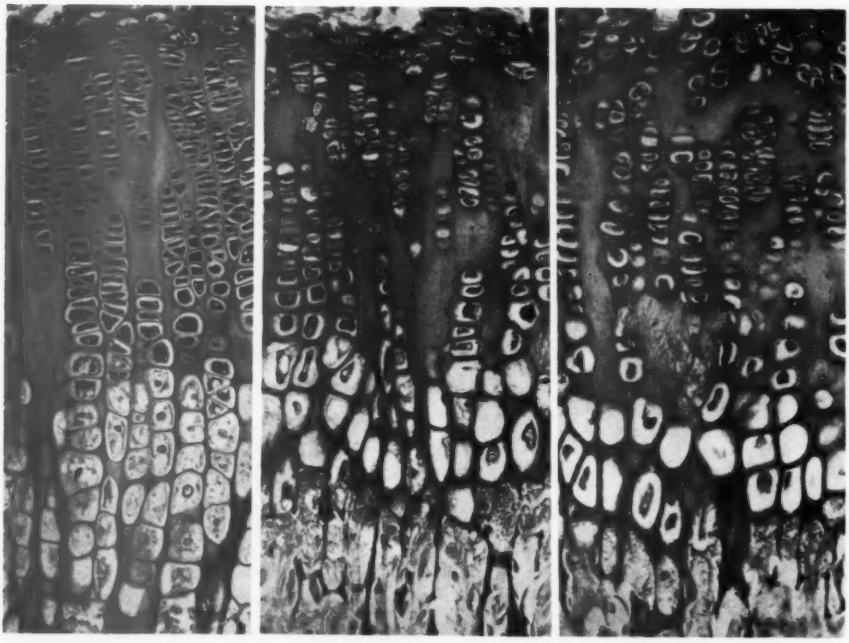

1

2, 3

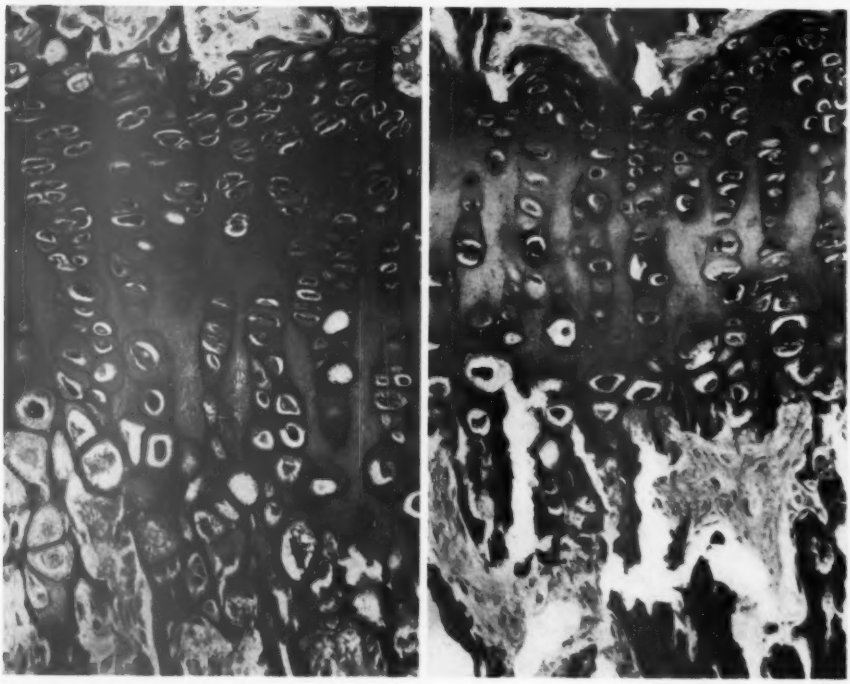

4

5

FIG. 6. Epiphysial cartilage, normal rat. Control for phosphatase reaction, shown in Figure 7. × 165.

FIG. 7. Epiphysial cartilage, normal rat. Gomori alkaline phosphatase procedure. Note the absence of reaction (blackening) in the upper portion of the plate. × 165.

FIG. 8. Epiphysial cartilage from a rat which had received 800 r 5 days earlier. Note the cells showing a positive phosphatase reaction in an area where ordinarily none would be present. × 165.

FIG. 9. Epiphysial cartilage from a rat which had received 1,200 r 6 days earlier. Note the loss of the phosphatase reaction in the hypertrophic zone and its spotty presence above. × 165.

FIG. 10. Epiphysial cartilage from a rat which had received 1,800 r 8 days earlier. Note the increasing loss of phosphatase reaction in the hypertrophic zone. × 165.

FIG. 11. Epiphysial cartilage from a rat which had received 1,800 r 9 days earlier. Note a focus of positive phosphatase reaction and spotty cell reactions elsewhere. × 165.

6

9

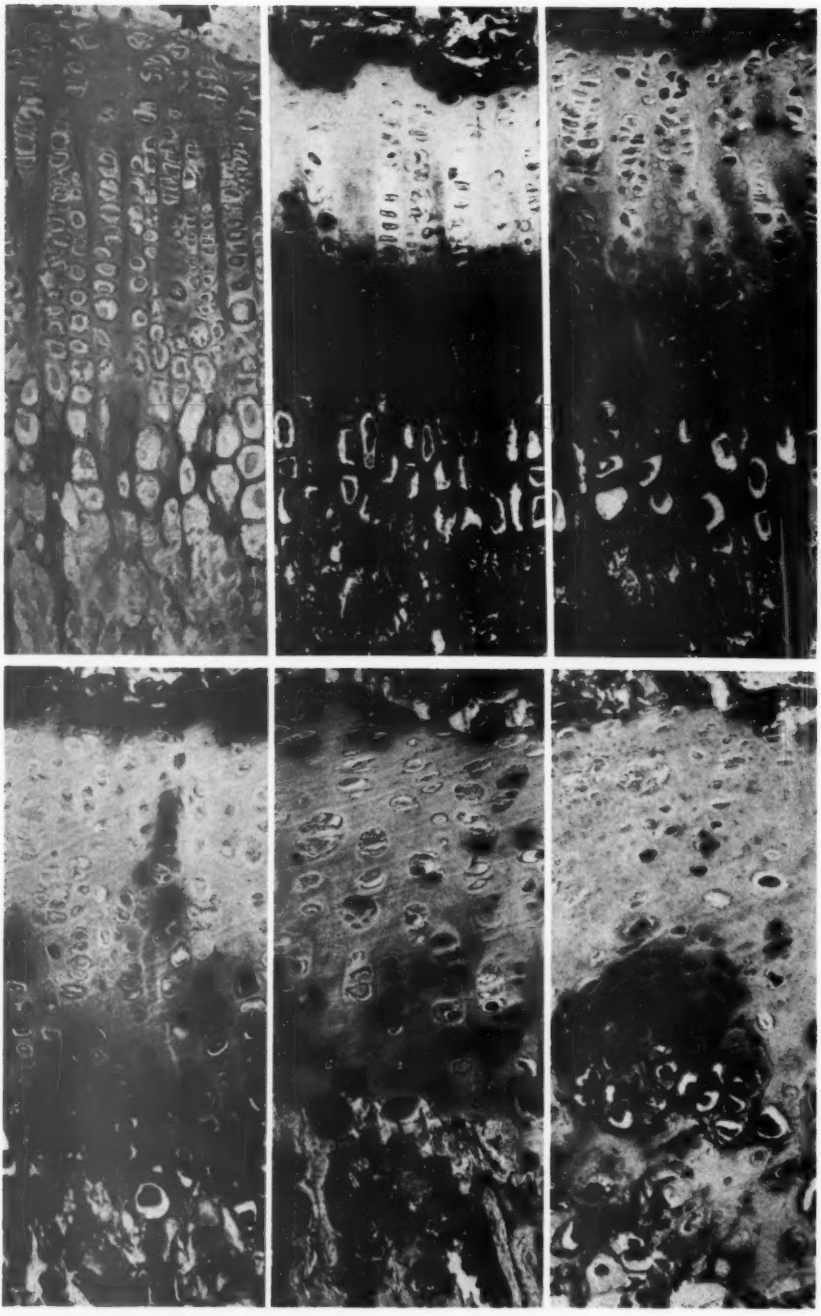

6

7, 8

9

10, 11

FIG. 12. Metaphysial area, normal rat. × 200.

FIG. 13. Metaphysial area from a rat which had received 400 r 6 days earlier. Note the increase in cellularity. × 200.

FIG. 14. Metaphysial area from a rat which had received 1,800 r 7 days earlier. Note the decrease in cellularity and disorganization. × 200.

FIG. 15. Trabeculae in the medulla of a rat which had received 800 r 6 days earlier. Note the increase in cellularity, osteoblast and fibroblast-like cells. × 150.

FIG. 16. The same trabeculae seen in Figure 15. A Snook stain to show an increase in argyrophilic fibers. × 150.

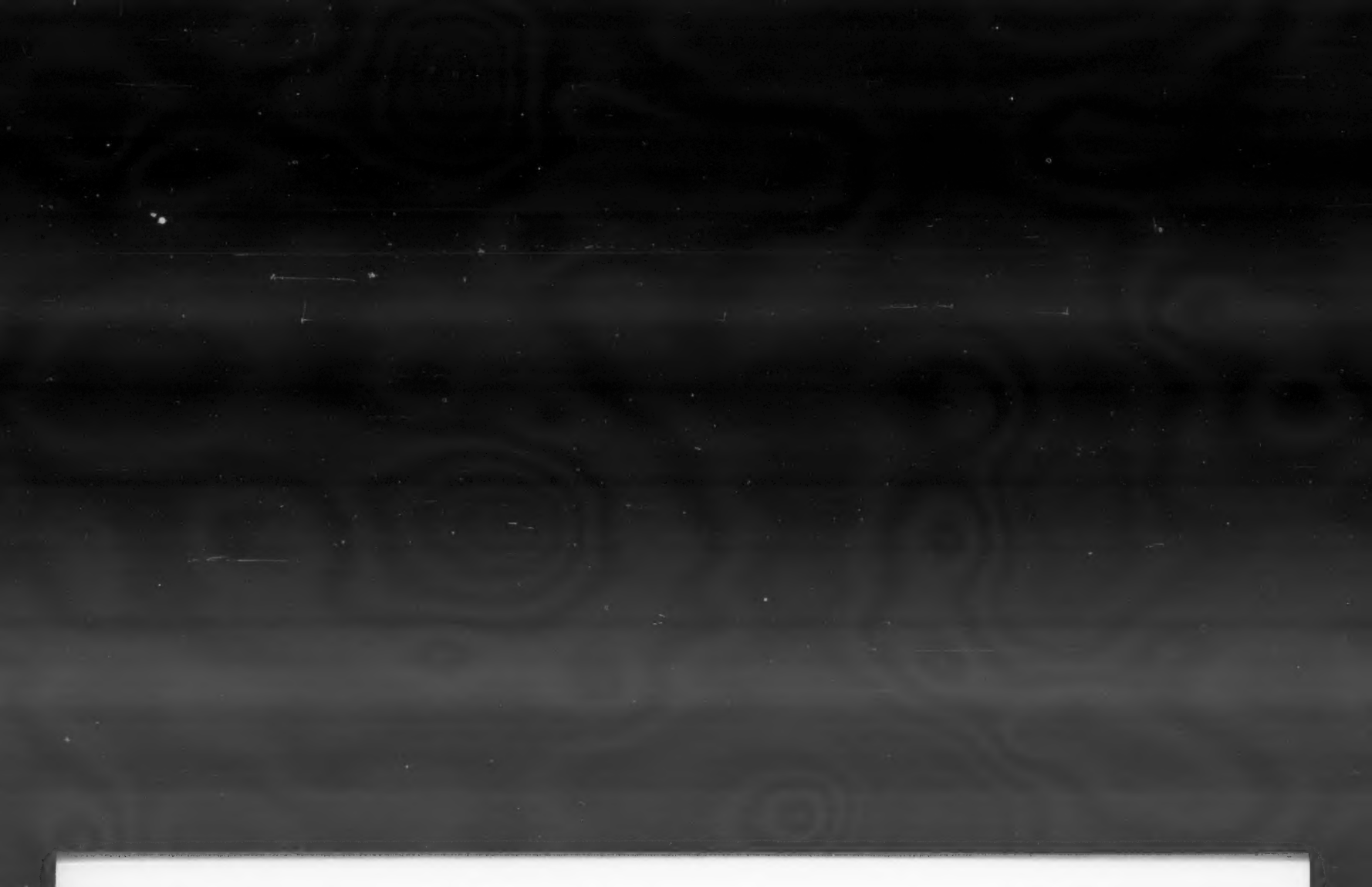

12

15

12

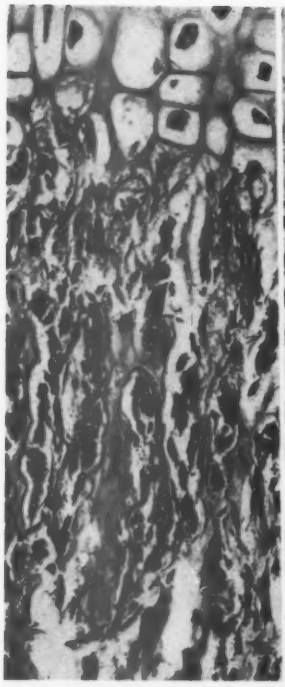

13, 14

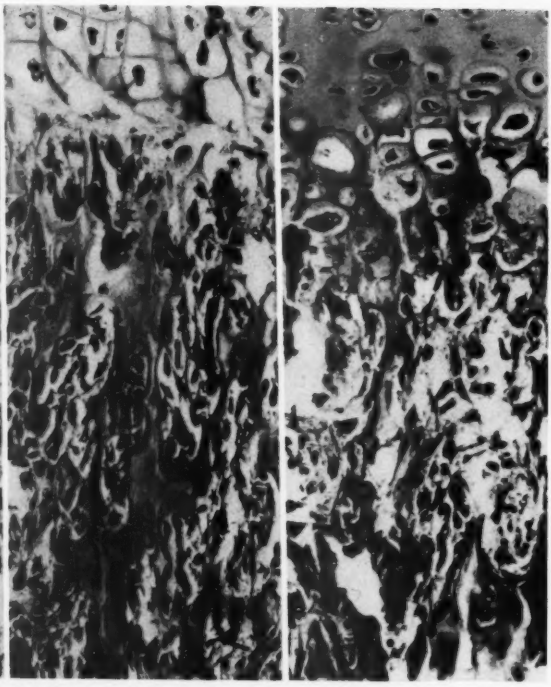

15

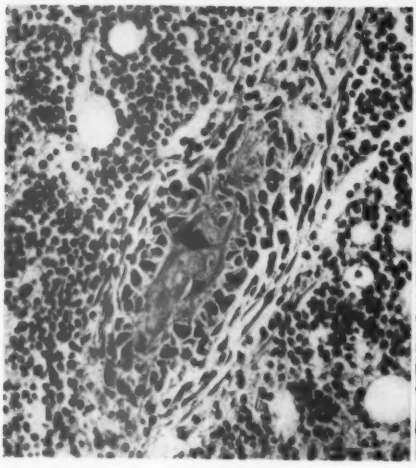

16

FIG. 17. Endosteal surface of the cortex from a control animal. There is a normal number of osteoblasts and stellate fibroblasts with close approximation of marrow cells. × 150.

FIG. 18. Endosteal surface of the cortex from a control to show the pattern of argyrophilic fibers in this area. Snook reticulum stain. × 150.

FIG. 19. Endosteal surface of the cortex, 2 days after 400 r. There are increasing numbers of osteoblasts and stellate cells. × 150.

FIG. 20. Endosteal surface of the cortex, 2 days after 400 r. An increase of argyrophilic fibrils is manifest. Snook stain. × 150.

FIG. 21. Endosteal surface of the cortex, 3 days after 1,800 r. The increase of stellate cells and regression of marrow cells are shown. × 150.

FIG. 22. Endosteal surface of the cortex, 3 days after 1,800 r. There is an increase of loose reticulum. Snook stain. × 150.

FIG. 23. Endosteal surface of the cortex, 4 days after 1,200 r. The excess of osteoblasts and bone matrix as well as stellate cells is apparent. × 150.

FIG. 24. Endosteal surface of the cortex, 4 days after 1,200 r. Note the increase in argyrophilic fibers and bone matrix. Snook stain. × 150.

FIG. 25. Endosteal surface of the cortex, 7 days after 1,800 r. There is increased cellularity and bone matrix. × 150.

FIG. 26. Endosteal surface of the cortex, 7 days after 1,800 r. Excessive bone matrix and argyrophilic fibers are shown. Snook stain. × 150.

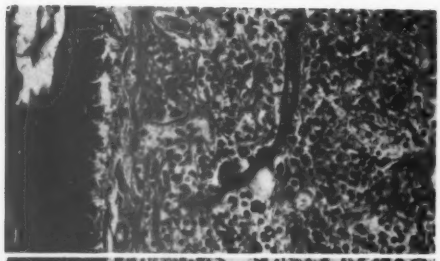

17

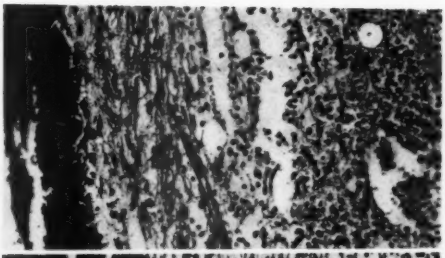

18

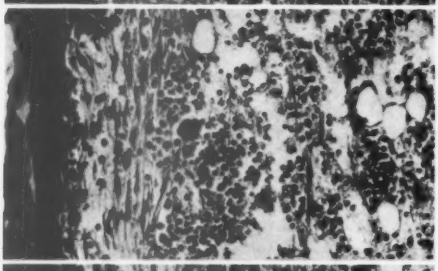

19

20

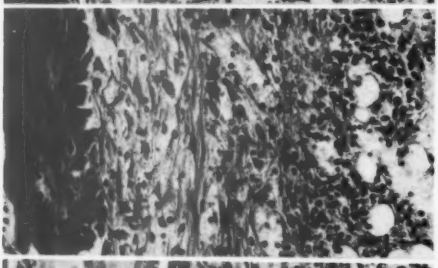

21

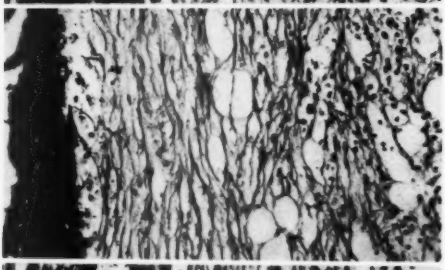

22

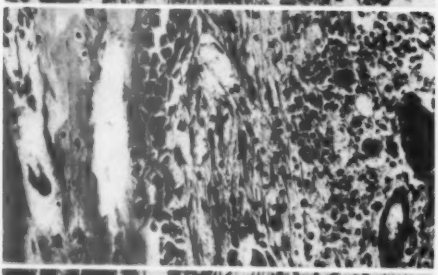

3

24

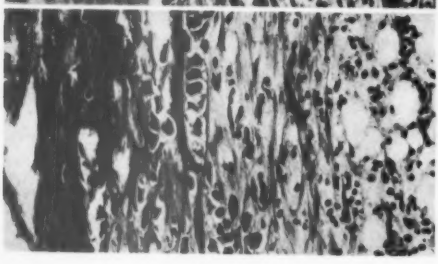

5

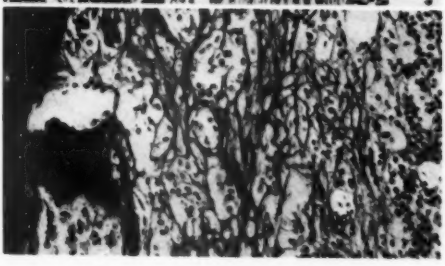

26

HISTOCHEMICAL OBSERVATIONS ON THE ROLE OF STROMAL AMINOPEPTIDASE ACTIVITY FOLLOWING NEOPLASTIC CELL (H.Ep.#3) INVASION

N. KARLE MOTTET, M.D.

From the Department of Pathology, University of Washington School of Medicine, Seattle, Wash.

Delineation of the role of peptidases in the destructive invasiveness of malignant tumor cells remains an important problem. Early experiments based on chemical analysis of homogenates of tumors did not define the nature or extent of their significance.[1] Topographic microchemical methods[2,3] revealed an increase in peptidases in the periphery of many animal neoplasms, but a causal relationship to invasiveness was not analyzed. Development of histochemical methods for demonstrating aminopeptidase-like activity[4,5] has led to an enlivened interest in the problem. The procedure utilizes the substrate L-leucyl-β-naphthylamide. Therefore, it would be more appropriately termed an amidase. However, to be consistent with the usage to date, the term aminopeptidase will be used in this report.

The presence of aminopeptidase activity in the stroma surrounding some tumors was reported[6,7] and confirmed[8] though there was disagreement as to the interpretation of the finding. One group[6,7] observed the enzyme activity in the connective tissues of a variety of neoplastic and inflammatory lesions and concluded that it was not specifically related to the invasiveness of neoplasms. Evidence supporting this has been produced.[9] Another group[8] was unable to detect elevated enzyme activity in stroma, other than that surrounding some invading malignant neoplasms, and concluded that the enzyme was specifically related to invasion. Evidence supporting this, too, has been produced.[10] The controversy remains unresolved.

Beyond identifying the presence of aminopeptidase activity in the stroma of many but not all invasive neoplasms, its role in the process has not been critically analyzed. Many rapidly invasive malignant neoplasms have had no demonstrable elevation of enzyme activity in their stroma. On the other hand, basal cell carcinomas, which rarely metasta-

This work was supported in part by Grant C-4570 of the National Institutes of Health, United States Public Health Service.

Accepted for publication, February 13, 1961.

size and differ somewhat from other types of carcinoma in their manner of infiltrating connective tissues, were reported to have positive activity.[8] Further, benign neoplasms reported[8] as showing no increase in aminopeptidase activity are types not ordinarily associated with a stromal proliferative response. The inconstancy of the presence of stromal enzyme activity in the neoplastic process suggested that the increased activity was a reflection of the host response to the neoplasm rather than a property of the neoplasm itself. The experiments herein reported were designed to test this hypothesis.

Material and Methods

A human epidermoid carcinoma, H.Ep.#3, was selected for transplantation because of its vigorous invasive properties.[11] It not only grows with ease on the chick chorio-allantoic membrane (CAM), invading extensively and usually metastasizing to the embryo proper, but it also infiltrates and metastasizes in the tissues of conditioned rats. Furthermore, the properties of this tumor have been extensively studied. Important among these properties is its morphologic and immunologic stability in spite of several years of serial transplantation.[12]

The experiments consisted of 4 parts:

Group 1. H.Ep.#3 on the Chorio-allantoic Membrane of Chick Embryos. A thick suspension of H.Ep.#3 cells in Earle's solution was placed on the CAM of 8-day embryos, then incubated for 5 days. Virtually 100 per cent "takes" resulted, and the tumors grew to approximately 1 cm. in diameter. A total of 60 blocks from 15 tumors were quick-frozen at −160° C. immediately upon removal from the CAM.

Group 2. H.Ep.#3 in Conditioned Weanling Wistar Rats. Twenty-four 30 to 60 gm. weanling Wistar rats were conditioned according to the method of Toolan.[13] Each rat received 150 r of total body x-radiation. On the third post-irradiation day each received 0.1 cc. of H.Ep.#3 suspension in each flank. Three mg. of cortisone were injected subcutaneously in the neck at the time of transplantation and every second day thereafter until a total of 4 doses was given. The animals were sacrificed 10 days after transplantation, and all had tumors of 2 cm. or more in diameter in each flank. Many had metastatic foci in the peritoneal cavity, liver, or lungs.

Group 3. H.Ep.#3 in Conditioned Nonweanling Wistar Rats. Thirteen Wistar rats were conditioned identically to the above. These rats had grown beyond the weanling size and weighed 80 to 100 gm. It has been reported that rats beyond weanling stage were not as susceptible to conditioning as weanlings.[13] Seventeen days after H.Ep.#3 transplantation, 7 rats were sacrificed, and the tumors were harvested and immediately frozen. They were grossly cystic, with central necrosis and liquefaction of the H.Ep.#3 and a dense fibrous peripheral capsule. Six of the rat tumors were harvested at 31 days. These had no detectable remaining H.Ep.#3. The transplantation site consisted of a fibrous scar.

Group 4. H.Ep.#3 in Nonconditioned Weanling Wistar Rats. Seven 30 to 60 gm. Wistar weanling rats received H.Ep.#3 transplants in each flank without conditioning. After 7 days they were sacrificed. Gross examination of these tumors revealed a necrotic core with surrounding tumor and a fibroproliferative zone. These tumors were also frozen.

In all the experiments, at least 4 quadrant blocks from each neoplasm were rapidly frozen in an isopentane-propane mixture producing temperatures of −160° C. The blocks were sectioned in a Pearse cryostat. At least 5 step sections were cut from each block. As many as 25 sections were made from some blocks. The recently modified histochemical method for demonstrating aminopeptidase activity, described by

Glenner, Burstone and Meyer,[8] was used. The substrate mixture consisted of 1 per cent L-leucyl-β-naphthylamide (supplied by Dajac Laboratories, 5000 Langdon Street, Philadelphia, Pennsylvania), 40 ml. of distilled water, 10 ml. of tris buffer to a final pH of 7.1 and 30 mg. of Corinth Fast Salt V (supplied by General Dyestuff Co. of General Aniline and Film Corp., Portland, Oregon). Following incubation (20 minutes at 37° C.) the slides were washed, placed in 2 per cent aqueous $CuSO_4$ solution, rinsed, then taken through 30, 50, 30 per cent alcohols, washed, then mounted in glycerol jelly. Rat kidney sections from the same animals served as positive controls. One control slide accompanied each 5 slides from the experiment through each reagent. A 20-minute substrate incubation time at 37° C. was optimal. However, from each block one 17 to 24 hour incubation was done. In addition, an adjacent section from each block was stained with hematoxylin and eosin.

Observations

Group 1. H.Ep.#3 on the Chorio-allantoic Membrane of Chick Embryos. The neoplastic cells were seen beneath the ectodermal epithelium in the form of a loose mass dispersed among the fibroblasts. Hematoxylin and eosin-stained sections did not reveal morphologic changes in the loose connective tissue adjacent to or within the tumor mass. On the edges of the tumor mass, individual and small groups of H.Ep.#3 cells were seen extending into and surrounded by the stroma. The H.Ep.#3 cell infiltration was very extensive. The sections for demonstrating aminopeptidase activity revealed no elevated stromal activity adjacent to the tumor (Fig. 3). The H.Ep.#3 cells were light tan in color, as were the fibroblasts. No black zone of elevated activity was seen adjacent to the tumor mass or surrounding the individual infiltrating cells. The simultaneously prepared positive control sections had intense black deposits, indicating aminopeptidase activity at the free border of the renal tubular cytoplasm.

Group 2. H.Ep.#3 in Conditioned Weanling Wistar Rats. Hematoxylin and eosin-stained sections revealed the H.Ep.#3 cells had formed a dense mass. On the periphery, small groups of cells extended into the adjacent loose and adipose connective tissue and striated muscle. In rare instances scant fibroproliferative change was seen adjacent to the H.Ep.#3. In most regions no connective tissue changes were found adjacent to the H.Ep.#3 cells. The fibroblasts throughout had a weakly positive cytoplasmic aminopeptidase activity (Fig. 1). However, no zone of increased activity was seen adjacent to the H.Ep.#3 cells, except in those areas where scant fibroproliferative changes were observed. At these sites the stromal aminopeptidase activity was slightly increased.

Group 3. H.Ep.#3 in Conditioned Nonweanling Rats. All of these sections revealed a core of necrotic H.Ep.#3 cells surrounded by a peripheral zone of some intact H.Ep.#3 cells. This, in turn, was sur-

rounded by a very dense zone of fibroblasts. Besides occurring in increased numbers, the collagen fibers seen were dense and more deeply acidophilic than the more peripheral loose areolar tissue. Within the dense fibroblast zone, the aminopeptidase activity was markedly increased above the level seen in the distant areolar connective tissue (Fig. 2). This was in sharp contrast to the findings in weanling rats described above. Control rat kidney sections were positive to a similar degree.

Group 4. H.Ep.#3 in Nonconditioned Weanling Rats. The findings in this group were similar to those in the conditioned nonweanling rats. Hematoxylin and eosin stains revealed a central necrotic zone of H.Ep.#3 cells surrounded by some intact H.Ep.#3 cells adjacent to a fibroproliferative zone in the stroma. The latter had an elevated aminopeptidase activity (Fig. 4) comparable to that seen in the preceding group.

Discussion

Recent developments in enzyme histochemistry have permitted initial explorations into some of the chemical mechanisms associated with the destructive invasiveness of neoplastic cells and the host response to it. Conventional histologic investigation has repeatedly shown morphologic alterations of the stroma at the border between neoplastic cells and the host's tissues. However, these changes *a priori* could just as well be ascribed to the host's reaction to the invasion by neoplastic cells as to the act of invasion itself. Thus the initial step in analysis of these changes was to separate those that were an integral part of the invasion from those that were the host's response to invasion.

Soon after the development of histochemical methods for localizing aminopeptidase activity, the originators of the methods applied them to neoplastic tissues.[4–7] A zone of increased enzyme activity was observed in the stroma at the periphery of many but not all malignant neoplasms. One group reported increased aminopeptidase activity in the connective tissue of benign neoplasms (colloid hyperplasia of thyroid, fibroadenomatosis of prostate) as well as inflammatory diseases (fibrocystic disease of breast, peptic ulcer, and ulcerative enteritis).[7] They concluded that in view of its abundance in proliferating connective tissue of neoplastic, inflammatory, and reparative processes, there was no reason to attribute the increased enzyme activity of the stroma in malignant neoplastic processes to the invasive properties of the tumor.

On the other hand, another group of workers[8] observed the sites of aminopeptidase activity in over 120 surgical specimens of human benign and malignant tumors. They noted a variability in the activity from

o to 4+ for some types of neoplasm and interpreted this variability to indicate aminopeptidase activity to be perhaps one of a series of proteolytic enzymes involved in invasiveness. They were unable to demonstrate elevated enzyme activity in inflammatory lesions and, therefore, concluded that the enzyme was specifically related to malignant neoplastic cell invasiveness. This contention had also been asserted by Braun-Falco.[10]

More recently Hess[9] examined the stromal aminopeptidase activity in 5 mouse and 4 rat carcinoma and sarcoma transplants. Those tumors that grew less well in the foreign host site generally had a higher stromal aminopeptidase activity. Thus, these experiments were consistent with the idea that the enzyme activity was part of the host's response to neoplastic cells.

Thus two conflicting views of the role of aminopeptidase in neoplastic cell invasion have developed: (a) the enzyme is part of the mechanism of destructive invasion by neoplastic cells; and alternately (b) the enzyme is part of the host's general reaction to injury. The experiments heretofore reported described the coincidence of the enzyme with a variety of pathologic processes. The observation that the enzyme was found in some inflammatory lesions did not necessarily elucidate, of itself, its role in invasiveness of neoplasms. To demonstrate a causal relationship between the host's fibroproliferative response to a neoplasm and the increased aminopeptidase, it was necessary to hold the properties of the neoplasm constant, then vary the host's fibroproliferative response.

To separate these two features I selected one stock type of carcinoma (H.Ep.#3) and transplanted it into hosts that had a varying response to the carcinoma. The growth characteristics of H.Ep.#3 on the CAM have been observed by conventional histologic methods.[14] The CAM fibroblasts were essentially nonreactive to the invading H.Ep.#3. The latter rapidly proliferated and infiltrated the membrane, invading blood vessels, and usually metastasized to the chick embryo proper. In this situation the stroma did not have histochemically detectable increased aminopeptidase activity.

Graded stromal response to H.Ep.#3 invasion was obtained by varying the extent of the conditioning of Wistar rats. One group was optimally conditioned, and in these the H.Ep.#3 grew so rapidly that the rats had to be sacrificed at 10 days post-transplantation. Luxuriant tumor growth and metastases were observed, with only traces of host fibroproliferative response. A second group of rats were conditioned in the usual manner except that they had grown beyond the weanling size. This has been observed by Toolan to reduce the conditioning effect,

and the host, in time, will destroy the tumor. Half of this group was sacrificed when the tumor was regressing and half later when the tumor had completely regressed. The third group consisted of nonconditioned weanlings. After a week of growth, the tumor grossly resembled that in the second group. A fibroproliferative response was prominent. The H.Ep.#3 carcinoma grown on the CAM and conditioned weanling rats did not have a peripheral zone of increased aminopeptidase activity. On the other hand, in those rats with a fibroproliferative response to the H.Ep.#3 transplant, an intense zone of aminopeptidase activity surrounded the tumor. I concluded from this that the aminopeptidase activity was related to the host's response to the tumor rather than constituting part of the mechanism of invasion.

These findings, along with those of Monis, Nachlas and Seligman[7] and of Hess,[9] seem to demonstrate clearly that stromal aminopeptidase activity is part of the host's response to the invasion of malignant tumor cells. Monis and co-workers showed increased stromal activity surrounding inflammatory lesions as well as benign and malignant neoplasms. Therefore, increased activity was not a unique feature of malignancies. Hess extended the observations to a variety of animal neoplasms. Tumors that grew poorly or regressed had the highest stromal aminopeptidase activity. The experiments reported herein demonstrated a close correlation of the aminopeptidase activity with the host's fibroproliferative reaction to a human epidermoid carcinoma and not with its invasiveness. The details of its specific function, whether in fibroblast metabolism, fiber formation, or "ground substance" properties, remain to be described. Further, how these changes may secondarily alter the invasiveness of malignant cells is also worthy of investigation.

Summary and Conclusions

When H.Ep.#3 carcinoma was grown on chorio-allantoic membranes of 15 chick embryos, no stromal proliferative response was detectable, and the stroma adjacent to the invading neoplastic cells was free from elevated aminopeptidase activity. Similarly, when H.Ep.#3 was grown in 24 conditioned weanling Wistar rats, there was no peripheral zone of elevated stromal aminopeptidase activity. However, when H.Ep.#3 was grown on 7 partially conditioned and 7 nonconditioned Wistar rats, the stromal fibroproliferative response was extensive and an intense zone of aminopeptidase activity was seen therein. The aminopeptidase activity was demonstrated histochemically using L-leucyl-β-naphthylamide as substrate. I concluded that the aminopeptidase activity represented the host's reaction to the invading neoplasm and was not part of

the mechanism by which malignant neoplasms invaded the host tissues.

References

1. Greenstein, J. P., and Meister, A. Tumor Enzymology. In: The Enzymes; Chemistry and Mechanism of Action. Sumner, J. B., and Myrbäck, K. (eds.). Academic Press, Inc., New York, 1952, Vol. 2, part 2, pp. 1134–1137.
2. Sylvén, B., and Malmgren, H. The histological distribution of proteinase and peptidase activity in solid tumor transplants; a histochemical study on the enzymic characteristics of the different tumor cell types. *Acta radiol.*, 1957, Suppl. 154, pp. 1–124.
3. Sylvén, B., and Bois, I. Protein content and enzymatic assays of interstitial fluid from some normal tissues and transplanted mouse tumors. *Cancer Res.*, 1960, **20**, 831–836.
4. Burstone, M. S., and Folk, J. E. Histochemical demonstration of aminopeptidase. *J. Histochem.*, 1956, **4**, 217–226.
5. Nachlas, M. M.; Crawford, D. T., and Seligman, A. M. The histochemical demonstration of leucine aminopeptidase. *J. Histochem.*, 1957, **5**, 264–278.
6. Monis, B.; Nachlas, M. M., and Seligman, A. M. Histochemical observations on leucine aminopeptidase activity in diseased tissues. (Abstract) *J. Histochem.*, 1958, **6**, 395.
7. Monis, B.; Nachlas, M. M., and Seligman, A. M. Study of leucine aminopeptidase in neoplastic and inflammatory tissues with a new histochemical method. *Cancer*, 1959, **12**, 601–608.
8. Glenner, G. G.; Burstone, M. S., and Meyer, D. B. A study of aminopeptidase activity in the stroma of neoplastic tissue with a comparison of histochemical techniques. *J. Nat. Cancer Inst.*, 1959, **23**, 857–872.
9. Hess, R. Localization of cathepsin-like and aminopeptidase activity in various solid tumor transplants. *Cancer Res.*, 1960, **20**, 940–943.
10. Braun-Falco, O. Histochemical demonstration of aminopeptidase in normal and pathological skin. (Letter to the editor) *J. Histochem.*, 1957, **5**, 94.
11. Toolan, H. W. Transplantable human neoplasms maintained in cortisone-treated laboratory animals: H.S.#1, H.Ep.#1, H.Ep.#2, H.Ep.#3, and H.Emb.Rh.#1. *Cancer Res.*, 1954, **14**, 660–666.
12. Toolan, H. W. Immunological responses elicited in the heterologous host by transplantable human tumors: use of the conditioned rat as a test medium. *Ann. New York Acad. Sc.*, 1957, **69**, 830–841.
13. Toolan, H. W. The Use of X-Irradiation and/or Cortisone to Condition Hosts for Grafting. In: Radiation Biology and Cancer. Symposium on Fundamental Cancer Research. University of Texas Press, Austin, Texas, 1958, pp. 400–408.
14. Mottet, N. K. Unpublished observations.

Acknowledgment and thanks are due to Professor E. P. Benditt and Dr. David Lagunoff for their encouragement and guidance throughout the course of these experiments. I also thank Miss Florence Woodworth for her technical assistance.

[*Illustrations follow*]

Legends for Figures

Photomicrographs were prepared from sections demonstrating aminopeptidase activity, using 1 per cent L-leucyl-β-naphthylamide as a substrate.

Fig. 1. Group 2. Edge of an H.Ep.#3 carcinoma mass (left) and adjacent subcutaneous connective tissues (right) of a "conditioned" weanling Wistar rat. Note the absence of elevated aminopeptidase activity. × 400.

Fig. 2. Group 3. Edge of an H.Ep.#3 carcinoma (left) and hyperplastic connective tissues (right) of a "conditioned" nonweanling Wistar rat. Note the intense black band of aminopeptidase activity at the interface. × 200.

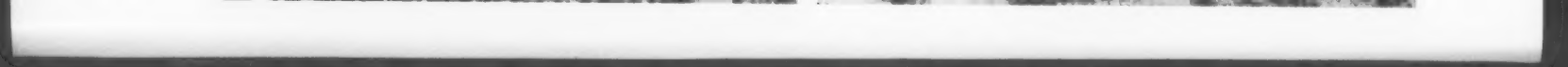

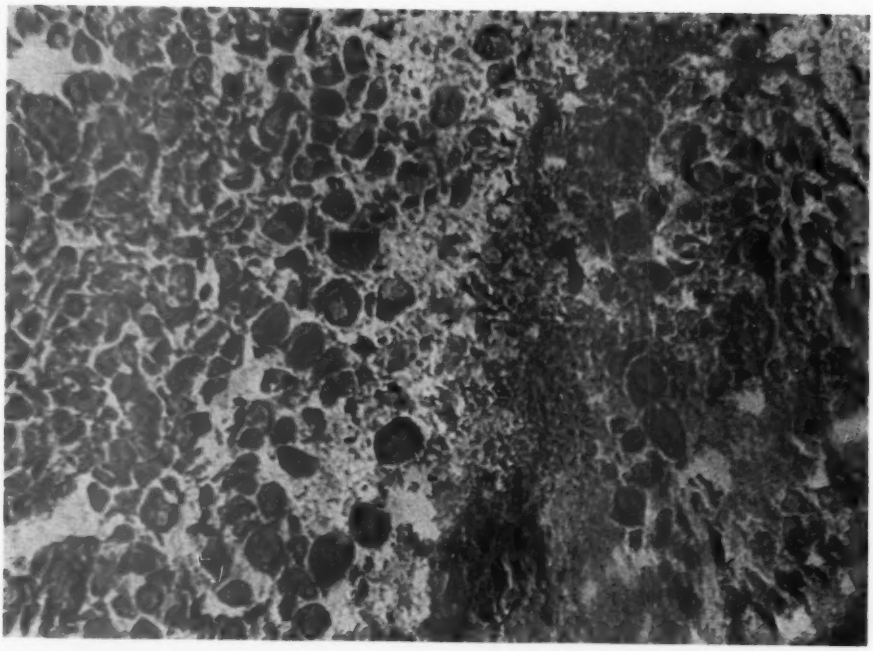

1

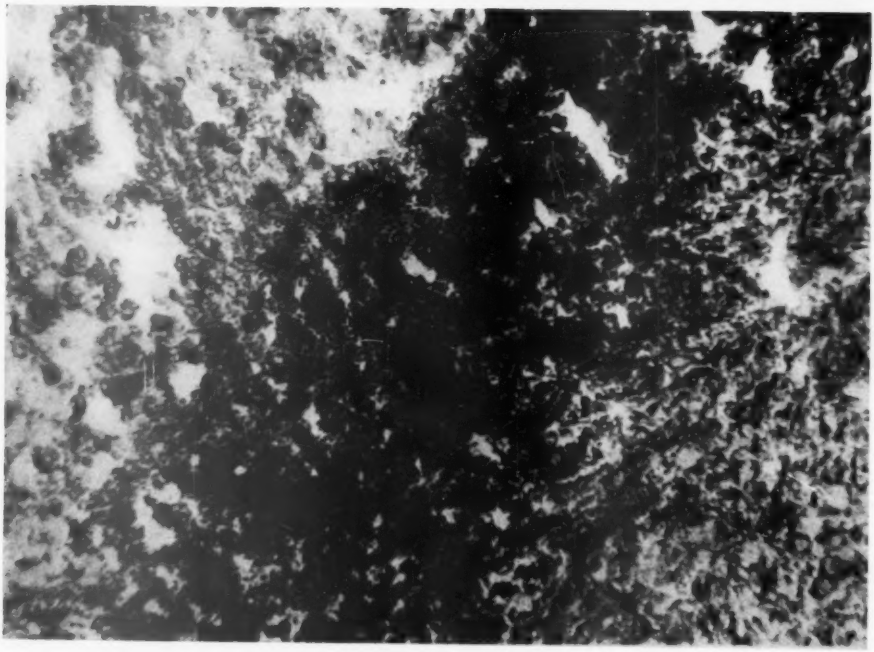

2

3

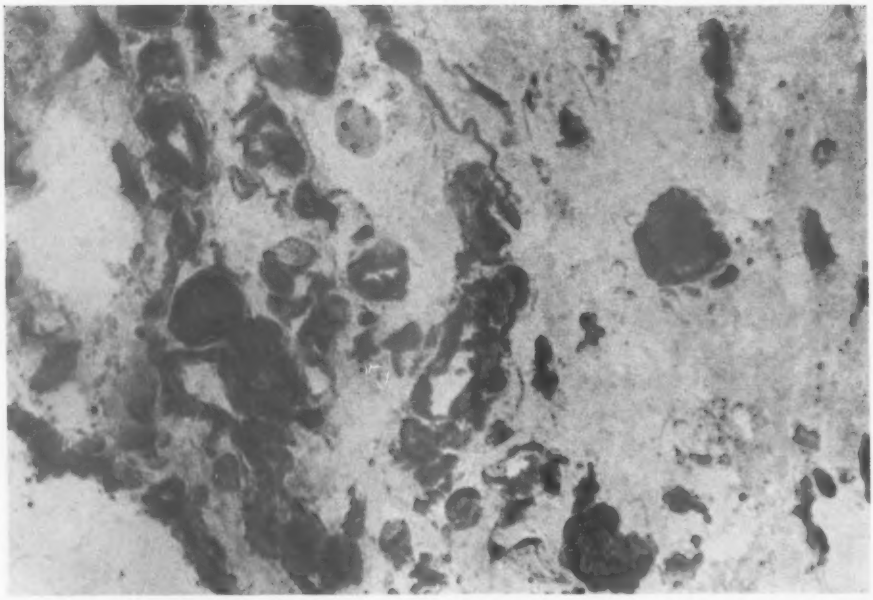

4

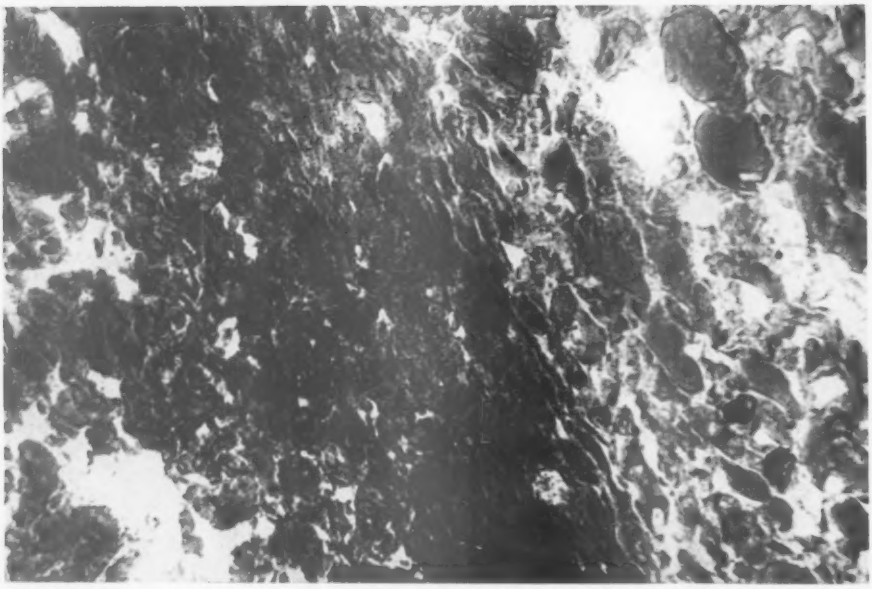

Fig. 3. Group 1. H.Ep.#3 carcinoma cells (left) infiltrating the chorio-allantoic membrane of a chick. Note the absence of aminopeptidase activity. × 600.

FIG. 4. Group 4. Edge of an H.Ep.#3 carcinoma (left) adjacent to the connective tissues and striated muscle of a nonconditioned weanling Wistar rat. The intense black band at the interface indicates intense aminopeptidase activity. × 300.

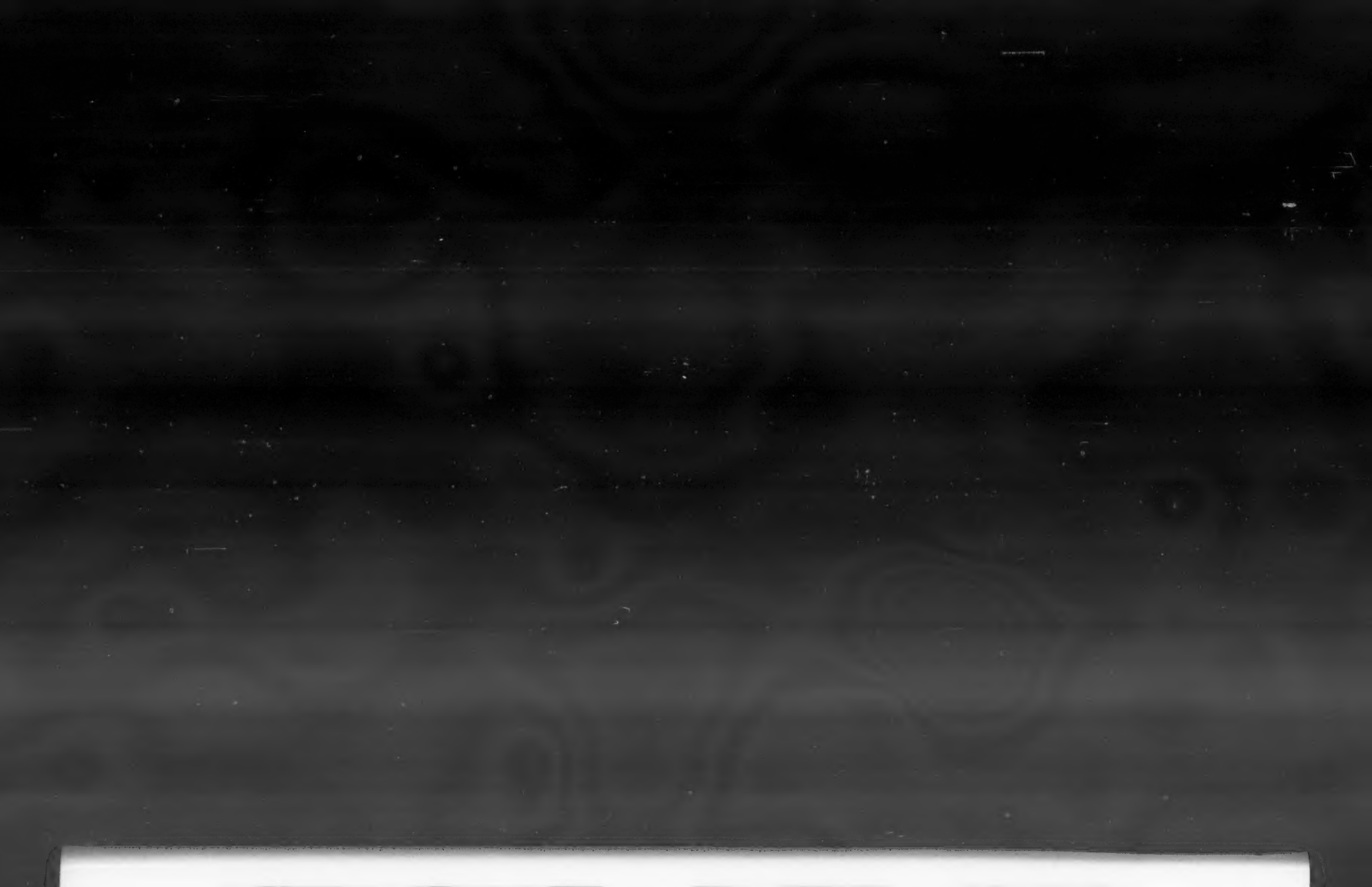

SPONTANEOUS MUSCULAR DYSTROPHY IN THE WHITE PEKIN DUCK

R. H. Rigdon, M.D.

From the Department of Pathology, The University of Texas Medical Branch, Galveston, Texas

Spontaneous focal necrosis has been observed in the striated muscle of white Pekin ducks.[1] Some of the birds with this lesion developed contractures of the legs. The necrosis is similar to that encountered in a variety of conditions, including bacterial[2] and viral[3,4] infections, vitamin E deficiency,[5,6] and following plasmocid administration.[7] A high percentage of the ducks in our laboratory have had the disorder, which occurs more frequently in the striated muscles of the legs than in the pectoral muscles. The extent of the necrosis varies in different ducks; usually it is only a microscopic finding. A similar lesion has been observed in the turkey, in which a pendulous crop appears as a result of necrosis in the crop-supporting muscle.[8] Some of the turkeys have shown difficulty in walking.[9] The morphologic alterations in the muscle, including histochemical changes, are the basis of this report.

Methods and Material

Normal white Pekin ducks one day of age were obtained at different intervals between 1956 and 1960 from the same commercial hatchery. The ducklings at first were kept in small groups in containers and later in a large outside pen. The food was a commercial ration (Ralston Purina Mills, St. Louis, Missouri) infrequently supplemented with cracked corn. Food and water were available at all times. Some of the ducks were used in different experiments, including the intratracheal injection of methylcholanthrene, tobacco condensate, polysorbate 80, and the oral administration of vitamin E. In each group, muscle necrosis was evident with varying frequency. Sixty-three of the ducks, however, were kept as untreated controls and were sacrificed at intervals of 1 to 347 days. As shown in Table I, 33 of these exhibited the muscle lesions to be described. Necropsy was performed immediately after death, and multiple specimens were removed from the muscle in each leg and in the pectoral region. These were fixed in a 4 per cent solution of formaldehyde. Paraffin sections were prepared and stained with hematoxylin and eosin. Selected sections were stained for glycogen with the periodic acid-Schiff (PAS) and Gomori methenamine silver techniques. The glycogen was removed with amylase by treating the sections either with a 1 per cent solution of diastase or human saliva before

This investigation was supported by PHS grants B-1439 (C_2) and B-2951 from the National Institute of Neurological Diseases and Blindness, National Institutes of Health, United States Public Health Service.

Accepted for publication, February 10, 1961.

staining by the PAS technique. Frozen sections of formalin-fixed tissues were stained for fat with oil red O.

Results

The frequency with which muscle necrosis occurred in the 63 control ducks is shown in Table I. It is evident from these data that muscle lesions first appeared when the ducks were 2 weeks old. After 28 days of

Table I

NECROSIS IN STRIATED MUSCLE OF WHITE PEKIN DUCKS
FREQUENCY OF OCCURRENCE

Number of ducks		Age	Sections per duck*	
Total	With necrosis	(days)	Number	With necrosis
9	0	1	6—7	0
5	0	5	4—6	0
5	4	14	7—13	1—2
10	0	15	10—12	0
5	3	16	9—10	1—3
5	4	28	6—13	2—4
2	2	41	7—13	3—4
1	1	42	11	2
4	3	44	11—19	2—4
5	5	54	9—10	1—5
1	1	78	11	7
1	1	88	26	21
1	1	170	7	7
1	1	244	7	4
5	4	298	6	1—3
1	1	328	7	7
2	2	347	6—8	2

* Usually removed from the legs and pectoral region.

age, necrosis was present in approximately 90 per cent of the birds, and the necrotic foci were more numerous in the older ducks. In 10 sections of muscle from a single bird, only 1 or 2 might show focal necrosis in 14-day-old ducks, but in those 100 days of age or older, necrotic foci were seen in as many as half of the sections. The necrotic lesions were evident in the striated muscle of ducks used in other experiments with essentially the same frequency.

The striated muscle of the normal duck contains a large amount of glycogen, appearing as small granules along the longitudinal striations (Fig. 1) and as larger masses widely distributed throughout the muscle fiber (Fig. 2). Focal accumulations of glycogen also occur within the muscle fiber, most frequently along its margin, immediately beneath the sarcolemma (Fig. 3). The glycogen stains as well with the Gomori technique as with the PAS stain. In many hematoxylin and eosin stained sections there are small, more or less uniform eosinophilic granules in

the same areas that stain for glycogen (Fig. 4). These persist after treatment with diastase. The larger glycogen masses (Fig. 2) are not visible in conventionally stained sections.

Lipid globules are also evident in the muscle fibers (Fig. 5). These frequently are present as small globules along the longitudinal striations (Fig. 6). Occasionally, larger globules appear with no special anatomic relation to the striations, however, and may be observed in the intermuscular spaces and about the small blood vessels. Lipid is also present in areas of muscle degeneration.

The most conspicuous microscopic alterations encountered were focal areas of "Zenker-like" necrosis affecting individual muscle fibers (Fig. 7). These varied in size and frequency in a single section and often exhibited a sharp line of demarcation between the necrotic portion and the adjacent normal muscle fibers (Fig. 8). Occasionally, neutrophils or mononuclear cells were manifest in relation to the necrotic foci. Globules of lipid-staining material were usually present, some within macrophages, while others lay free within the areas of inflammation. Clear spaces were evident within some of the muscle fibers (Fig. 9), their number and size varying within a single fiber. Occasionally, the spaces filled the greater part of the fiber and contained glycogen granules (Fig. 10). The sarcoplasm adjacent to the clear spaces did not always have visible striation (Fig. 11).

In addition to vacuolated spaces and the Zenker-like foci of necrosis, the sarcolemmal cells frequently were greatly enlarged (Fig. 12); the cytoplasm of some of them stained lightly with eosin and was vacuolated. Their nuclei appeared normal. The cytoplasm of enlarged sarcolemmal elements contained groups of glycogen-staining granules (Fig. 13). When treated with amylase, the cytoplasmic glycogen content disappeared. In many instances nuclei were distributed throughout the muscle substance (Fig. 14). The fibers in muscle exhibiting this atypical nuclear arrangement appeared to be normal. Evidence of regeneration in areas of necrosis was frequent (Fig. 15).

In view of the excessive amount of glycogen in the muscle of the duck, special attention was given to the relationship of glycogen to the areas of vacuolation and the Zenker-like necrosis. As previously stated, large granules of glycogen were frequently present within the muscle vacuoles (Fig. 10). Often large portions of fibers stained reddish purple with the PAS technique (Fig. 16); the areas of necrosis usually stained similarly. Moreover, the latter areas retained some of the glycogen after treatment with amylase. To remove all the glycogen, it was necessary to keep amylase in contact with the sections for long intervals.

As noted above, many of the individual muscle fibers were filled with

small globules of fat. This was occasionally the case in the fibers adjacent to an area of necrosis. However, fragments of sarcoplasm might not show excessive lipid content although globules of fat usually surrounded the fragments. It would seem, therefore, that the lipid substance in these locations followed necrosis rather than having been present in the muscle at the time the degenerative process began.

Discussion

Glycogen and fat are normally present in striated muscle. Their location within muscle fibers was discussed many years ago by Bullard.[10] A small amount of glycogen-staining material is evident in striated muscle of ducks at one day of age. At two weeks and older a large amount is manifest; it is at this age that ducks are more likely to exhibit muscle degeneration. Large amounts of glycogen continue to be present throughout the life of the duck. The glycogen has a focal distribution in normal muscle but may be present in areas of vacuolation, in foci of Zenker-like necrosis, and in the cytoplasm of enlarged sarcolemmal cells. The existence of large amounts of glycogen in foci of muscle degeneration suggests a relationship between the deposit of glycogen and the necrosis.

It is of interest to know that muscle necrosis, similar to that in the duck, has been observed in the horse with "glycogen-rich muscle fibers." Carlström[11] apparently was the first to describe this, in 1931. It occurred in horses that were actively exercised after a few days of rest and rich feeding. According to Carlström, the disease was due to rapid glycolysis in glycogen-rich muscle fibers. Smith and Jones[12] called this same disorder "azoturia." According to them, "As a muscle performs work, lactic acid . . . is known to accumulate in it. The accepted concept [for azoturia] is that the stored glycogen is changed by a series of intermediate steps into pyruvic acid, approximately one-fifth of which is oxidized to $CO_2 + H_2O$ with the production of energy. When the amount of oxygen immediately available is limited, the remaining four-fifths is converted to lactic acid, which may be oxidized later. Pursuant to the above concept it may well be that the amount of lactic acid formed is especially large when the supply of stored glycogen is large, not being directly proportional to the amount of work done."

Spontaneous necrosis in the striated muscle of man has been observed in 2 of 7 cases of acute paralytic myohemoglobinuria.[13] Bywaters and Dible[13] made this diagnosis in a human subject because of the close resemblance of the symptoms to the paralytic equine myohemoglobinuria described by Carlström.[11] In Bywaters and Dible's case the pectoral muscle fibers showed a marked tendency to fragmentation, a feature

not observed in well-stained normal fibers. Occasional fibers were vacuolated and had an increase in muscle nuclei; some fibers underwent hyaline necrosis. Buchanan and Steiner[14] reported an instance of myoglobinuria in which "all the skeletal muscles had evidence of a severe recent progressive degeneration. This change was characterized by a waxy degeneration with vacuolation and necrosis with liquefaction." It would be of considerable interest to know if excessive amounts of glycogen were present in the human examples of myoglobinuria as it was in those described by Carlström[11] and Smith and Jones[12] in the horse.

McArdle[15] described a form of glycogenesis in man in which there was a defect in the breakdown of muscle glycogen. On exercise the muscles underwent prolonged painful contracture. The myopathy in the McArdle syndrome, according to Grollman,[16] was attributable to a deficiency of 1,3-diphosphoglyceraldehyde dehydrogenase. It may be that an abnormality in glycogen metabolism in the white Pekin duck could account for the muscle necrosis. Additional studies are being made in an attempt to support this hypothesis.

Abnormality in carbohydrate metabolism has been described in patients with progressive muscular dystrophy.[17] McCrudden[18] expressed the opinion that an abnormality in muscle glucose metabolism was an underlying factor in this disease. Delayed utilization of glucose[19] and low levels of blood sugar[19–21] have been reported in patients with this condition. Mosberg[22] found the level of lactic acid to be higher than normal in patients with muscular dystrophy. Zenker-like muscle necrosis has been described in individuals with muscular dystrophy.[23] It has been postulated that this disorder and spontaneous myohemoglobinuria may be related, the former being a chronic and the latter an acute variety of the same process.[23]

Humphreys and Kato[24] in 1934 described an unusual form of vacuolar degeneration in the skeletal muscle of an infant with glycogen-storage disease (von Gierke); coarse and fine glycogen granules were present in many of the vacuoles. Similar degenerative changes have been reported by di Sant'Agnese and his colleagues.[25,26] It is obvious that a metabolic error leading to excessive accumulation of glycogen is a feature in individuals with glycogen-storage disease.[25] The description of the morphologic changes in muscle, reported by Humphreys and Kato[24] in von Gierke's disease, and the illustrations of the lesions are similar to the alterations observed in the muscles of the duck.

Since similar muscle necrosis has been observed in ducks fed a ration deficient in vitamin E,[5] 10 ducks were given a dietary supplement of vitamin E orally. Necrosis was present, however, in the striated muscle of 9 of these birds when they were 23 days of age. If a nutritional de-

ficiency other than vitamin E is responsible for this disorder, there is nothing at this time to suggest what it may be. The food given to these ducks was a commercially prepared ration. The degenerative lesions were observed over a period of more than a year. The absence of vitamin E or any other known dietary factor, within a specific shipment of food, therefore, would appear unlikely.

Since degeneration associated with large deposits of glycogen occurs spontaneously in the striated muscle of turkeys, ducks and chickens, it is possible that an abnormal carbohydrate metabolic process is frequent in birds. However, only a few birds in this laboratory have shown clinical manifestations attributable to the effects of muscle necrosis. A genetic factor is present in von Gierke's disease and in progressive muscular atrophy; whether this may also be the case in this muscular dystrophy in birds is not known.

A recent publication [27a] gives an excellent review of muscle and includes a discussion of a variety of conditions in which muscle necrosis may occur. It is stated: "It must be emphasized that the histological changes in muscle fibers are not specific to a particular etiology and that the histological appearance often shows little correlation with the clinical state." It is further stated: "The cause of muscular dystrophy of any type is quite unknown, but the diseases are thought to be essentially 'degenerative' and possibly due to inborn errors of metabolism or endocrine disturbance." In view of the histochemical features observed in the affected muscle of ducks, it is of considerable interest to find that Wells [28] in 1909 sought to relate Zenker's necrosis to local lactic acid production. Although this concept has not been confirmed, Field [27b] said that "at the moment the question remains open."

Wells [28] performed a number of experiments *in vitro* and *in vivo* to show that lactic acid produced changes in striated muscle that were quite similar microscopically to those observed in typical Zenker's degeneration. He concluded that the evidence seemed to strongly favor an association of lactic acid and hyaline transformation as cause and effect. Fishback and Fishback [29] pointed out that an accumulation of lactic acid occurred in injured muscles. This indicated damage to the metabolic function with a resulting incomplete cycle of carbohydrate change.

Summary

Focal areas of degeneration occurring spontaneously in the striated muscle of the white Pekin duck have been described. This lesion is characterized by vacuolation and Zenker-like necrosis within individual muscle fibers. Large granules of glycogen are associated with the process. Sarcolemmal cells are frequently swollen, and their cytoplasm con-

tains glycogen. Muscle striations are occasionally absent when vacuoles are present.

Contractures are present in some of the ducks with the degenerative muscle lesions in the extremities.

A similar lesion has been observed in striated muscle of the horse and has been attributed to a disturbance in glycogen metabolism. An apparently similar lesion has been described in the muscle of an infant with von Gierke's disease.

Necrosis in striated muscle and abnormal carbohydrate changes have been observed in human subjects with primary muscular diseases. It would seem that the spontaneous muscular degeneration in the white Pekin duck could be related to a local disturbance in carbohydrate metabolism.

References

1. Rigdon, R. H. Muscular dystrophy: spontaneous occurrence in ducks. *Texas Rep. Biol. & Med.*, 1961, **19**, 167–177.
2. Forbus, W. D. Pathologic changes in voluntary muscle. I. Degeneration and regeneration of the rectus abdominis in pneumonia. *Arch. Path. & Lab. Med.*, 1926, **2**, 318–339.
3. Dalldorf, G.; Sickles, G. M.; Plager, H., and Gifford, R. A virus recovered from the feces of "poliomyelitis" patients pathogenic for suckling mice. *J. Exper. Med.*, 1949, **89**, 567–582.
4. Godman, G. C.; Bunting, H., and Melnick, J. L. The histopathology of Coxsackie virus infection in mice. I. Morphologic observations with four different viral types. *Am. J. Path.*, 1952, **28**, 223–257.
5. Pappenheimer, A. M., and Goettsch, M. Nutritional myopathy in ducklings. *J. Exper. Med.*, 1934, **59**, 35–42.
6. Nesheim, M. C.; Leonard, S. L., and Scott, M. L. Alterations in some biochemical constituents of skeletal muscle of vitamin E-deficient chicks. *J. Nutrition*, 1959, **68**, 359–369.
7. Hicks, S. P. Brain metabolism *in vivo*. II. The distribution of lesions caused by azide, malononitrile, plasmocid and dinitrophenol poisoning in rats. *Arch. Path.*, 1950, **50**, 545–561.
8. Rigdon, R. H.; Ferguson, T. M., and Couch, J. R. Pendulous crops in turkeys—an anatomical and pathologic study. *Am. J. Vet. Res.*, 1960, **21**, 979–986.
9. Rigdon, R. H.; Ferguson, T. M., and Couch, J. R. Spontaneous occurring muscular necrosis and encephalomalacia in the turkey. *Poultry Sc.* (To be published)
10. Bullard, H. H. On the interstitial granules and fat droplets of striated muscle. *Am. J. Anat.*, 1912–1913, **14**, 1–46.
11. Carlström, B. Ueber die Aetiologie und Pathogenese der Kreuzlähme des Pferds (Haemoglobinaemia paralytica). IV. Die Aetiologie und Pathogenese der Muskelveranderungen bie des Kreuzlähme. *Skandinav. Arch. Physiol.*, 1931, **62**, 1–69.
12. Smith, H. A., and Jones, T. C. Veterinary Pathology. Lea & Febiger, Philadelphia, 1957, p. 653.

13. BYWATERS, E. G. L., and DIBLE, J. H. Acute paralytic myohaemoglobinuria in man. *J. Path. & Bact.*, 1943, **55**, 7–15.

14. BUCHANAN, D., and STEINER, P. E. Myoglobinuria with paralysis (Meyer-Betz disease); report of a case. *Arch. Neurol. & Psychiat.*, 1951, **66**, 107–109.

15. MCARDLE, B. Myopathy due to a defect in muscle glycogen breakdown. *Clin. Sc.*, 1951, **10**, 13–35.

16. GROLLMAN, A. Metabolic Diseases. In: Clinical Physiology; the Functional Pathology of Disease. Blakiston Div., McGraw-Hill Book Co., Inc., New York, 1957, Chapt. 7, p. 229.

17. HOAGLAND, C. L. States of Altered Metabolism in Diseases of Muscle. In: Advances in Enzymology and Related Subjects of Biochemistry. NORD, F. F. (ed.). Interscience Publishers, Inc., New York, 1946, pp. 193–230.

18. MCCRUDDEN, F. H. The nature of the pathologic process in progressive muscular dystrophy. *Arch. Int. Med.*, 1918, **21**, 256–262.

19. JANNEY, N. W.; GOODHART, S. P., and ISAACSON, V. I. The endocrine origin of muscular dystrophy. *Arch. Int. Med.*, 1918, **21**, 188–215.

20. BYARD, D. S. Four cases of muscular dystrophy. *Internat. Clin.*, 1923, 33rd series, **1**, 174–177.

21. MCCRUDDEN, R. H., and SARGENT, C. S. Hypoglycemia and progressive muscular dystrophy. *Arch. Int. Med.*, 1916, **17**, 465–475.

22. MOSBERG, G. Beitrag zur Kenntnis des Stoffwechsels der Dystrophia musculorum progressiva. *Klin. Wchnschr.*, 1930, **9**, 2051–2052. (Cited by Hoagland [17])

23. ADAMS, R. D.; DENNY-BROWN, D., and PEARSON, C. M. Diseases of Muscle; a Study in Pathology. Paul B. Hoeber, Inc., New York, 1953, 556 pp.

24. HUMPHREYS, E. M., and KATO, K. Glycogen-storage disease: thesaurismosis glycogenica (von Gierke). *Am. J. Path.*, 1934, **10**, 589–614.

25. DISANT'AGNESE, P. A.; ANDERSEN, D. H., and MASON, H. H. Glycogen storage disease of the heart. II. Critical review of the literature. *Pediatrics*, 1950, **6**, 607–623.

26. DISANT'AGNESE, P. A.; ANDERSEN, D. H.; MASON, H. H., and BAUMAN, W. A. Glycogen storage disease of the heart. I. Report of 2 cases in siblings with chemical and pathologic studies. *Pediatrics*, 1950, **6**, 402–424.

27. BOURNE, G. H. (ed.). The Structure and Function of Muscle. Vol. III. Pharmacology and Disease. Academic Press, New York, 1960. (a) BOSANQUET, F. D.; DANIEL, P. M., and PARRY, H. B. Myopathy: the Pathological Changes in Intrinsic Diseases of Muscle. Chapt. 10, pp. 321–358. (b) FIELD, E. J. Muscle Regeneration and Repair. Chapt. 5, pp. 139–170.

28. WELLS, H. G. The pathogenesis of waxy degeneration of striated muscles (Zenker's degeneration). *J. Exper. Med.*, 1909, **11**, 1–9.

29. FISHBACK, D. K., and FISHBACK, H. R. Metabolism in acute molecular degeneration of striated muscle. III. Variations produced in the glycogen, lactic acid and phosphorus of the muscle. *Arch. Path.*, 1932, **14**, 204–212.

[*Illustrations follow*]

Legends for Figures

Fig. 1. Small glycogen-staining granules are deposited along the longitudinal striations. Periodic acid-Schiff (PAS) stain. × 807.

Fig. 2. Large glycogen-staining granules are distributed throughout muscle fiber. PAS stain. × 902.

Fig. 3. Glycogen-staining granules are deposited at the margin of muscle fibers. One fiber has several vacuoles containing glycogen-staining granules. PAS stain. × 460.

Fig. 4. Eosinophilic granules in a muscle fiber. These granules usually are concentrated along the fiber margin. Hematoxylin and eosin (H and E) stain. × 360.

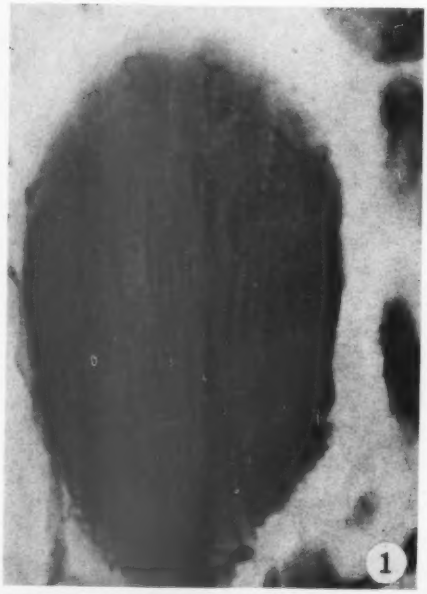

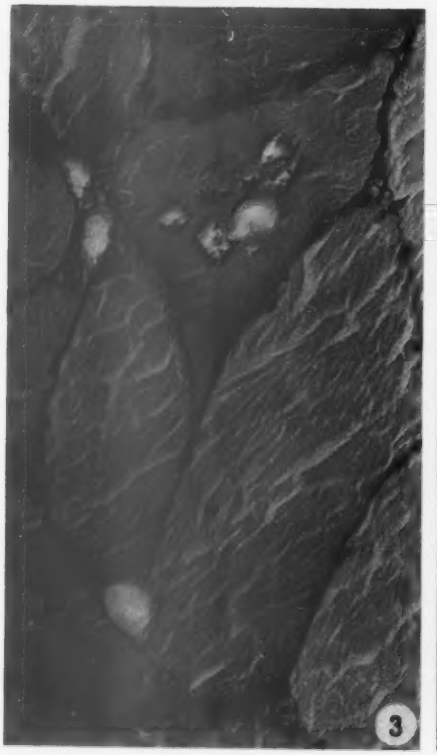

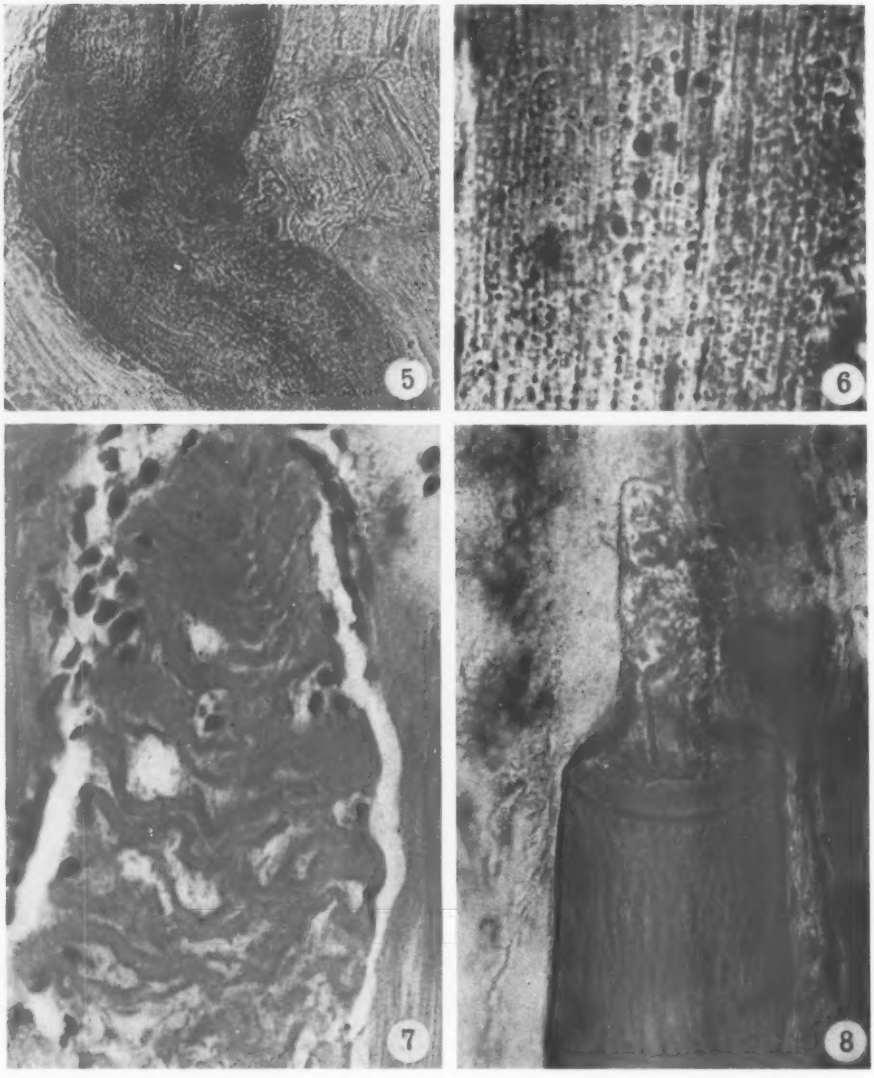

FIG. 5. Lipid granules fill two of the muscle fibers. Oil red O stain. × 280.

FIG. 6. Lipid granules are located along the longitudinal striations within a muscle fiber. Oil red O stain. × 855.

FIG. 7. A focal area of Zenker-like necrosis in a striated muscle fiber. H and E stain. × 517.

FIG. 8. There is a sharp line of demarcation between the necrotic and the well-preserved portion of this muscle fiber. Oil red O stain. × 360.

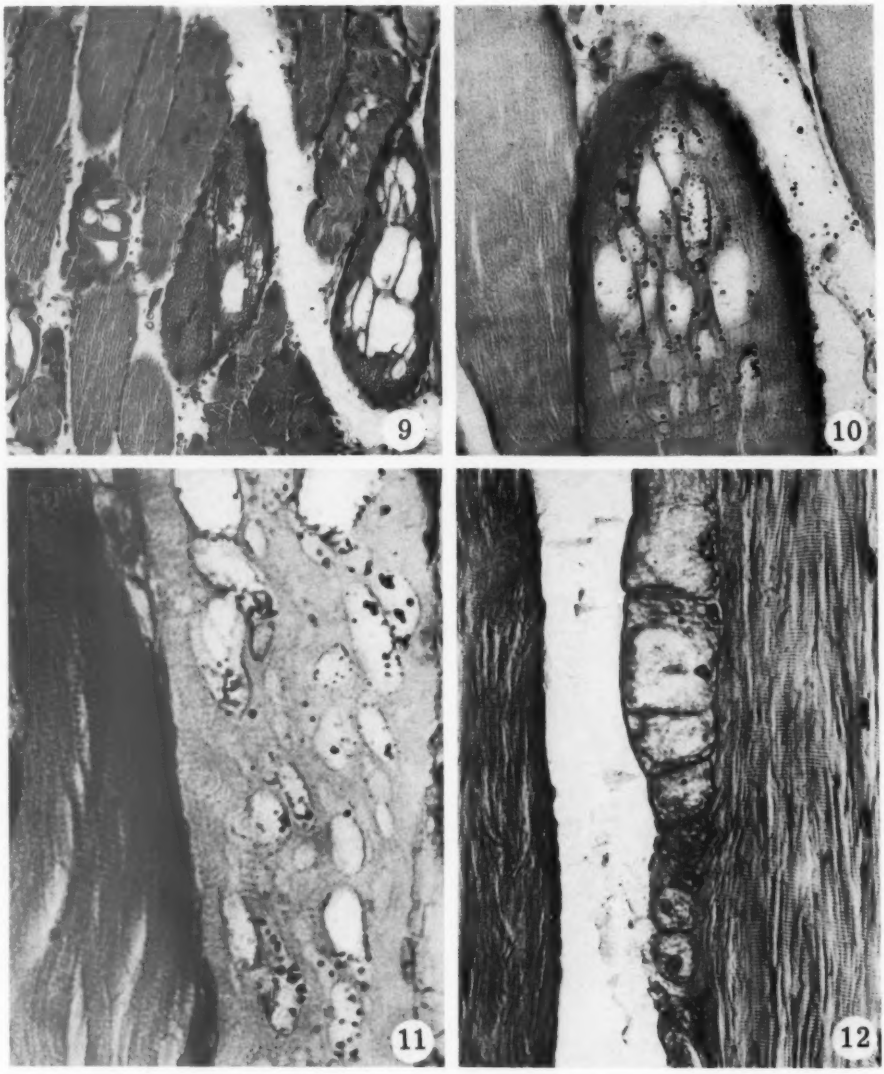

FIG. 9. Clear areas of varied size are present in many of the muscle fibers. H and E stain. × 120.

FIG. 10. The clear spaces within muscle fibers are filled with glycogen granules. PAS stain. × 340.

FIG. 11 Longitudinal striations are absent in muscle fibers filled with large clear spaces. An adjacent fiber exhibits glycogen granules along one margin. PAS stain. × 522.

FIG. 12. Sarcolemmal cells are greatly enlarged. Their cytoplasm stains lightly with eosin. H and E stain. × 240.

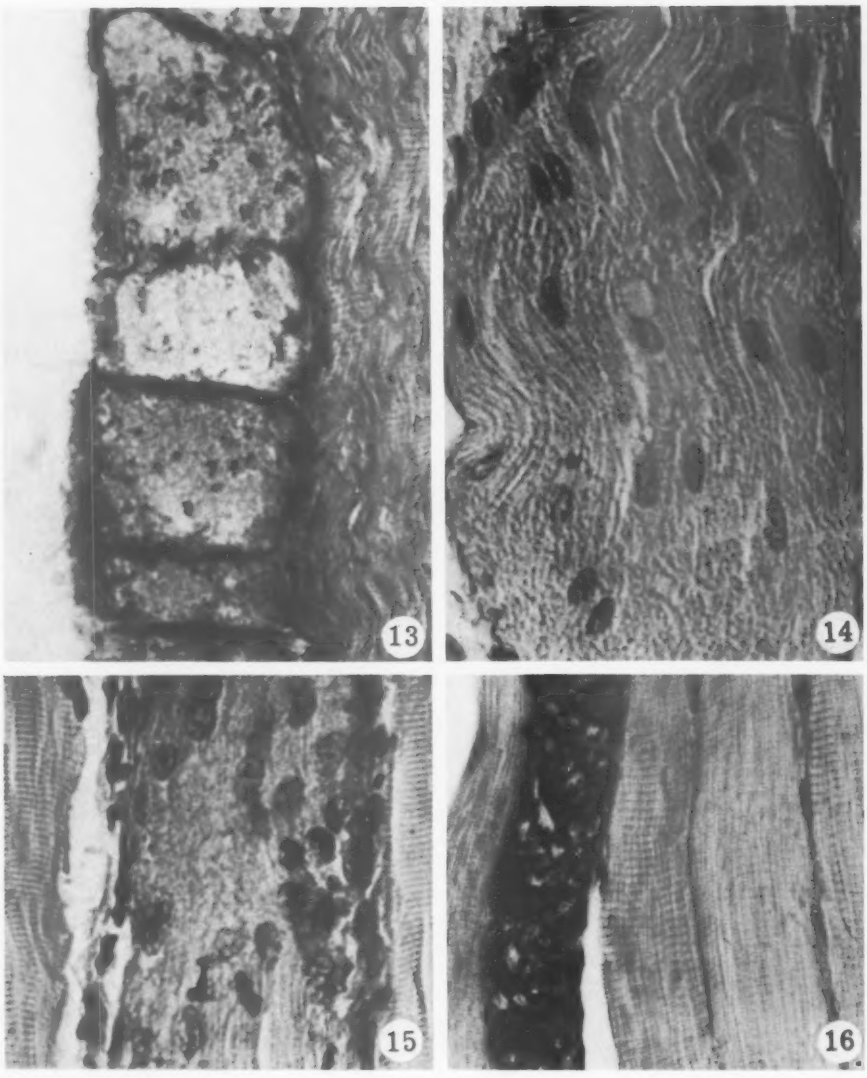

FIG. 13. Many large glycogen masses are present in the cytoplasm of sarcolemmal cells. Gomori's methenamine silver stain. × 712.

FIG. 14. Many nuclei are present in a muscle fiber. Saliva treated, PAS stain. × 617.

FIG. 15. Regeneration of a muscle fiber. H and E stain. × 632.

FIG. 16. A single muscle fiber with early degenerative changes stains for glycogen. PAS stain. × 712.

STUDIES ON THE FINE STRUCTURE OF THE TERMINAL BRANCHES OF THE BILIARY TREE

II. Observations of Pathologically Altered Bile Canaliculi

Jan W. Steiner, M.D., and John S. Carruthers, M.D.

From the Department of Pathology, University of Toronto, Toronto, Ontario, Canada

In the course of studies designed to elucidate the cause of intrahepatic biliary obstruction, changes were noted in the microvilli of parenchymal liver cells where these project into the lumens of biliary passages. It will be shown that widespread edema of the microvilli produces a subtotal or total obstruction of the lumens of bile canaliculi. Such alterations have not been recorded in previous studies of the fine structural changes in intrahepatic or extrahepatic cholestasis.[1-4]

In order to investigate the specificity of this change and the reciprocal behavior of parenchymal liver cells and their microvilli in bile canaliculi, tissues were subsequently examined from cases with extrahepatic biliary obstruction and from cases of human and experimental liver injury not associated with clinical evidence of cholestasis. It will be shown that in all such instances qualitatively similar alterations of the microvilli can be demonstrated. Their distribution is less widespread than in intrahepatic cholestasis.

Material and Methods

Biopsy tissue was examined from the following disorders; the diagnosis was based upon the clinical pattern in the patient or experimental animal.

Intrahepatic Biliary Obstruction. Two patients with intrahepatic cholestasis, both of whom were found to have no obstruction to their extrahepatic biliary tree at operation. The relevant microscopic finding in each case was plugging of bile canaliculi. A second biopsy specimen obtained from one patient showed early evidence of biliary cirrhosis. The cause of the original intrahepatic biliary obstruction could not be determined in either case.

Extrahepatic Biliary Obstruction. (a) Two patients with congenital biliary atresia which had progressed to biliary cirrhosis; (b) rabbits with early complete experimental extrahepatic biliary obstruction.[5]

Hepatic Lesions Not Associated with Clinical Evidence of Cholestasis. (a) An example of "fatty" liver in a human subject; (b) a patient with portal cirrhosis; (c) rabbits receiving portal vein injections of nonspecific soluble immune complexes. Some

Supported by a Grant-in-Aid (MA 785) of the National Research Council of Canada.
Accepted for publication, January 31, 1961.

aspects of the histologic features in these lesions have been reported separately[6]; (d) rabbits receiving a prolonged series of systemic injections with heterologous protein (human gamma globulin).

Tissues obtained by surgical biopsy or, in the case of animals, immediately prior to sacrifice, were fixed, impregnated and stained by the methods outlined previously.[7] Care was taken not to pass judgment on any altered tissue which was inadequately preserved. The criteria of good preservation employed were the following: (a) even distribution of the karyoplasm in the central portions of parenchymal cell nuclei; (b) preservation of the reciprocal relationship between Kupffer cells and their trabeculae and the parenchymal microvilli where these project into the space of Disse; and (c) uninterrupted cell membranes.

In all the cases under review, sections stained with phosphotungstic acid (PTA) and with silver methenamine (SM), with or without prior periodic acid oxidation, were examined. The purpose of this was to facilitate distinction between bile canaliculi and sinusoids. The spaces of Disse surrounding the latter contained demonstrable reticulin fibrils and an amorphous ground substance-like material[6] whereas bile canaliculi were devoid of them. Despite these precautions, channels were found where it was not possible to make a distinction. These were ignored in arriving at conclusions.

Results

Alterations of Microvilli of Bile Canaliculi

It was noted previously that variations in size, shape and distribution of microvilli in the ultimate branches of the biliary tree occurred even normally.[7] Only marked deviations were considered to be of pathologic significance.

Edema of Microvilli. This was seen in all cases under review though the distribution and severity of this change varied (Figs. 10 to 16). In the cases of intrahepatic biliary obstruction, almost total or total occlusion was seen frequently. In all other instances such alterations were patchy and involved only a very few areas and often only a single villus in an occasional canaliculus. Observations of large numbers of swollen microvilli indicated that the evolution of the edema was not uniform. In many it commenced in the tip, producing a clublike dilatation of the extremity, a narrow neck of cytoplasm connecting it to the main parenchymal cell mass (Fig. 11). In other instances the edema began near the base of the villus, producing a broad-based structure with a delicate finger-like projection at the extremity (Fig. 10). Finally, the entire villus became edematous and progressively more broad-based (Figs. 13 to 15). Occasionally such a large villus filled the entire lumen (Fig. 14). This was seen more frequently in bile pre-ductules and ductules (Fig. 21) than in canaliculi, in which the obstruction was usually caused by more numerous interlocking microvilli. The internal structure of the edematous microvilli differed little from their normal counterparts except for a reduction in over-all electron density (Fig. 12). Occasional small smooth-surfaced vesicles (Fig. 11) or aggregates of crystals, thought to be cholesterol (Fig. 7), were found in the cytoplasmic matrix

of the enlarged microvilli. Particles of ribose-nucleoprotein (RNP) were seen rarely in their cytoplasm (Fig. 10).

Reduction and Distortion in the Number of Microvilli. Apart from the reduction of microvilli in those canaliculi where a few edematous villi were found filling the lumen (Figs. 13 to 16), decrease in the number of microvilli was noted most frequently in dilated canaliculi (Figs. 3 and 4). Only very marked reduction was considered to be of pathologic significance since variations in the density distribution of these structures were found even normally.[7] Reduction in the number of microvilli contributed occasionally to the impression that canaliculi were dilated (Figs. 3 and 4). Many microvilli in dilated and occluded channels were found to be stunted or distorted (Figs. 4 and 13 to 16).

Changes of Canalicular Size

Markedly dilated bile canaliculi were found in all cases under review. In general, their numbers were greater and their presence ubiquitous in a given lobule in instances associated with clinical evidence of cholestasis (Figs. 1 to 5). In all other cases their distribution was patchy, and often they could be found only after a prolonged search. Assessment of pathologic dilatation of bile canaliculi could only be made in electron micrographs not exceeding an original magnification of approximately 6,000 times (Figs. 1 and 2). At higher magnifications, where a comparison between the average size of cells and of bile canaliculi could not be made, conclusions could not be reached on the existence of this form of alteration. Moreover, dilatation may be merely apparent in those channels in which the number of microvilli projecting into the lumen is reduced (Figs. 3 and 4).

The Relationship of Dilated to Occluded Canaliculi

In general, in intrahepatic cholestasis the number of occluded canaliculi exceeded the number of dilated ones, and the opposite was observed in extrahepatic biliary obstruction. It was, however, of importance to note that both pathologically dilated and occluded canaliculi were found in all the material under review. Despite attempts to localize exactly the site and distribution of the obstruction and dilatations respectively in a given lobule, no definitive conclusions could be reached on this point. It is noteworthy that in intrahepatic biliary obstruction, dilated canaliculi were often found in the marginal zones of lobules. In these instances the cause of the obstruction was occasionally found to be occlusion of the lumens of bile pre-ductules or ductules as a result of edema of their microvilli (Fig. 21).

In extrahepatic cholestasis, dilatation of bile canaliculi and of bile

ductules was not always accompanied by a dilatation of the intervening pre-ductule (duct of Hering).

Disturbances of Bile Canalicular Topography

As a result of both distention of most and opening up of some pre-existing partially or totally closed canaliculi, the topographic relationship between the spaces of Disse, perisinusoidal recesses and canals and bile canaliculi was found to be altered. They were often found to be in closer contact with each other than normally, yet actual communications could not be demonstrated. In well-preserved tissue, canalicular ruptures were not observed.

Numbers of Bile Canaliculi

In animals with experimentally induced complete extrahepatic biliary obstruction, an apparent increase in the number of bile canaliculi was observed. This was thought to be due to an opening up of channels which were normally partially or totally closed.[7] A reduction in the number of bile canaliculi was not seen in any of the cases under review.

Morphologic Evidence of Bile Stasis

It was stated previously that small quantities of a faintly electron-opaque material could be found occasionally in the lumens of bile canaliculi under normal circumstances.[7] In general, the presence of more highly electron-dense or particulate material in bile canalicular lumens was most marked in instances associated with clinical evidence of cholestasis. However, even in cases of total extrahepatic biliary obstruction, completely empty bile canaliculi were found (Fig. 2).

The retained products of bile in the canaliculi assumed several forms: (a) a diffuse, moderately electron-dense material partially or totally filling the lumen (Fig. 5); (b) a coarsely granular amorphous material of a fairly marked electron density, less evenly distributed and often intermingled with the material described under (a) above (Figs. 3 and 4); (c) precipitates with a crystalline structure forming rosettes of needles. Small ringlike structures of the same material were occasionally found in the vicinity of the crystalline aggregates. It was thought that this material represented cholesterol (Fig. 8); (d) aggregates of lipid of a variable, but usually marked, electron density, closely resembling the so-called peribiliary and lipofuscin bodies. These intraluminal aggregates will be referred to as lipid emboli since they were never found to adhere to the lining of canaliculi and therefore could not be designated as bile thrombi (Fig. 5). The mode of entry of these lipid bodies into the lumen was never observed at a canalicular level, but was seen fairly

frequently in bile pre-ductules and ductules. Figure 6 shows the extrusion of such material from a biliary epithelial cell across its cell membrane.

Alterations of Parenchymal Liver Cells

The main cytoplasmic mass of parenchymal liver cells, which formed the boundary and microvilli of pathologically altered bile canaliculi, was frequently found to behave independently of the pathologic processes in the latter. Markedly dilated canaliculi with reduced numbers of microvilli or with edematous microvilli were often found to be bounded by otherwise normal or almost normal parenchymal cells (Figs. 2 and 13 to 16). On the other hand, cells with severe degrees of vacuolar (hydropic) degeneration were frequently provided with microvilli of average dimensions protruding into bile canaliculi of average appearance (Fig. 9). In many instances, particularly in extrahepatic biliary obstruction, both changes in canaliculi and in the adjacent parenchymal cells were found to have developed simultaneously.

The changes of parenchymal cells which were noted in relation to altered canaliculi can be summarized as follows:

Condensation of Peri-canalicular Cytoplasmic Matrix. A band of dense cytoplasmic matrix devoid of organelles surrounded the canalicular lumen (Fig. 2). A similar condensation may be noted even in normal tissues.[7] However, in SM-stained sections of pathologically altered tissues, the zone of condensation assumed an intense argentophilia, possibly as a result of the presence of carbohydrate-containing material (e.g., glycoprotein) in this region (Fig. 2). In sections stained with lead hydroxide, the zone was usually found to be entirely devoid of RNP granules (Fig. 12).

Increase of Peribiliary and Lipid Bodies. Pericanalicular, "dense," lipid, and lipofuscin bodies were often markedly increased in number in the vicinity of pathologically altered bile canaliculi (Figs. 3 and 4).

Vacuolar (Hydropic) Degeneration. As was previously noted, this change was seen frequently in the parenchymal cells adjoining altered canaliculi. It consisted of a dilatation of the endoplasmic reticulum, thus forming spaces usually devoid of any electron-dense material in the lumen. Neither the change itself nor the size of dilated sacs bore any obvious direct relation to the severity of the canalicular changes.

Alterations of Mitochondria. In the vicinity of altered bile canaliculi from any cause, abnormal mitochondria were found in the parenchymal cells (Figs. 17 to 20). These changes were patchy in distribution and usually had to be searched for. They may be summarized as follows: (a) an over-all increase in size of the corpuscles; (b) a distortion of the

shape of the entire mitochondrion (Fig. 17); (c) an elongation of the cristae mitochondriales, thus forming long, tortuous partitions within the mitochondrial matrix (Fig. 20); (d) formation of "ring-shaped" cristae which surrounded a lumen containing part of the mitochondrial matrix (Fig. 19); and (e) an increase in size of the usual opaque or dense bodies within the matrix (Fig. 18).

Development of Abnormal Resorptive or Secretory Cell Surfaces. In most of the cases under review in which bile canalicular alterations were demonstrated, microvilli were found on surfaces of liver cells where they are not normally present. Thus, cells were frequently found to be provided with microvilli on all surfaces in addition to those which faced the space of Disse and bile canaliculi (Fig. 22). Such aberrant microvilli were particularly numerous on those surfaces which were in direct contact with portal tracts or with fibrous connective tissue septums in regenerating lobules. Lipid and bile-laden macrophages were often found in these areas in direct apposition to such microvillous borders, suggesting that their predominant function was to provide an alternate pathway of bile secretion.

The various changes in parenchymal liver cells will be analyzed in detail later.

Discussion

This paper reports morphologic observations of pathologically altered bile canaliculi in intrahepatic cholestasis. These changes consisted of edema of microvilli, leading to subtotal or total obstruction of the canaliculi. In other areas the canalicular lumens were widened and their over-all topography was consequently disturbed so that they came to lie in close proximity to the perisinusoidal spaces of Disse. The contents of the dilated canaliculi were altered and were seen to consist of more or less particulate bile constituents.

In order to establish the specificity of these changes, human and experimental animal tissues were examined from cases with extrahepatic biliary obstruction and from others with liver injury not associated with clinical evidence of cholestasis. In these, changes were found which were qualitatively identical with those described in intrahepatic cholestasis. It is one of the purposes of this paper to show that alterations of bile canaliculi occurred not only in conditions associated with clinical evidence of cholestasis but also in its absence. This point seems to us of importance since interpretation of canalicular alterations based upon observations of a very few altered canaliculi in a given liver biopsy specimen cannot be used as definite evidence of a specific form of cholestasis.

The changes in canaliculi were extremely variable, and it was only by an assessment and estimation of their reciprocal frequency and distribution that some attempt could be made to arrive at a diagnosis. Since quantitation of changes at an electron microscopic level of observation is extremely difficult, the results serve mainly to advance the frontiers of microscopy to areas which could not be previously resolved and studied.

With the above considerations and limitations in mind, bile canalicular occlusion by edematous microvilli in intrahepatic cholestasis is seen considerably more frequently than canalicular dilatation. In extrahepatic biliary obstruction the reverse holds true. In the latter condition and in others not associated with clinical evidence of cholestasis, occlusions of lumens by edematous microvilli were seen only sporadically, though edema of individual microvilli was encountered frequently.

It has been suggested that precipitated bile plugs may be the cause of bile canalicular obstruction in intrahepatic cholestasis.[1,3] Our observations failed to substantiate this view. Where particulate material was observed in canalicular lumens, it was never of a consistency or size adequate to account for total obstruction. We considered it probable that bile plugs were a secondary phenomenon resulting from either hydrodynamic disturbances or from changes in the composition of bile. The edema of microvilli may be the primary cause of intrahepatic biliary obstruction. In view of the finding of an identical change in extrahepatic biliary obstruction, it cannot be denied that this change may itself be secondary to prolonged contact of microvilli with static bile constituents.

On the basis of these considerations, the following hypothesis is suggested to explain the morphogenesis of intrahepatic biliary obstruction: The primary cause may be a disturbance of bile formation (e.g., inadequate hydration) leading to faulty drainage of bile from canaliculi. The edema of microvilli may be secondary to prolonged contact with such inspissated bile constituents and may lead in turn to the hydrodynamic disturbances evidenced morphologically by dilatation of some canaliculi. The occlusion of lumens by edematous microvilli may further increase the retention of bile products in the biliary passages. The swollen microvilli may themselves constitute an obstacle to the elimination of bile constituents from cells by producing an increase in the cell-lumen barrier. Thus a vicious circle may be established (Text-fig. 1).

Observation of the reciprocal behavior of parenchymal liver cells on the one hand, and of their microvilli where these project into the lumens of bile canaliculi on the other, shows a remarkable autonomy of behavior of the latter structures. A similar observation was made previ-

ously in the study of microvilli in the space of Disse when these came in contact with soluble immune complexes.[6] It is clear that the microvilli may undergo changes when the main cytoplasmic mass of parenchymal cells remains unaltered.

Our observations of the parenchymal liver cells adjacent to altered bile canaliculi differ from those of others.[1] Schaffner and Popper noted inconstant and irregular alteration of endoplasmic reticulum and normal

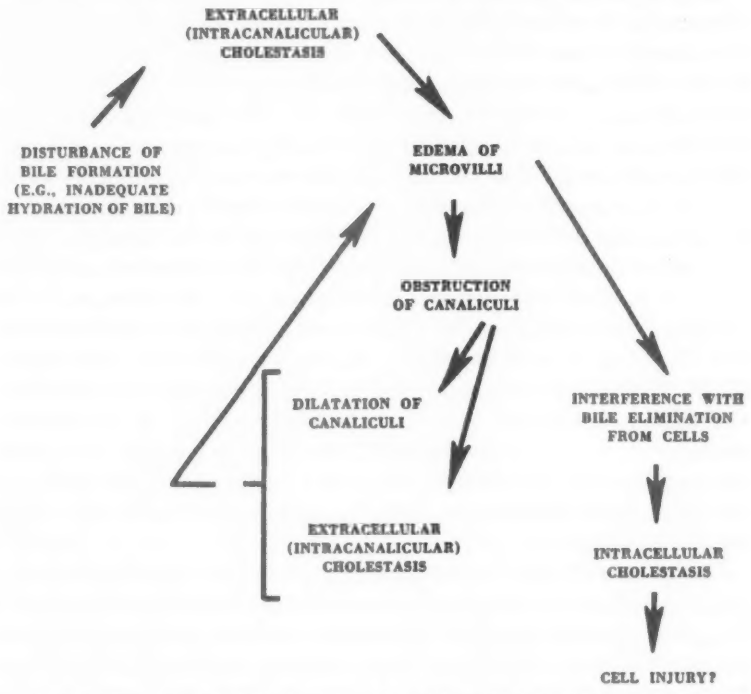

TEXT-FIGURE 1. Hypothetical concept of a vicious circle in intrahepatic cholestasis.

mitochondria in intrahepatic cholestasis, and disruption of the normal profiles of the endoplasmic reticulum and increased lipofuscin pigment structures in extrahepatic cholestasis. They stated that the mitochondria were not significantly altered in the latter condition.[1] Although the exact significance of the cytoplasmic alterations of liver cells reported in this paper is at present not apparent, they occur with a sufficient degree of constancy in relation to altered bile canaliculi to suggest some etiologic connection.

Disturbances of cell hydration (e.g., hydropic or vacuolar degeneration) can be anticipated when the outflow of bile from the pertinent

canaliculi is obstructed. It should be noted, however, that the dilatation of the endoplasmic reticulum which we designate as hydropic or vacuolar degeneration is considered by others as not necessarily related to water retention,[8] though an alternative explanation is not offered.

The increase in the number of intracytoplasmic "bodies" of various composition and the pericanalicular cytoplasmic condensation probably of glycoprotein material may be similarly related to the interference with elimination of bile or its constituents. Abnormal liver cell mitochondria have been reported in a case of biliary carcinoma and in a case of prolonged viral hepatitis.[9] The alterations in those instances consisted of the formation of intramitochondrial structures resembling myelin figures. The abnormality reported here is different in that it consists of an elongation and irregular coiling of the cristae mitochondriales. Since mitochondria are known to be highly integrated structures, concerned with many enzymatic functions,[10] it can be anticipated that such altered mitochondria may have a profound effect on the metabolism of the cells.

The use of auxiliary stains, i.e., PTA and SM, and the strict observance of the criteria of good preservation of tissues, outlined earlier in this paper, are essential in the study of bile canaliculi. It was found repeatedly that differentiation between bile canaliculi and sinusoids was impossible without these measures. It is significant that with these precautions abnormal communications could not be demonstrated between these two structures. This finding differs from those of others.[1]

Demonstration of canalicular ruptures or abnormal communications between bile canaliculi and sinusoids are essential prerequisites for the assumption of direct bile leakage into the space of Disse. Since this finding could not be confirmed in this study, evidence was sought for a possible alternate aberrant pathway of bile excretion. A preliminary observation suggests that this could occur via abnormally located microvilli on surfaces of liver cells not normally provided with them. Bile or its constituents may thus reach the connective tissues of the liver and percolate through into vascular channels, e.g., lymphatics, which are not always provided with a basement membrane. This suggestion does not exclude the possibility of bile regurgitation into the space of Disse by a trans-cellular transport mechanism as suggested by the investigations of Hampton.[11]

Summary

Morphologic alterations of bile canaliculi were found to occur in conditions associated with clinical signs of cholestasis as well as in others in the absence of such clinical evidence. It was suggested that

canalicular dilatation, obstruction by edematous microvilli and inspissation of bile observed with the electron microscope should not be considered as evidence of cholestasis or of a specific form of cholestasis unless quantitation and assessment of the reciprocal frequency of these changes could be achieved.

In intrahepatic cholestasis, obstruction of canaliculi by edematous microvilli was seen relatively more frequently than dilatation. It was suggested that the underlying anomaly in intrahepatic cholestasis might be a disturbance of bile formation (e.g., hydration) leading to stasis of bile in canaliculi. The edema of microvilli could then be the result of prolonged contact of these structures with inspissated bile constituents and might in turn lead to hydrodynamic disturbances evidenced morphologically by dilatation of some canaliculi. The swollen microvilli might themselves constitute an obstacle to the efficient elimination of bile constituents from cells.

In extrahepatic cholestasis, similar changes were noted in bile canaliculi though dilatation was seen more frequently than obstruction by edematous microvilli.

References

1. Schaffner, F., and Popper, H. Morphologic studies of cholestasis. *Gastroenterology*, 1959, **37**, 565–573.
2. Schaffner, F., and Popper, H. Electron microscopic studies of human cholestasis. *Proc. Soc. Exper. Biol. & Med.*, 1959, **101**, 777–779.
3. Reichel, J.; Goldberg, S. E.; Ellenberg, M., and Schaffner, F. Intrahepatic cholestasis following administration of chlorpropamide; report of a case with electron microscopic observations. *Am. J. Med.*, 1960, **28**, 654–660.
4. Rouiller, C. Les canalicules biliaires; étude au microscope électronique. *Acta anat.*, 1956, **26**, 94–109.
5. Steiner, J. W., and Carruthers, J. S. Unpublished observations.
6. Steiner, J. W. Investigations of allergic liver injury. I. Light, fluorescent and electron microscopic study of the effects of soluble immune aggregates. *Am. J. Path.*, 1961, **38**, 411–436.
7. Steiner, J. W., and Carruthers, J. S. Studies on the fine structure of the terminal branches of the biliary tree. I. The morphology of normal bile canaliculi, bile pre-ductules (ducts of Hering) and bile ductules. *Am. J. Path.*, 1961, **38**, 639–661.
8. Jezequel, A.-M.; Albot, G., and Nezelof, C. Les cellules clarifiées dans l'hépatite parenchymateuse. Étude comparée en microscopie optique et électronique. *Presse méd.*, 1960, **68**, 567–570.
9. Jezequel, A. M. Dégénérescence des mitochondries de foie humain dans un épithélioma du cholédoque et un ictère viral. Étude au microscope électronique. *J. Ultrastructure Res.*, 1959, **3**, 210–215.
10. Novikoff, A. B., and Essner, E. The liver cell; some new approaches to its study. *Am. J. Med.*, 1960, **29**, 102–131.
11. Hampton, J. C. An electron microscope study of the hepatic uptake and ex-

cretion of submicroscopic particles injected into the blood stream and into the bile duct. *Acta anat.*, 1958, **32**, 262–291.

The authors wish to thank Professor J. D. Hamilton for his valuable advice and Drs. W. L. Donohue, A. Sass-Kortsak and H. Ghadimi of the Hospital for Sick Children, Toronto, for permission to examine some of the liver biopsy material and for their cooperation. Thanks are also due to Dr. J. C. Sinclair and to Professor J. A. Dauphinee for their encouragement, and to Miss B. F. Lambert and Mr. H. Layne for technical assistance.

[*Illustrations follow*]

Legends for Figures

Key:

bc, c = bile canaliculus
d = bile ductule
e = bile embolus
f = fibroblastic processes
gl = glycogen
k = Kupffer cell
l = lumen
m = mitochondrion
mb = microbodies (lipid, lipofuscin, "peribiliary," glycoprotein cytoplasmic inclusions)
mv = microvillus
n = nucleus
ncl = nucleolus
pd = bile pre-ductule (duct of Hering)
plc = parenchymal liver cell
pt = portal tract
pv = pinocytic vesicle
rbc = red blood cell
rnp = ribose-nucleoprotein granules
S = sinusoid
V = intracytoplasmic vacuole
ZC = zone of cytoplasmic condensation

Fig. 1. Congenital biliary atresia. Moderately dilated bile canaliculi devoid of content lie between parenchymal cells which contain large irregular lipid deposits. The canalicular dilatation can only be assessed in relation to the size of the neighboring cells. Uranyl acetate impregnation. × 3,920.

Fig. 2. Experimental extrahepatic biliary obstruction (2 days). Widely dilated empty canaliculi show condensation of parenchymal cytoplasm in their margins. Note that some canaliculi are of average size. A perisinusoidal recess reaches to within a short distance of one canaliculus. Silver methenamine stain. × 5,760.

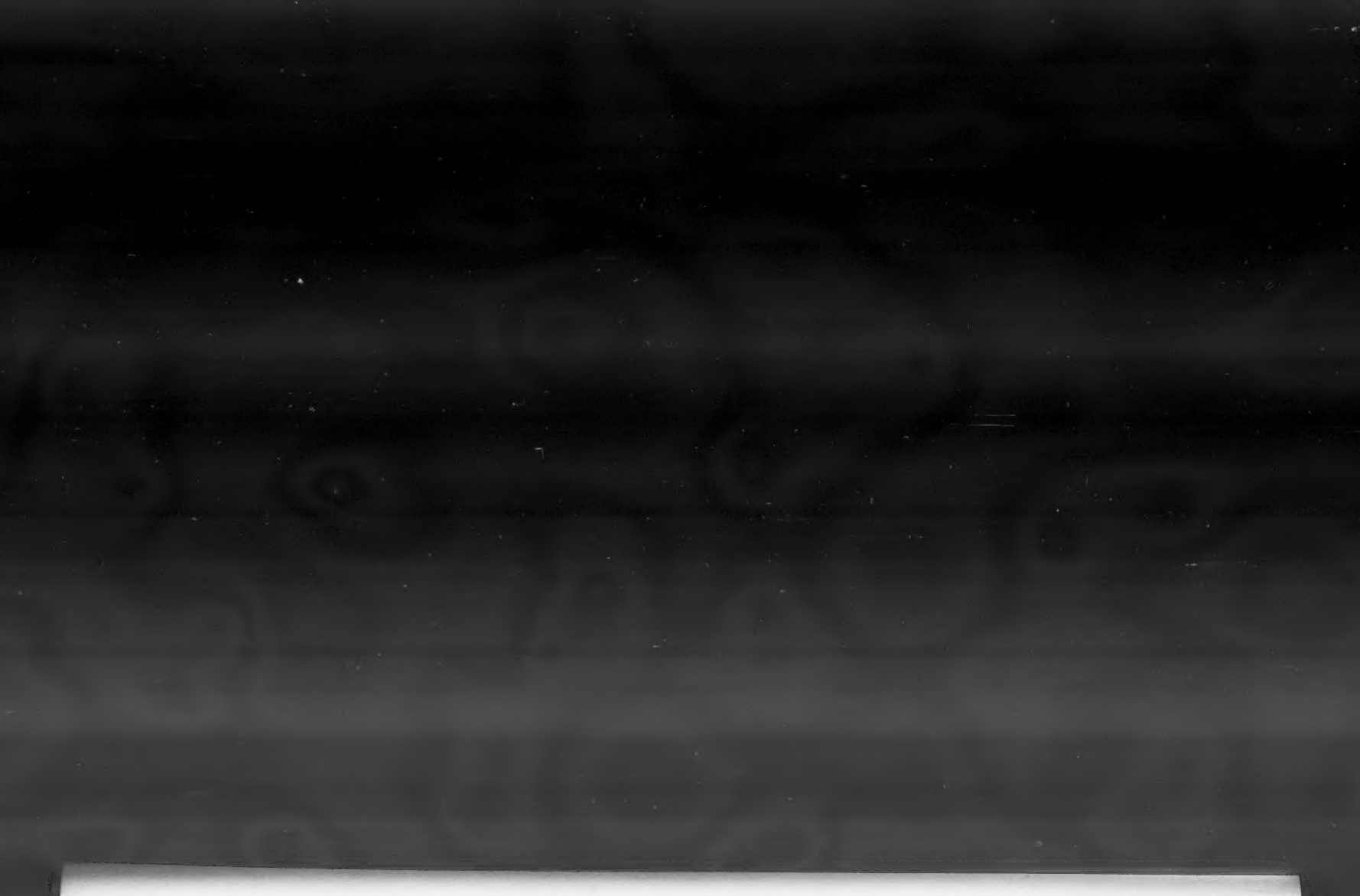

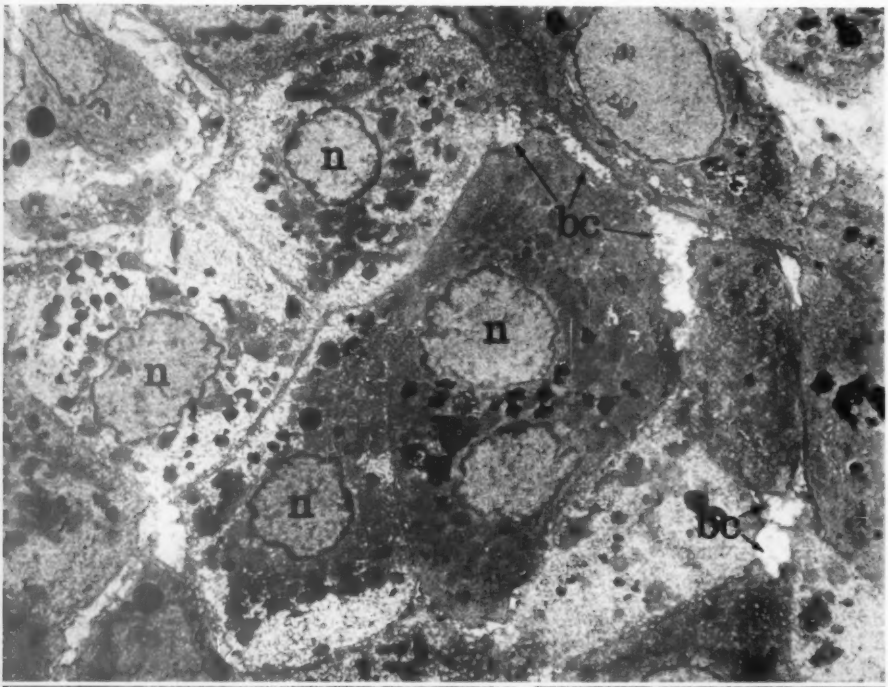

1

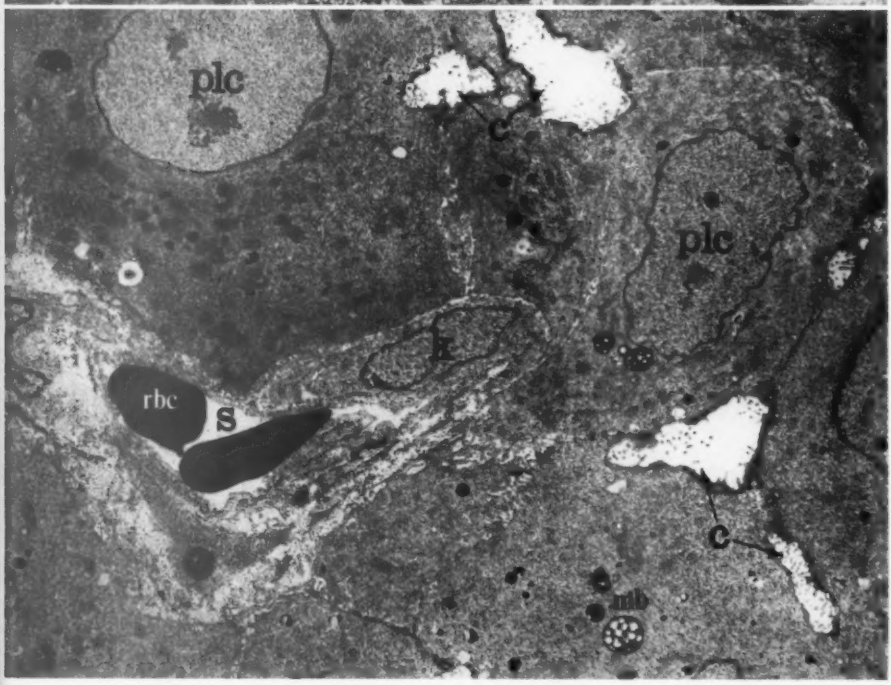

2

FIG. 3. Intrahepatic biliary obstruction. Two adjacent dilated bile canaliculi with a marked reduction of their microvilli. The lumens contain a granular argentophilic material. Note the complex structure and increased number of peribiliary lipid bodies. Protargol stain. × 5,600.

FIG. 4. Intrahepatic biliary obstruction. The microvilli which project into the dilated lumen of the bile canaliculus are stunted and distorted. The inspissated bile is seen as a faintly diffuse argentophilic cloudlike substance with a scattering of electron-dense particles. Protargol stain. × 9,800.

FIG. 5. Biliary cirrhosis. A dilated bile canaliculus containing a granular, faintly electron-dense substance in addition to an embolus of marked but variable argentophilia. The microvilli of the canaliculus are reduced in number, stunted and often distorted. Protargol stain. × 10,000.

FIG. 6. Congenital biliary atresia. The lumen of a bile ductule with reduced and stunted microvilli is seen. The biliary epithelium around the lumen contains several lipid bodies. One of these appears to have been extruded into the lumen where several small lipid emboli are present. Protargol stain. × 20,000.

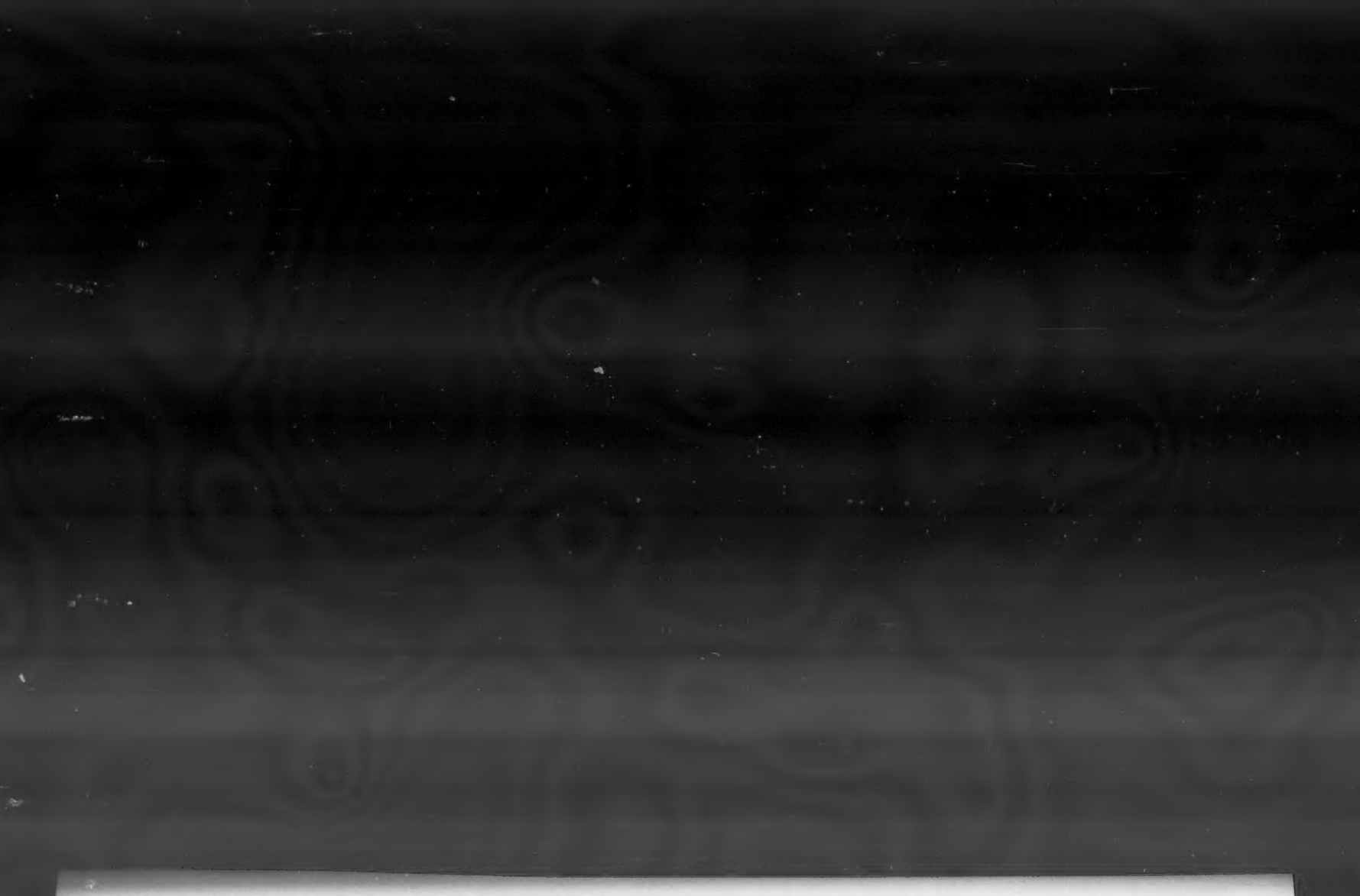

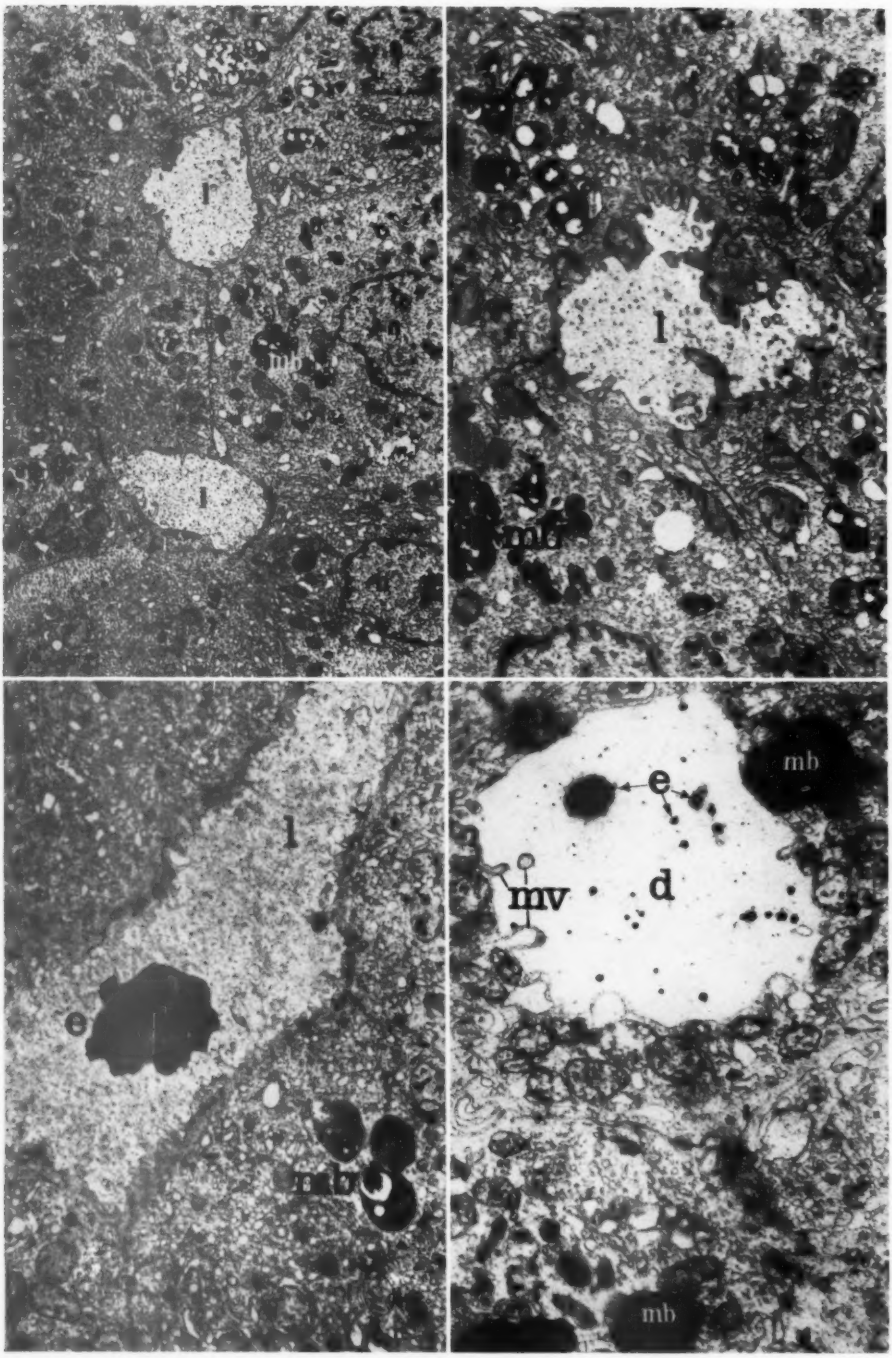
l
mb
l
3
l
mb
4
l
e
mb
5
mb
e
mv
d
mb
6

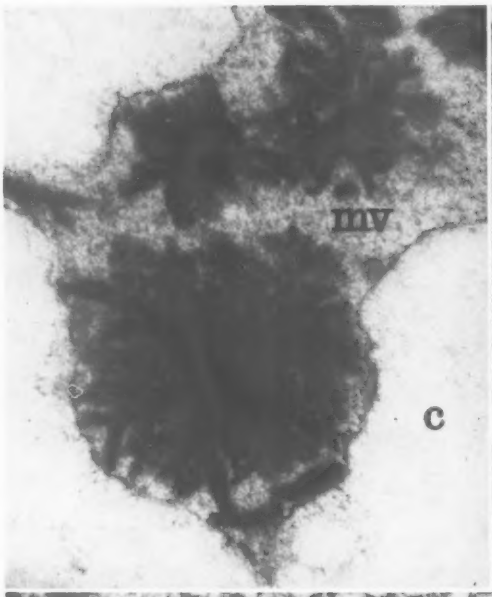

7

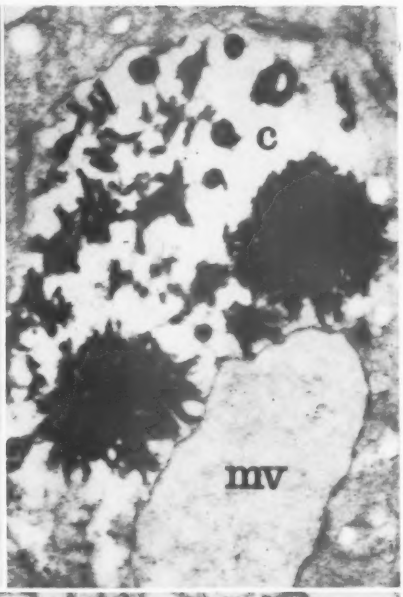

8

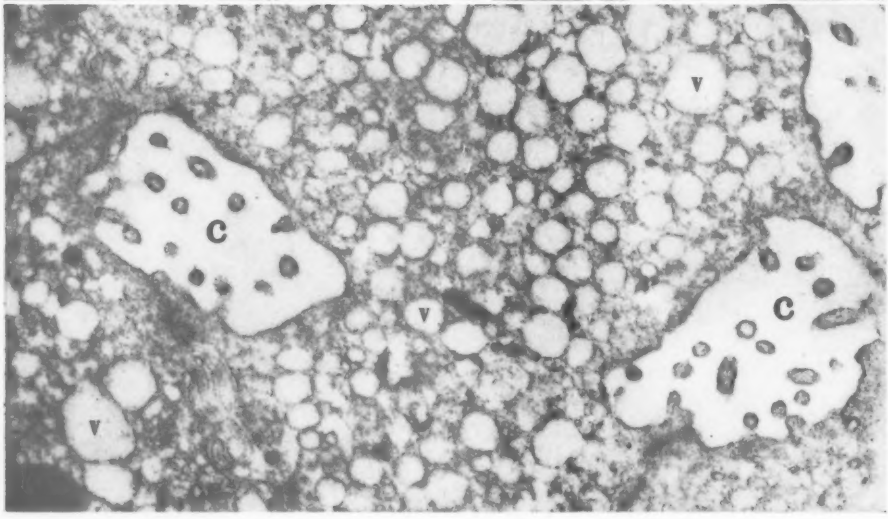

9

FIG. 7. Congenital biliary atresia. Needle-shaped crystals within a bile canalicular microvillus. These are interpreted as representing cholesterol. Phosphotungstic acid stain. × 59,200.

FIG. 8. Intrahepatic biliary obstruction. Needle-shaped crystals and ring forms of these in the lumen of a bile canaliculus containing also a large edematous microvillus. The material is interpreted as representing cholesterol. Phosphotungstic acid stain. × 29,600.

FIG. 9. Experimental immunologic liver injury (72 hours following the injection of soluble immune aggregates into the portal vein). Diffuse hydropic (vacuolar) degeneration is manifest in parenchymal cells. The two bile canaliculi show no changes in their microvilli. Phosphotungstic acid stain. × 24,640.

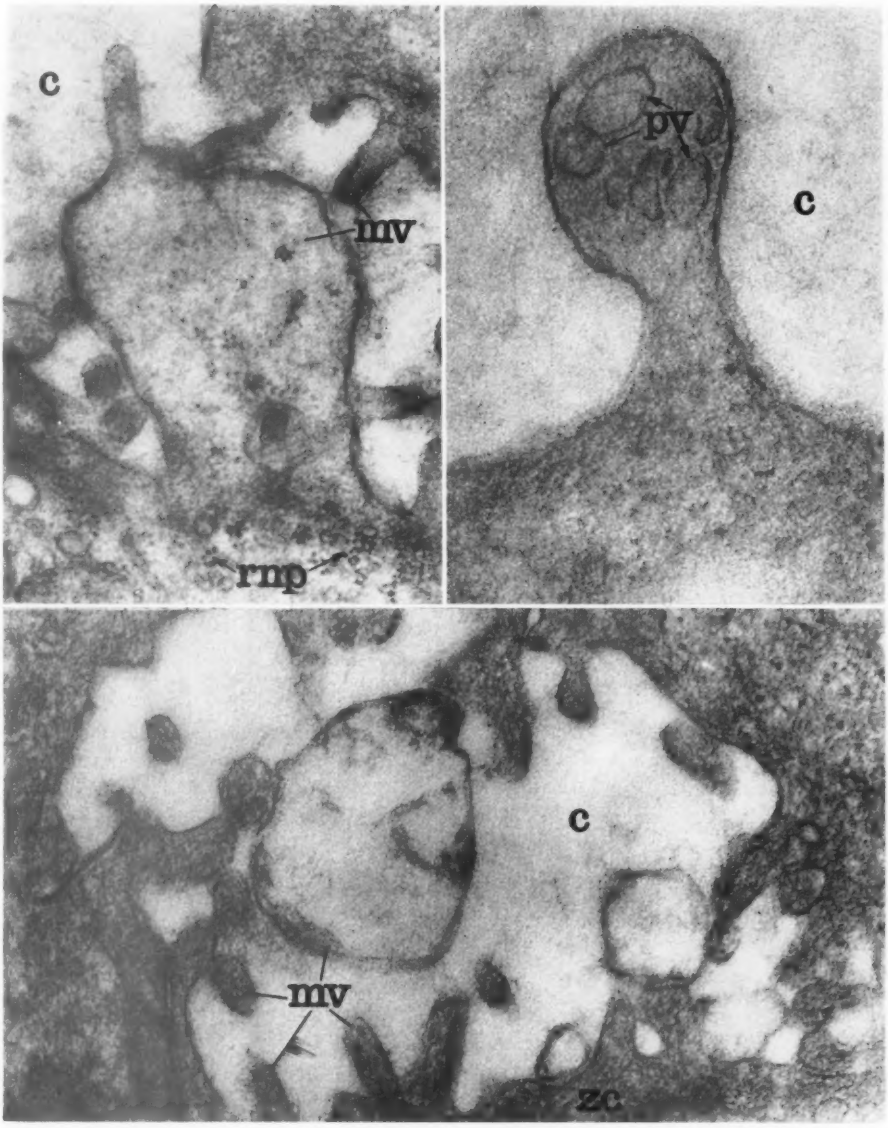

10 11 12

FIG. 10. Experimental extrahepatic biliary obstruction (2 days). Edema of a microvillus commencing at its base and as yet not involving the extremity. Neighboring microvilli are of average size. Lead hydroxide stain. × 47,260.

FIG. 11. Experimental extrahepatic biliary obstruction (2 days). Early edema of the extremity of a microvillus with a relatively normal waist. Note the presence of smooth-surfaced vesicles in the matrix of the microvillus. Lead hydroxide stain. × 69,500.

FIG. 12. Experimental extrahepatic biliary obstruction (3 days). Ballooned microvilli are cross-sectioned in the lumen of an apparently empty canaliculus with other intact microvilli in other parts of the lining. Note the zone of condensed cytoplasm adjacent to the canaliculus. Lead hydroxide stain. × 58,380.

FIG. 13. Portal cirrhosis. Edematous microvilli almost totally occlude the lumen of a bile canaliculus; others are stunted. The adjacent cells show no evidence of hydropic (vacuolar) degeneration. Protargol stain. × 7,840.

FIG. 14. Intrahepatic biliary obstruction. The canaliculus in the center of the electron micrograph is almost totally occluded by a massively edematous microvillus and several others less severely affected. Note the absence of hydropic (vacuolar) degeneration in adjacent parenchymal cells. Protargol stain. × 8,400.

FIG. 15. Biliary cirrhosis. A partially occluded bile canaliculus. The microvilli are partly edematous and many are markedly distorted. Note the densely argentophilic granules representing glycogen in the cytoplasm. They are not present in the mitochondria. A few are located within the lumen. Periodic acid-silver methenamine stain. × 13,440.

FIG. 16. Intrahepatic biliary obstruction. Markedly edematous microvilli project into a lumen which contains a diffuse, faintly electron-opaque substance. Note the particles of glycogen in the cells and in the lumen. Periodic acid-silver methenamine stain. × 16,800.

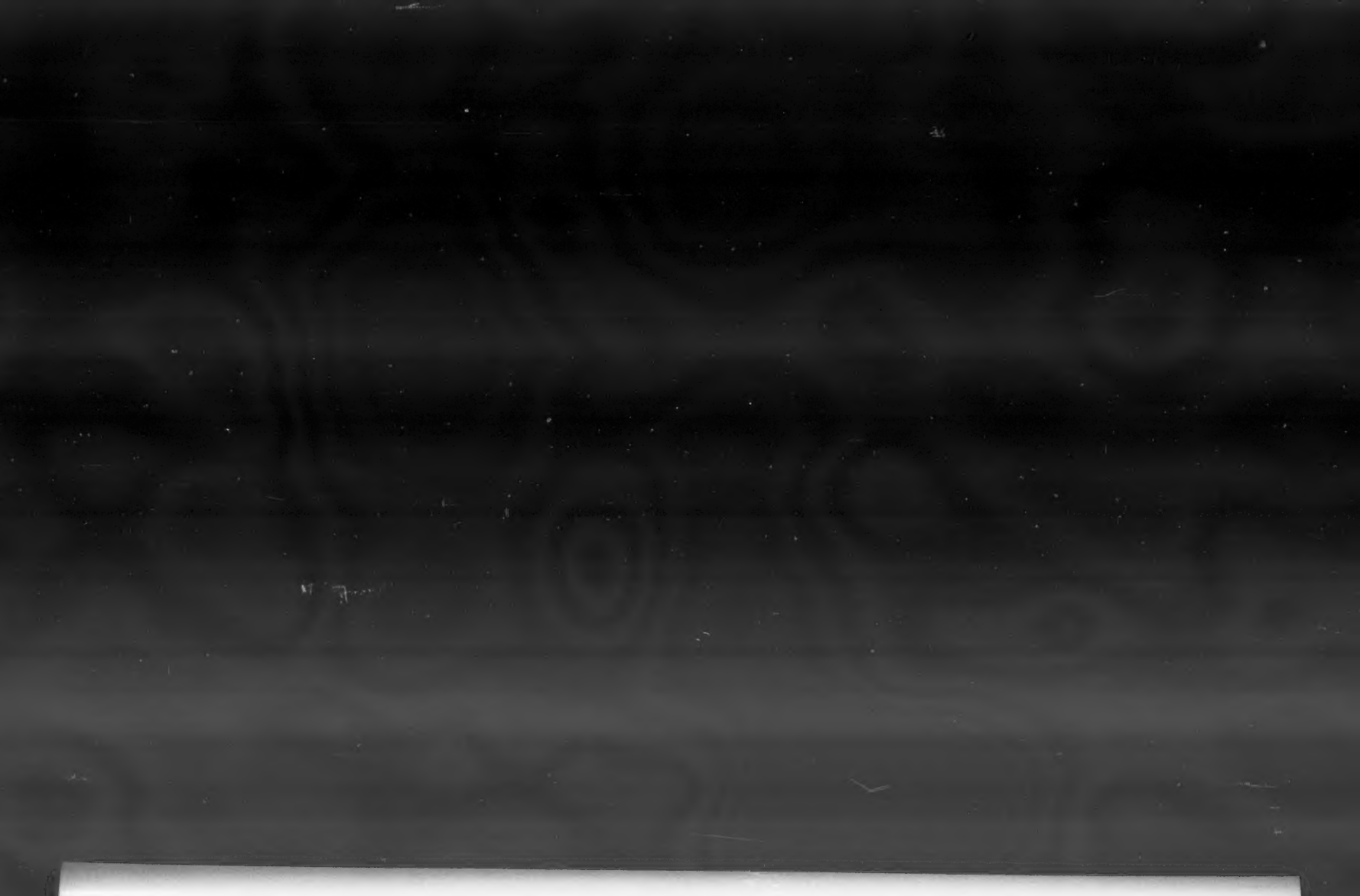

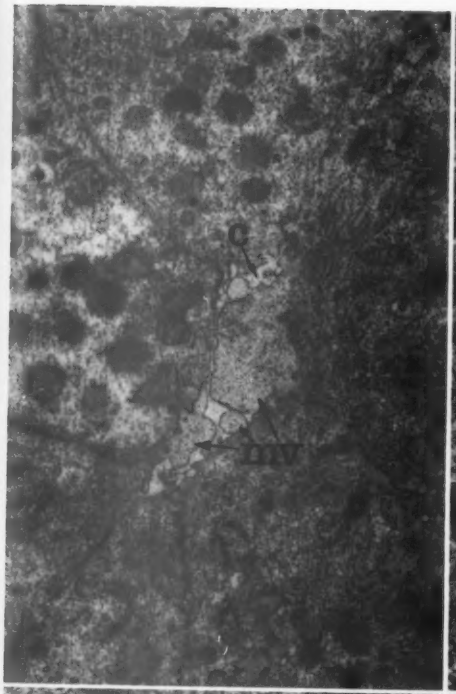

13

14

15

16

FIG. 17. Congenital biliary atresia. Mitochondria of a parenchymal liver cell show distortion of over-all shape, elongation of some cristae mitochondriales and a "ring" form in the mitochondrion in the right upper corner (arrow). Protargol stain. × 20,800.

FIG. 18. Portal cirrhosis. A mitochondrion in a cell in the vicinity of an altered bile canaliculus. Note the irregular enlargement of the dense body in the mitochondrial matrix. Lead hydroxide stain. × 73,600.

FIG. 19. Intrahepatic biliary obstruction. An abnormal mitochondrion shows a ring-shaped crista and others which are elongated and abnormally oriented. Phosphotungstic acid stain. × 68,200.

FIG. 20. Biliary cirrhosis. An abnormal mitochondrion with elongated tortuous cristae mitochondriales. The fine black precipitate is an artifact caused by staining. Lead hydroxide stain. × 59,400.

17
19

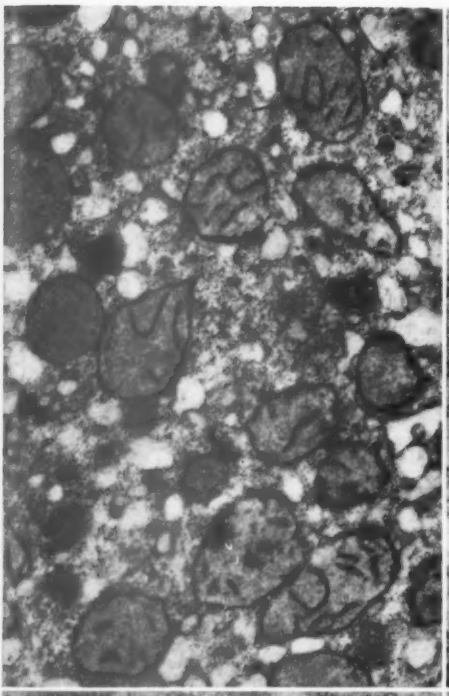

17

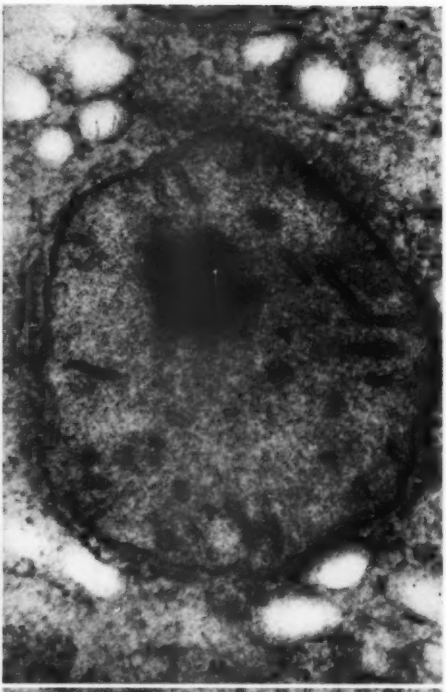

18

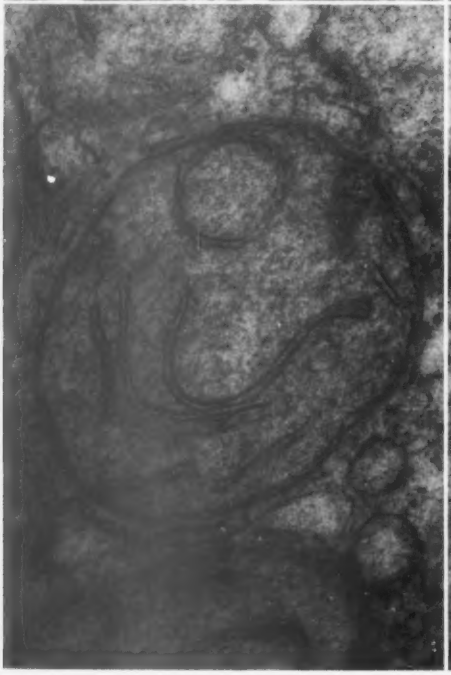

19

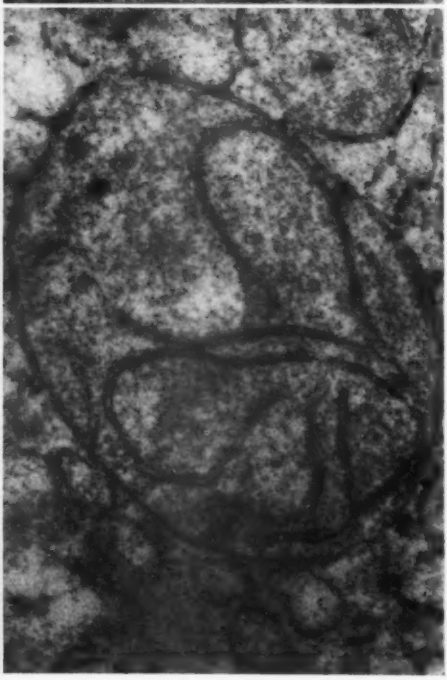

20

FIG. 21. Congenital biliary atresia. A large edematous microvillus is obstructing the lumen of a bile ductule. Very few apparently normal microvilli can still be recognized. Protargol stain. × 10,800.

FIG. 22. Biliary cirrhosis. A portion of the orifice of a dilated bile pre-ductule is seen on the right. The pre-ductule can be recognized since part of its lining is formed by a biliary epithelial cell. Note the different mitochondria in the latter epithelium (arrows) as compared to parenchymal cells. A liver cell adjoins a portal tract in which cytoplasmic processes of fibroblasts can be recognized. Note that the parenchymal liver cell is provided with microvilli on all its surfaces, including that which faces the portal tract. These are thought to constitute a possible pathway of aberrant bile secretion. Protargol stain. × 9,600.

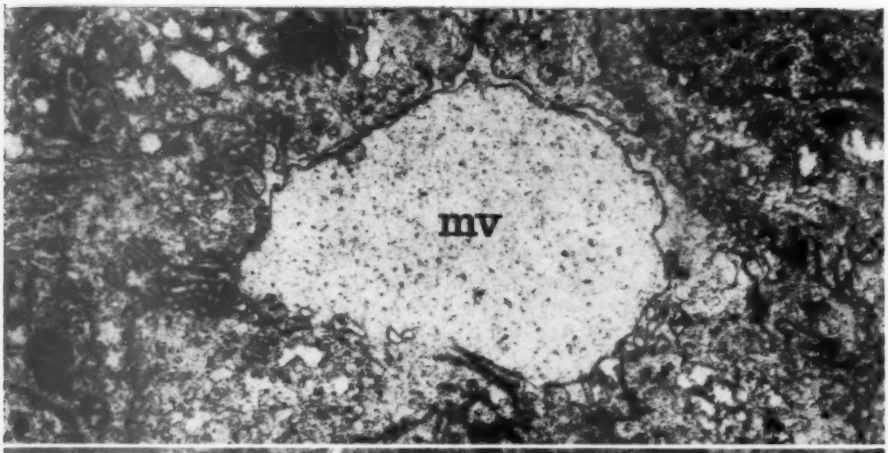

21

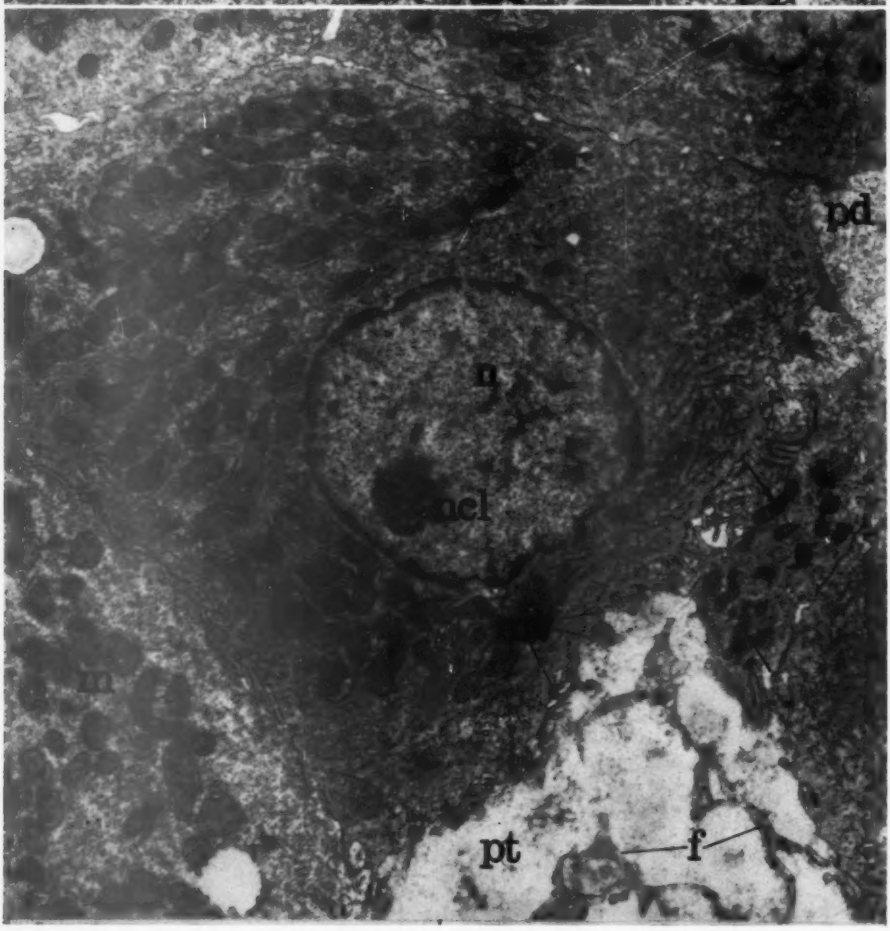

22

DEPOSITION OF GLOBULAR LIPID IN ARTERIAL CELLS IN RELATION TO ANOXIA

KENDAL C. DIXON, M.D., PH.D.

From the Department of Pathology, Cambridge University, Cambridge, England

Intracellular deposition of visible droplets of liquid lipid is frequently initiated by anoxia. Anoxic cells lack the capacity to synthesize protein and phospholipid and therefore may not be able to emulsify and disperse the fat which they contain.[1] This paper considers anoxia as a possible determinant of fatty deposition in the intimal cells of arterial walls and records observations on the content of protein in these lipid-laden cells. A brief account is also given of some of the factors which determine fatty deposition in general, by affecting the physical state of cellular fat.

STATE OF CELLULAR FAT

In the healthy cells of many tissues, such as liver, kidney, cardiac muscle and arterial walls, fat is dispersed in an invisible state. This invisible fat may be held inside laminar micelles formed by orientated molecules of phospholipid covered by an adherent film of protein.[1] Fat in this dispersed state has neither the optical nor the solvent properties of a liquid and is masked or concealed in the cells; it may conveniently be called *micellar fat*. Cells, which in health contain no visible fat, may in illness contain droplets of liquid fat in abundance. This fat, like that of the lipocytes, dissolves the nonpolar Sudan dyes and has the physical properties of a liquid. It is not masked by dispersion, is plainly visible by microscopy as spherical droplets, and gives the tissues a creamy or fatty appearance. It is conveniently called *globular fat*.

Micellar and globular fat differ greatly in their cellular reactivity.[1] Micellar fat is the form which takes part in metabolism and transport. Globular fat is in a phase apart from these activities and must be converted into micellar fat, with which it is in equilibrium, before it can be utilized or mobilized from the cell. The dominant position of micellar fat in cellular economy is indicated in Text-figure 1.

Fatty Deposition in Disordered Cells

Deposition of visible droplets of fat inside cells consists in the transition of invisible or concealed [2] micellar fat into the visible globular form.

Accepted for publication, March 10, 1961.

This transition occurs[1] firstly when the susceptibility to dispersion is impaired, as by deficiency in phospholipid or protein, and secondly when fat accumulates to such an extent that it cannot be held in the micellar state. Thus when, either by deficiency in emulsifying agents or by excess of fat, a certain ratio of fat to emulsifiers is surpassed, visible globular fat is aggregated or deposited inside the cell.

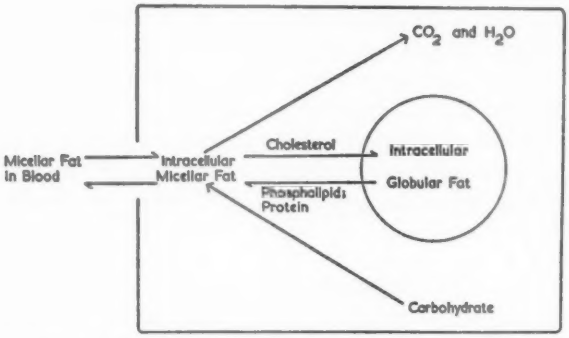

TEXT-FIGURE 1. Intracellular equilibrium between micellar and globular fat.

There are, thus, two basic determinants of fatty deposition in disordered cells: (a) interference with micellar dispersion of fat; and (b) increase of intracellular fat to an extent which cannot be held in the micelles.

Interference with Micellar Dispersion. Lack of phospholipid and protein,[3] which are essential constituents of the micelles, and excess of cholesterol, which antagonizes[4] the emulsifying action of phospholipid, alike cause fatty deposition by interfering with micellar dispersion.[1] Anoxia is probably an important determinant of intracellular lack of phospholipid and protein, since the synthesis of these substances is dependent on oxidative phosphorylation; anoxia is responsible for the intense fatty deposition in heart failure and anemia. Excess of cholesterol, as in diabetes, probably interferes with dispersion of fat and thus accounts for fatty change in the liver and arterial walls, so conspicuous in this disease.

Increase of Intracellular Fat. Excess of fat to an extent which cannot be held in the dispersed micellar state arises by (a) increased entry of fat into the cell, which follows excessive mobilization from the depots in starvation and wasting diseases; and (b) diminished removal of fat from the cell. This may result from defective oxidation or from defective mobilization. Actually both oxidation and mobilization may be inhibited by interference with dispersion, since micellar fat is the reactive form

which takes part in both these processes (Text-fig. 1). Thus, defective dispersion, which itself causes deposition of visible fat, also promotes increase of intracellular fat. This in turn accounts for further deposition.[1] Even when fat is not entering the cell as such, inhibition of removal causes accumulation, since fat is formed *de novo* in the cell from carbohydrate (Fig. 1).

The determinants of fatty deposition inside the cells of arterial walls are likely to be the same in principle as those outlined above for disordered cells in general. The zonal prominence of lipid-laden cells in the intima, moreover, suggests that anoxia may be an important factor in promoting deposition. Since anoxia would result in intracellular lack of protein as well as lack of phospholipid, a study was made of the content of protein in the lipid-laden cells of the intima.

Material and Methods

The location of protein and fat was studied in atheromatous plaques and lipoid spots of human arterial walls (aorta, subclavian and coronary arteries). Necropsy material from 5 patients (men aged 50 and 75, and women 54, 78 and 83 years) suffering from coronary atheroma was examined. Each piece of affected vessel wall containing lesions was divided into two parts, one of which was fixed in Carnoy's fluid and the other in formol-saline. The tissues fixed in Carnoy's fluid were then embedded in wax; sections were cut, mounted on slides without adhesive, and stained by the oxidized tannin-azo (OTA) method [5] for protein. The techniques of fixing, embedding and staining by OTA were the same as those used earlier [5] except that the time of immersion in cold buffered diazotized o-dianisidine (after tanning and oxidation) was increased from 10 to 20 minutes. Sections of the tissues fixed in Carnoy's fluid were also stained by hematoxylin and eosin. Fat was demonstrated in the tissues fixed in formol-saline: for this purpose, frozen sections were cut and stained with a mixture of Sudan III and Sudan IV (saturated solution of the two dyes in 70 per cent ethanol), Carazzi's hematoxylin being employed as a counterstain. Frozen sections of lesions in 9 different vessels and wax sections from lesions in 8 different vessels were examined after staining by the various techniques employed.

Results

Fusiform, stellate or spherical cells filled with droplets of lipid were visible in the intima in all the arterial lesions examined (Figs. 1 and 2). These large fatty cells were confined to the intima; they abutted the internal elastic lamina in some of the lesions, but subendothelial and mid-intimal aggregations of fatty cells were also encountered. Only very occasional minute fusiform fatty cells were visible in the media. Extracellular and intrafibrillar droplets of fat were also seen; this fat occurred in finer droplets and appeared to be more diffuse than the intracellular fat. Moreover, some of the extracellular and intrafibrillar droplets were present in the media as well as in the intima, although the intimal deposits were much more substantial. Intracellular fat was almost entirely restricted to the intima.

With the OTA method the intimal fatty cells appeared foamy, and their cytoplasm contained little tannophilic protein (Figs. 3 to 6). In contrast, the surrounding collagen and vascular endothelium were rich in protein stainable by OTA. The internal elastic lamina (Figs. 5 and 6) and the elastic fibers of the media were uncolored by OTA; the rest of the media was intensely stained. Extracellular droplets of lipid appeared as foamy material only faintly colored by OTA. The foam cells with scanty protein were entirely intimal in location. In one lesion, foam cells rich in protein were seen around extravasated plasma.

Discussion

The purpose of this paper is not to consider the cause of atheromatous thickening which has been discussed so fully in recent years,[6-8] but to focus attention on the process of fatty deposition within the intimal cells.

An admirable account of the cellular deposition of visible lipid in arterial walls was given by Virchow.[9] He emphasized that droplets of lipid first appeared inside the cells of intimal connective tissue: the fatty cells occurred both in superficial whitish spots (*weissliche Flecke*) and in the depths of atheromatous foci (*Heerde*). Hueper[7] suggested that there was, indeed, no fundamental distinction between the genesis of these lipid spots and the more deeply situated atheromatous plaques; at any rate connective tissue cells bloated with droplets of liquid lipid and containing scanty protein occur in both types of lesion (Figs. 3 and 6). The cells containing the fatty droplets may be elongated (Fig. 1), stellate or spherical (Fig. 2); they thus vary from the spindle-shaped and stellate elements (*spindel-oder sternförmig*) to the spherical granular cells (*rundlichen Körnchenzellen*) so graphically described by Virchow.

The determinants of fatty deposition in these intimal cells are probably very similar to those responsible for intracellular fatty change in general. Indeed, Virchow[9] regarded the initial fatty change (*Fettemetamorphose*) in intimal cells as in no wise different (*absolut nicht verschieden*) from fatty alterations which he had already described in the cells of other tissues. Recently, Geer, McGill, Strong and Holman,[10] using electron microscopy, found droplets of fat in the muscle cells of atheromatous arteries, and they suggested that fat was formed as the result of metabolic processes in the cells.

The most remarkable feature of fatty change in the cells of arterial walls is its zonal character. The usual outer limit of intense intracellular fatty deposition is the internal elastic lamina. Outside this membrane, deposition is absent (Fig. 1) or much less intense. In atheromatous plaques the cells containing the most abundant droplets of lipid are often

situated in the outer intima just internal to the elastic lamina. This zonal disposition of fatty cells, moreover, indicates that the droplets of fat have an intracellular origin and that they do not arise by ingestion of extracellular deposits which would form in a more random manner. Extracellular lipids may arise from disintegration of lipid-laden cells.

There is, indeed, a striking resemblance between the zonal distribution of lipid-laden cells in arterial walls and the zonal limits of visible lipid in the liver and heart when globular fat appears in these organs. The deposition of fat in hepatic lobules is frequently determined by relative anoxia of the centrally situated cells; in these cells fatty deposition is most prevalent, since in them the relatively low tension of oxygen probably interferes with synthesis of protein and phospholipid necessary for the dispersion of fat. Similarly, in the heart, the muscle fibers close to the cavities are those most prone to anoxia, and these fibers are also most affected by fatty deposition in disease.[11]

It seems likely that relative anoxia alone determines the zonal distribution of visible lipid in arterial disease. In normal arterial walls the vasa vasorum supply the adventitia and penetrate the media; but the intima is usually devoid of blood vessels. Hueper [6] supposed that arteriosclerosis could be caused by ischemic hypoxia, which interfered with the oxidative metabolism and nutrition of the vascular wall and was followed by increased permeability with infiltration by constituents of the plasma. Dible [12] also emphasized that the deeper layers of the intima were deficient in vascular supply and designated the internal elastic lamina as a barrier to vascularization of the intima. It is now suggested that ischemic anoxia is the principal determinant of fatty deposition within the intimal cells.

Defective oxygenation may cause fatty deposition by interference with the synthesis of protein and phospholipid. Both of these substances are necessary for the micellar dispersion of fat, and their synthesis is dependent on oxidative phosphorylation within the cell. Phospholipid appears to be absent from the hydrophobic lipids of intimal macrophages.[13] The observations recorded above show that the cytoplasm of the fatty intimal cells contains hardly any tannophilic protein (Figs. 3 to 6). This lack of protein is not a universal characteristic of all fatty cells, since abundant tannophilic protein is present in fatty hepatic cells of rats poisoned by carbon tetrachloride (unpublished observations). Loss of protein is therefore not an obligatory sequel to fatty deposition. Many of the intimal fatty cells, indeed, contain so little protein that it seems reasonable to suppose that lack of protein interferes with micellar dispersion and is thus the determinant of the deposition of globular fat. Moreover, the transition of micellar to globular fat (Text-fig. 1) would

interrupt utilization and so promote accumulation of excessive fat which may in turn lead to further deposition.

Interference with dispersion may even promote accumulation when no fat is entering the cell as such, since fat may be formed *de novo* in the cell from carbohydrate (Text-fig. 1). This cycle of events initiated by anoxia would thus result in the formation of lipid-laden cells containing scanty protein which are confined to the intima.

This view of the deposition of globular lipid in the intimal cells accords well with the conditions which are known to predispose to atheroma. Firstly, in the aging or hypertensive patient, narrowing of the vasa vasorum and reduplication of the internal elastic lamina would tend to increase intimal anoxia and so cause intracellular deficiency in protein and phospholipid. Secondly, the attachment of mural thrombi [14,15] and also subsequent organization [15] would impede oxygenation of the intimal cells and so promote deposition. Finally, in diabetes, excessive amounts of cholesterol may antagonize the emulsifying action of phospholipid,[4] and this would be likely to affect most severely the intimal cells, where lack of oxygen diminishes the available phospholipid and protein. In all these instances interference with intracellular dispersion of fat may thus herald fatty deposition in the intimal cells.

Summary

Fatty deposition or aggregation consists in the appearance of visible droplets of liquid lipid in disordered cells which in health contain no visible fat. This change involves the transition from micellar fat, which is dispersed and invisible in the cell, into globular fat, which has all the physical properties of a liquid lipid. Fat appears as visible droplets firstly, when its susceptibility to dispersion is impaired, and secondly, when it accumulates to such excess that it can no longer be dispersed completely by phospholipid and protein in the micellar form. Moreover, since undispersed globular fat cannot be oxidized or mobilized from the cell, interference with dispersion may itself promote accumulation and thus herald further deposition of visible droplets of fat. Thus, deposition may occur even when no fat is entering the cell, since fat can be formed within the cell from carbohydrate.

Protein and phospholipid are essential intracellular emulsifiers for the dispersion of fat in the micellar state. Lack of these substances within the cells thus promotes deposition of globular fat. Since intracellular oxidative phosphorylation is necessary for the synthesis of both protein and phospholipid, anoxia is likely to be a basic determinant of fatty deposition.

In arterial walls the cytoplasm of lipid-laden cells (in atheromatous

plaques and lipoid spots) contains but little tannophilic protein. It is suggested that this intracellular lack of protein coupled with lack of phospholipid is responsible for the appearance of fat.

Lipid-laden cells with scanty cytoplasmic protein are confined to the intima of arteries. This zonal distribution of fatty cells in the most anoxic region of the arterial tissue suggests that anoxia may be the underlying cause of lack of protein and lack of phospholipid, which in turn lead to fatty deposition in atheroma.

References

1. Dixon, K. C. Fatty deposition: a disorder of the cell. *Quart. J. Exper. Physiol.*, 1958, **43**, 139–159.
2. Masson, P. Tumeurs humaines: Histologie—diagnostics et techniques. N. Maloine, Paris, 1956, ed. 2, p. 10.
3. Best, C. H.; Hartroft, W. S.; Lucas, C. C., and Ridout, J. H. Effects of dietary protein, lipotropic factors, and re-alimentation on total hepatic lipids and their distribution. *Brit. M.J.*, 1955, **1**, 1439–1444.
4. Corran, J. W., and Lewis, W. C. M. Lecithin and cholesterol in relation to the physical nature of cell membranes. *Biochem. J.*, 1924, **18**, 1364–1370.
5. Dixon, K. C. Oxidized tannin-azo method for protein in tissues. *Am. J. Path.*, 1959, **35**, 199–211.
6. Hueper, W. C. Arteriosclerosis. *Arch. Path.*, 1944, **38**, 162–181; 245–285; 350–364.
7. Hueper, W. C. Arteriosclerosis. *Arch. Path.*, 1945, **39**, 51–65; 117–131; 187–216.
8. Florey, H. Coronary artery disease. *Brit. M.J.*, 1960, **2**, 1329–1335.
9. Virchow, R. Die Cellularpathologie in ihrer Begründung auf physiologische und pathologische Gewebelehre. A. Hirschwald, Berlin, 1858, pp. 309–310; 327–328.
10. Geer, J. C.; McGill, H. C., Jr.; Strong, J. P., and Holman, R. L. Electron microscopy of human atherosclerotic lesions. (Abstract) *Fed. Proc.*, 1960, **19**, 15.
11. Dible, J. H. Is fatty degeneration of the heart muscle a phanerosis? *J. Path. & Bact.*, 1934, **39**, 197–207.
12. Dible, J. H. Atheroma. In: Pathogenesis and Treatment of Occlusive Arterial Disease; the Proceedings of a Conference Held in London at the Royal College of Physicians of London, 13–14 Nov., 1959. McDonald, L. (ed.). Pitman Medical Publishing Co., Ltd., London, 1959, pp. 7–9.
13. Adams, C. W. M. Role of lipids of aortic elastic fibres in atherogenesis. *Lancet*, 1959, **1**, 1075–1076.
14. Rokitansky, C. A Manual of Pathological Anatomy. Day, G. E. (tran. Sydenham Society, London, 1852, Vol. 4, p. 272.
15. Duguid, J. B. Thrombosis as a factor in the pathogenesis of cor atherosclerosis. *J. Path. & Bact.*, 1946, **58**, 207–212.

The author wishes to thank Dr. A. M. Barrett for the postmortem material, A. J. King for technical assistance and S. W. Patman for the photomicrography.

[*Illustrations follow*]

Legends for Figures

Fig. 1. Elongated intimal cells situated inside the internal elastic lamina (which crosses the field) are filled with droplets of globular lipid stained by Sudan III and IV. The media outside this lamina contains no fatty cells. Subclavian artery. ×400.

Fig. 2. Stellate and spherical intimal cells are filled with globular lipid stained by Sudan III and IV. Coronary artery. × 400.

Fig. 3. Empty-looking intimal cells are stained for protein by the oxidized tannin-azo (OTA) method. These cells are deeply situated in thickened intimal connective tissue. The internal elastic lamina is visible at the lower edge of the field. This is the same vessel shown in Figure 2. × 400.

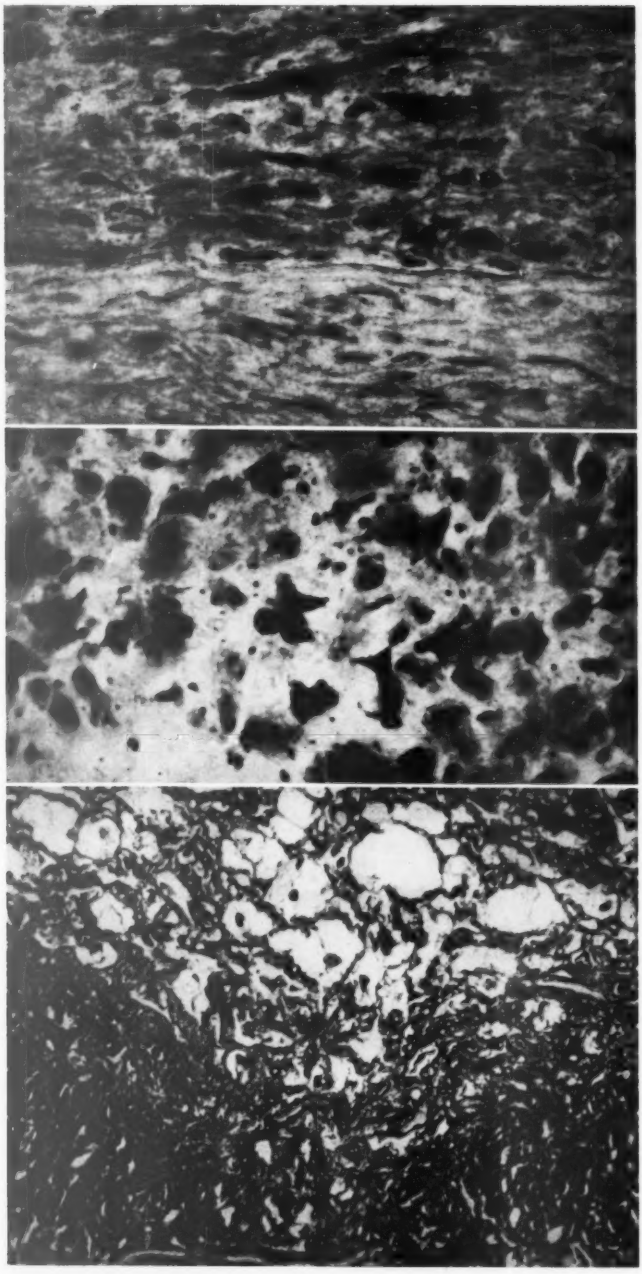

1

2

3

4

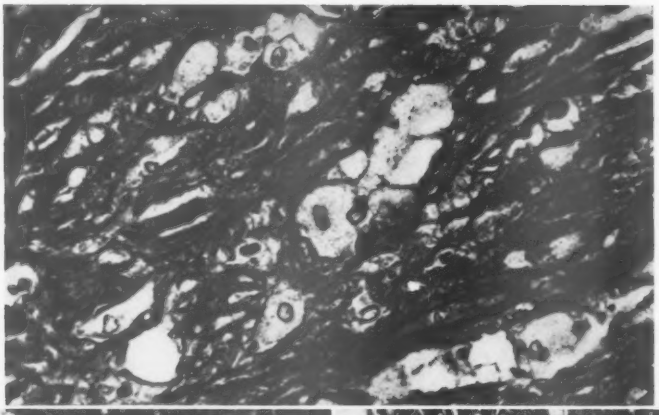

5

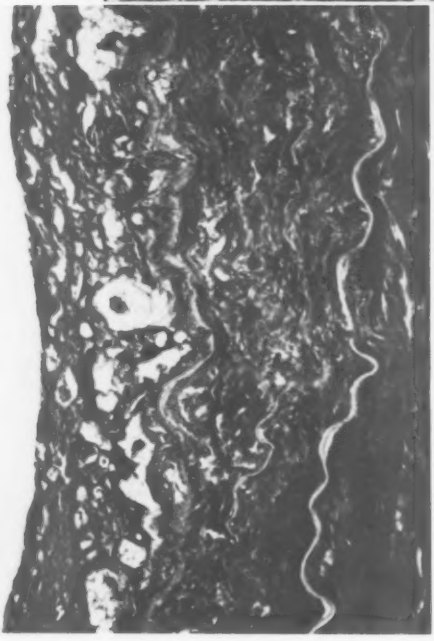

6

FIG. 4. Intimal fatty cells are stained for protein by OTA. These cells are embedded in a thickened intimal connective tissue. Their cytoplasm contains only traces of tannophilic protein. This is the same vessel shown in Figure 1. × 400.

FIG. 5. Scattered subendothelial fatty cells are stained for protein by OTA. There is little tannophilic protein in the cytoplasm of these intimal cells; but the connective tissue, except for the internal elastic lamina, contains abundant tannophilic protein. Same vessel as shown in Figure 1. ×400.

FIG. 6. A zone of more numerous subendothelial fatty cells stained for protein by OTA. Their cytoplasm is conspicuously lacking in tannophilic protein. Same vessel as shown in Figure 1. × 400.

HYPERTENSION OF THE PULMONARY CIRCULATION DUE TO CONGENITAL GLOMOID OBSTRUCTION OF THE PULMONARY ARTERIES

E. Moschcowitz, M.D.; E. Rubin, M.D.,* and L. Strauss, M.D.

From the Department of Pathology, The Mount Sinai Hospital, New York, N.Y.

Our purpose is to report a hitherto unrecognized cause of hypertension of the pulmonary circulation. Although the histologic structure of the lesion has been frequently described, there has been a wide divergence in the interpretation of the pathogenesis and significance of the lesions. With a single exception,[1] the lesion has been viewed as the result and not the cause of hypertension in the pulmonary circulation. The probability is strong, now that more attention may be paid to it, that the lesion will be reported more frequently. The fact that the 4 cases we have described were encountered within the space of a few years supports this surmise.

Case Reports

Case 1

A 7-month-old boy entered the hospital with bronchopneumonia and congestive failure. The child suddenly developed respiratory failure and died.

Necropsy Observations. The fifth fingers were shorter than normal, and there was an unusually wide separation between the first and second toes. The heart weighed 55 gm. (normal, 35.5 gm.). The right atrium was enlarged and lined by thickened endocardium. The foramen ovale was patent and bridged by a narrow fibrous band. The atrial septum was short, and a large defect was present. This constituted a combined ostium primum and a ventricular septal defect; it measured 2 cm. in diameter. As a result, a common atrioventricular canal with wide communication connected all chambers of the heart. Complete clefts were present in the septal leaf of the tricuspid and the anterior leaf of the mitral valve. The pulmonary artery was dilated, and its entire wall was thickened. The left ventricle was dilated. The ductus arteriosus was closed. The right lung weighed 70 gm., and the left, 30 gm. (normal right, 49; left, 41 gm.). There was some emphysema at the margins of the lower lobes bilaterally. The lungs were edematous and congested. Intrapulmonary arterial branches were slightly thickened and dilated. The liver was yellow, and the remaining organs were normal.

Anatomic Diagnoses. Mongolism; congenital heart disease, persistent ostium primum and common atrioventricular canal (complete form), hypertrophy of the right ventricle, thickened right atrial endocardium, patent foramen ovale, dilated and thickened pulmonary artery and branches, dilatation of the left ventricle; bronchopneumonia, pulmonary emphysema; fatty liver.

Microscopic Examination. All branches of the pulmonary artery with diameters between 210 and 278 μ showed marked thickening of the

Accepted for publication, February 17, 1961.

* Dazian Fellow.

intima and hyperplasia of the elastica. The majority of the vessels exhibited the following sequences in serial section: The most conspicuous lesion was a hernia-like projection from the lumen through an opening in the elastica. The elastica was completely interrupted at the mouth of the projection. The latter was round, somewhat smaller than the main vessel and consisted of a cellular "glomus" or plexiform structure of fine capillaries. The capillary lumens contained some red cells and a granular substance resembling fibrin. These structures were contained within vessels with thin muscular walls continuous with the muscle of a parent artery. They were covered at the periphery by a thin layer of elastic fibers (Fig. 1). In its further course, the cellular elements of the "glomus" disintegrated, and a thin-walled vessel containing blood and fibrin emerged (Fig. 2). This structure left the parent artery completely and acquired the appearance of a vein (Fig. 3). Distally, at a level well beyond the circumference of the main channel, the vessel acquired a well-defined muscular wall (Fig. 4), and if followed along its considerable length (Fig. 5), it became progressively smaller in diameter. Eventually it emptied into pulmonary alveolar capillaries.

The length of the entire vessel from "glomus" to capillaries corresponded to 54 serial sections. Not infrequently 2 branches containing "glomuses" arose from the same artery only a short distance apart. The parent artery showed medial hypertrophy and severe intimal proliferation with narrowing of the lumen. In larger arteries, having a diameter of 500 μ or more, the sequences were somewhat modified. At the site of branching, a cleft appeared in the wall, and its opening was surrounded by a much thickened intima (Fig. 6). The glomus-like structure was embedded in the media and adventitia of the parent artery and made its exit into the surrounding parenchyma (Fig. 7), soon emptying into an efferent vessel with a well-defined muscular media (Fig. 8). The latter vessel divided into smaller branches which eventually entered pulmonary capillaries. This was the invariable termination of every vessel containing a "glomus," which had been traced in serial sections. The efferent vessel thus must be viewed as an artery. We observed no arteriovenous shunts.

The main trunk of the pulmonary artery exhibited intimal proliferation 40 to 80 μ in thickness. The elastica showed no hyperplasia. The aorta was normal, and the intima of the vena cava was not sclerotic.

Comment. A boy aged 7 months with congenital heart disease (common atrioventricular canal) exhibited arteriosclerosis of the pulmonary artery. The intrapulmonary vessels of smaller caliber showed secondary branches occluded by glomoid structures which continued into efferent normal-appearing vessels, ultimately entering pulmonary capillaries.

The parent artery was the seat of severe arteriosclerosis; its lumen was considerably narrowed by intimal thickening.

Case 2

A boy aged 2 and 4/12 years was admitted on April 3, 1958. Up to 7 months the child's development had been normal. Since then his activity was progressively limited. The mother noted swelling of the ankles and eyelids, and puffiness of the face, as well as dyspnea. A thrill was felt over the apex of the heart, and a soft systolic murmur was heard over the entire cardiac area. The heart was enlarged both to the right and to the left. The second sound was split. P2 was greater than A2. The liver edge was felt 3 finger breadths below the costal margin. The femoral blood pressure was 140/100. An electrocardiogram showed right ventricular hypertrophy. A chest roentgenogram revealed globular enlargement of the heart, predominantly of the right side. An angiocardiogram demonstrated marked dilatation of the right atrium and ventricle. The child developed congestive failure; sudden cardiac arrest caused death a month after entry.

Necropsy Observations. The heart was greatly enlarged, weighing 110 gm. (normal, 56 gm.). There was enormous hypertrophy and dilatation of the right atrium and ventricle; the left heart was within normal limits of size or rather small. The pulmonary artery was wider than the aorta. The foramen ovale was closed, and there were no septal defects. The mural endocardium of the right atrium was thickened, but the cardiac valves were normal. The pulmonary artery was dilated; its intima appeared smooth to the naked eye, but the wall was thickened. This was true also of its branches. The ductus arteriosus was closed. The pulmonary veins were small. The lungs were smaller than usual, and the left lung was devoid of an interlobar fissure; the right lung had only two lobes. No bronchial abnormalities were noted. The pleura was smooth. In the right lung were a few patchy areas of atelectasis. Pulmonary vasculature was prominent on the cut surfaces of the lungs because of dilatation and thickening of the proximal intrapulmonary branches. At the periphery of the lungs this vascular prominence was absent. The liver showed pronounced lobular markings and fatty changes. The remaining viscera were normal except for congestion.

Anatomic Diagnoses. Cardiomegaly, hypertrophy and dilatation of the right atrium and ventricle; dilatation and arteriosclerosis of the pulmonary artery; chronic congestion and fatty changes of the liver; abnormal division of the pulmonary lobes.

Microscopic Examination. The wall of the aorta was 1 mm. thick and normal. The pulmonary arterial wall measured 880 μ in thickness; its intima was markedly thickened by collagen to the extent of 168 μ. The muscular and elastic coats appeared normal. The inferior vena cava exhibited appreciable collagenous thickening of the intima, an evidence of prolonged congestive failure. Serial sections of the lung were examined. Practically all of the arteries accompanying smaller bronchi with diameters varying from 340 to 1,000 μ exhibited glomoid lesions. The earliest phase was a deep indentation of the muscular wall on the intimal surface, with a break in the elastica interna. The intima in this portion of the vessel was profoundly thickened, usually with a hyaline substance almost occluding the lumen. As it penetrated beyond the wall, the vessel became a semicircular cellular whorl containing small narrow clefts less than the diameter of a red blood cell; the whole resembled a

cellular angioma (Fig. 9). When traced further by serial section, the cellular mass became progressively smaller until it disappeared by merging into the neighboring connective tissue. More often, however, the structure became much more cellular, resembling a glomus with well-defined, blood-filled capillaries. Distally a triangular space remained filled with erythrocytes (Fig. 10). Traced further, the "glomus" became progressively more fibrous and extensively hyalinized. Eventually the triangular space mentioned above merged almost abruptly into a vessel with a well-defined media that resembled a vein in structure (Fig. 11). If our observation had ceased at this point, it would have appeared as though we were dealing with an arteriovenous shunt. With further tracing, however, the vessel became progressively smaller until it was observed to become the vascular channel accompanying the next smaller bronchus; this in turn eventually merged into the pulmonary capillaries. This channel was therefore anatomically an artery and simply a continuation of the efferent vessel.

Comment. A boy aged 2 years and 4 months had all of the signs and symptoms of pulmonary hypertension. At necropsy no congenital malformation was found, but the characteristic gross lesions of hypertension of the pulmonary circulation were manifest. Microscopically, as in case 1, glomoid lesions were encountered. Here, however, the histologic structure was of greater maturity, as evidenced by more widespread fibrosis and hyalinization.

Case 3

An 11-year-old girl was known to have had a cardiac murmur since birth. Cardiac catheterization in November, 1958, revealed marked right ventricular systolic hypertension with identical pressure in the pulmonary artery (102/60). There was no gradient across the pulmonary valve, and the pressures in the right ventricle and pulmonary artery were equal to the systolic systemic pressure. A_2 was less loud than P_2, and the latter was split. There was a grade III harsh systolic murmur and a diastolic murmur along the left border of the sternum. No clubbing of the fingers was apparent. In April, 1959, operation showed a small patent ductus arteriosus which was tied. Two defects in the interventricular septum were closed. The patient died two hours later.

Necropsy Observations. The heart weighed 190 gm. (normal, 122 gm.). The right atrium was somewhat dilated, and there was slight endocardial thickening. The foramen ovale was closed. Just behind the septal leaflet of the tricuspid valve, a defect leading into the left ventricle was manifest high in the interventricular septum. Two additional defects were present lower in the septum; the largest of these measured 2.2 cm. in diameter. The infundibular portion of the right ventricle was dilated, and its wall hypertrophied. The pulmonary artery trunk exhibited marked widening and thickening, and there were many yellow intimal plaques extending into both the major and intrapulmonary branches. The latter also were dilated and thickened. The left atrium was small and lined by thickened endocardium. The pulmonary veins were dilated. The left ventricular myocardium measured 1.1 cm. in thickness. The combined weight of the lungs was 240 gm. (normal, 390 gm.). The liver was small, and the remaining organs were unremarkable.

Anatomic Diagnoses. Partial surgical repair of multiple interventricular septal defects, right and left ventricular hypertrophy; marked pulmonary arteriosclerosis with dilatation and thickening; small patent ductus arteriosus (surgically repaired); pulmonary atelectasis.

Microscopic Examination. Arteries with caliber between 600 and 900 μ showed marked collagenous thickening of the intima. There was moderate fibrosis of the media and some hyperplasia of the elastica. In serial sections many branches were occluded by glomoid structures often multiple in the same vessel at short distances apart. Proximally this was characterized by a cleft in the parent vessel wall, penetrating the media and elastica. The cleft was narrowed and sometimes almost completely filled by fibrous tissue that had become completely hyalinized. At the distal end the vessel was completely occluded by a glomoid cellular mass (Fig. 12). The vessels containing these structures were wider than in the two previous cases, and between the capillary spaces there was moderate fibrosis and often hyalinization (Fig. 13). The lumens contained eosinophilic material with the staining characteristics of fibrin. In other sections the "glomus" was observed to pass directly into a normal-appearing vessel with a well-defined thin muscular wall. The lumen contained remnants of the "glomus." This vessel, which was relatively long, became smaller and eventually entered pulmonary capillaries. Anatomically, therefore, it was an artery.

The main stem of the pulmonary artery exhibited marked collagenous thickening of the intima and occasional hyalinization. The media was thickened. Capillaries of the lung were widened, and the alveolar walls thickened.

Comment. An 11-year-old female child suffering from congenital heart disease with patent ductus arteriosus and multiple interventricular septal defects succumbed shortly after an open heart operation. The lungs were the seat of fairly advanced pulmonary arteriosclerosis. From the smaller divisions of the pulmonary arteries there arose secondary branches with advanced mural fibrosis and hyalinization. These terminated in glomoid structures showing fairly marked intercapillary sclerosis. Distally these glomoid structures merged into normal-appearing efferent vessels which terminated in pulmonary capillaries.

*Case 4**

A 24-year-old woman had been found by roentgen examination at 6 months of age to have an enlarged heart. At that time, there were systolic and diastolic murmurs in the pulmonary area, and the pulmonic second sound was accentuated. Fluoroscopic study showed a dilated pulmonary artery and moderate enlargement of both ventricles. An electrocardiogram disclosed right axis deviation. The diagnosis was patent ductus arteriosus.

* This case was previously reported by Gordon, Donoso, Kuhn, Ravitch and Himmelstein.[2]

She was admitted to the Mount Sinai Hospital for the first time in December, 1947, at the age of 19 years. On examination, prominence of the pulmonary arterial segment and widening of the smaller vessels throughout the lungs were apparent. An electrocardiogram suggested enlargement of the right ventricle. In January, 1950, the patient was again admitted. On this occasion a transient systolic murmur was heard at the apex. Cardiac catheterization was performed, and no abnormal communications were demonstrated.

In October, 1952, at 24 years of age, she was admitted to the hospital for the third time. The second sound at the apex was split, and the pulmonic second sound was also split and accentuated. There were no murmurs except in the pulmonic area, where a rough, medium-loud late systolic murmur was heard only during expiration. An electrocardiogram indicated hypertrophy of the right ventricle. A reparative operation was attempted.

The ductus was completely isolated, but before any attempt was made to ligate it, ventricular tachycardia and fibrillation developed, and death ensued soon after.

Necropsy Observations. The heart weighed 400 gm. From the left pulmonary artery (near the bifurcation) arose the ductus arteriosus, measuring 2 cm. in width and 0.8 cm. in length. It entered the descending limb of the aortic arch. The aorta contained a few irregularly placed, raised yellow subintimal elevations, 2 to 3 mm. in size. The right atrium was mildly dilated, and the foramen ovale was closed. The right ventricle was markedly hypertrophied. The left atrium was normal, but the mitral valve exhibited marked thickening of the anterior cusp along the line of closure. The left ventricle was normal. The lungs weighed 1,200 gm. The intima of the pulmonary artery was wrinkled and exhibited extreme arteriosclerosis with irregularly situated, raised smooth yellow atheromatous nodules. There were also many depressed gray foci, measuring 1 to 3 mm.

Anatomic Diagnoses. Patent ductus arteriosus, pulmonary arteriosclerosis, chronic mitral valvulitis, right ventricular hypertrophy; pulmonary congestion, thoracotomy and cardiac manipulation.

Microscopic Examination. The main stem of the pulmonary artery showed a profound arterio- and atherosclerosis. The intrapulmonary branches exhibited an unusually severe collagenous thickening of the intima and hyperplasia of the elastica. Alveolar capillaries were dilated; the walls of the alveoli were thickened, and there was patchy consolidation of the parenchyma.

Most of the intrapulmonary arteries measuring 550 and 1,500 μ in diameter contained the glomoid complexes described in the 3 previous cases. In serial sections they began as clefts in the muscular and elastic coats lined by intima with marked fibrous thickening and almost complete hyalinization (Fig. 14). After the cleft had penetrated the arterial wall, it proceeded into a glomoid structure composed of dilated capillaries separated from one another by connective tissue of considerable thickness (Fig. 15). The lumens of the glomus capillaries contained a granular substance probably composed of fibrin and erythrocytes. Distally the glomoid structure entered an efferent vessel with a normal vein-like structure. This diminished progressively in caliber until it terminated in pulmonary capillaries. In other words, anatomically this vessel was an artery (Fig. 16). Occasionally the penetrating vessel

ended in a fibrotic whorl containing tiny capillaries; this structure did not continue into an efferent vessel but melted imperceptibly into the surrounding fibrous parenchyma of the adventitia. In many instances the penetrating branch was almost occluded by hyalinization.

Comment. A 24-year-old woman with patent ductus arteriosus showed the obstruction of numerous intrapulmonary arterial branches by glomoid structures. These were profoundly fibrotic. Proximal to the structures, the vessels exhibited unusually advanced sclerotic changes; distally the continuing vessel was normal and terminated in pulmonary capillaries. The main trunk of the pulmonary artery was the seat of advanced arteriosclerosis.

Discussion

The four cases cited exhibited graded lesions of similar structure. The senescent progression of the lesions was directly related to the age of the individual. The youngest patient died at 7½ months, the second at 2 years, the third at 11 years, and the fourth at 24 years. All showed the clinical evidences of pulmonary hypertension with cyanosis, dyspnea, and congestive failure. Three patients had an accompanying congenital anomaly of the heart. In one it was a persistent ductus arteriosus; in the second, a ventricular septal defect, and in the third, a persistent common atrioventricular canal. In the fourth, a 2-year-old child, no cardiac anomaly was found, and the case was considered to be a "primary" hypertension of the pulmonary circulation. Direct proof that pulmonary hypertension existed in all 4 cases was attested by marked collagenous intimal thickening of the pulmonary artery and its branches and, in the oldest individual, by conspicuous atheroma of the pulmonary artery. Furthermore, in this patient, hypertension of the pulmonary circulation was demonstrated by cardiac catheterization. Additional corroboration was provided by dilatation and thickening of the capillaries in the walls of pulmonary alveoli.

In all instances, a distinctive vascular morphologic pattern was revealed in serial sections. Along the path of the intrapulmonary arterial divisions of small caliber, branches penetrated the muscular and elastic coat of the artery and ended abruptly either in glomoid structures or in semicircular whorls of fibroblasts containing narrow capillaries and resembling a fibro-angioma. Some of the whorls then passed into a "glomus" or merged directly into the surrounding fibrous tissue. The "glomus" completely filled the vessel lumen. Communication between the capillaries of the "glomus" and the distal continuing channel was demonstrated. In subsequent sections the vessel assumed the appearance of a normal vein which penetrated the lung for a considerable

distance, became smaller or divided and eventually merged with pulmonary capillaries. Anatomically, therefore, this efferent vessel was an artery and a continuation of the efferent vessel.

It seems obvious that the complete or nearly complete block of the subsidiary vascular channel by a "glomus" was directly responsible for hypertension of the pulmonary circulation. This was associated with pulmonary arteriosclerosis, the degree of which varied with the age of the patient. The sclerosis was manifest at the point of origin of the affected vessel, as indicated by a considerable collagenous intimal thickening which spread on either side of the opening along the wall of the parent vessel. The thickening appeared to proceed along the affected vessel distally, narrowing the lumen to almost complete obliteration. The muscular coat was thickened, although this was difficult to determine with accuracy. There was little hyperplasia of the elastica. Early the "glomus" showed little or no fibrosis. In a later stage, as in the 2-year-old child, intimal hyperplasia of the parent vessel was more intense and had undergone partial hyalinization. The glomus also exhibited intercapillary fibrosis and partial hyalinization. The fibrosis was greater in the 11-year-old child, and in the patient aged 24 the fibrosis was so intense that the intima was enormously thickened and hyalinized. The lumens in some of the smaller vessels were completely obliterated.

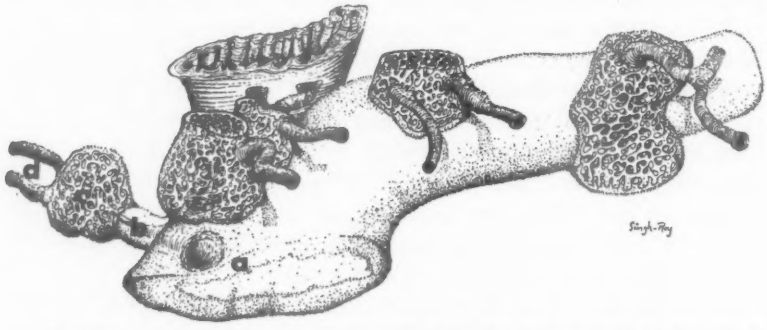

TEXT-FIGURE 1. A schematic representation indicating the anatomic relationship of glomoid structures. Drawn directly from 3-dimensional planes. (a) Parent artery. (b) Arterial branch. (c) Glomoid structure. (d) Efferent artery, which terminates in pulmonary capillaries.

Here, the glomoid structures were densely fibrotic, and the individual capillaries had been largely obliterated. In contrast, the efferent vessels in which the pressure had apparently been neutralized showed no sclerosis. Text-figure 1 is a schematic 3-dimensional representation of the lesion, derived from serial microscopic examinations.

Glomoid structures of this nature have been described repeatedly

and designated by such terms as "plexiform structures,"[3] "endothelial hyperplasia,"[4] "angiomatoid cushions,"[5] "vasoformative tissue,"[6] "recanalization of thrombi,"[7] "glomerulus-like bodies,"[8,9] and "arteriovenous shunts."[10–13] One may surmise from this diversity that their pathogenesis has been subject to varied interpretation.

The earliest pertinent description available is that of Bredt[7] in 1932, who reported a case in a woman aged 53. He believed the lesion was the result of revascularization of a thrombus. A year later Gombert[5] recorded a case in a man aged 42 with a wide foramen ovale. The glomoid structure consisted of "angiomatous endothelial cushions," the cause of which was not clear; despite the cardiac anomaly, he argued against a congenital origin. Spencer,[10] in reporting 6 cases of "primary" pulmonary hypertension, described pulmonary vascular lesions in one case of a child aged 6 with patent ductus arteriosus and foramen ovale and congenital stenosis of the pulmonary artery. His description fits that of the glomoid lesions that we have recorded. He viewed the process as an occlusive intimal proliferation with the formation of arteriovenous shunts, the result of recanalization. He admitted, nevertheless, that he saw no evidence of thrombosis distal to the points of occlusion. Rutishauser and Blanc[11] cited a boy aged 2 years with all the clinical and anatomic evidences of pulmonary hypertension but without any cardiac malformation. They considered the lesions to be arteriovenous shunts, but in a later communication, Rutishauser and Feuardent[1] retracted this view. By means of injection techniques, these authors concluded that the lesions represented congenital glomoid obliterations of the arterioles, a view which is in accord with our own.

Cross and Kobayashi[4] described a case in a 20-month-old child without cardiac malformation. They ascribed the lesion to "endothelial hyperplasia" occluding the lumens of smaller arterial branches. Kucsko[12] reported two patients with hypertension of the pulmonary circulation without congenital cardiac lesions. The first was a man aged 45 and the second, a woman aged 22; both had intrapulmonary glomoid lesions which he thought represented arteriovenous shunts. Brewer[14] described typical glomoid lesions in a 26-year-old patient with a patent ductus arteriosus; he considered the lesions to be the result of fibrous occlusions of smaller arteries with resulting anastomoses. Hufner and McNicol[13] described pulmonary vascular shunts in 3 cases; one, a child of 13 with an interventricular septal defect; a second, a child of 11 months with patent ductus arteriosus and interventricular septal defect; and a third, a child of 22 months without a congenital cardiac lesion but with other congenital defects such as hare lip and meningocele. Harrison[8] reported "glomerulus"-like bodies in a patient with an atrial

septal defect; he believed the lesions were caused by recanalization of small thrombi. Rossall and Thompson[6] recorded a 38-year-old woman with the signs and symptoms of pulmonary hypertension; the patient had two large defects in the interatrial septum. They thought the glomus-like lesions were the result of the production of "vasoformative tissue" which communicated with large angiomatoid channels terminating in capillaries. Wagenvoort[9] demonstrated glomerulus-like bodies in 10 cases; all but one occurred in individuals with communications between the systemic and pulmonary circulations. He did not observe such lesions in 40 cases of mitral stenosis. He considered the mechanism to be "hyperkinetic." McCormack[15] reported 16 instances in 38 necropsy examinations of individuals with congenital heart disease. As his report has appeared only in abstract form, a detailed review of his findings is not possible. Naeye and Vennart[16] reported 6 cases, 3 associated with patent ductus arteriosus, 2 with large interatrial septal defects and one with "primary" hypertension of the pulmonary circulation. They offered no explanation but were inclined to favor the mechanism of recanalization of thrombi. Heath and Edwards[3] described plexiform and angiomatoid lesions in lungs, associated with congenital cardiac disease, and viewed these as stages in the development of pulmonary hypertension. They related the early glomoid lesions to granulation tissue consequent to necrosis of the media.

Some of these views concerning pathogenesis may be dismissed summarily. That the lesions do not represent arteriovenous anastomoses is shown by serial section observations that the efferent vessel ultimately enters pulmonary capillaries. In other words, this vessel is a continuation of the same artery. The glomoid structures could not stem from endothelial hyperplasia because in no other bodily site, as far as we are aware, does hyperplastic endothelium form glomerular or angioma-like blood spaces. Nor is there any evidence that the bodies arise by recanalization of thrombi, first, because the affected lungs were remarkably free from thrombi, and second, because the lesion lacked entirely the morphologic characteristics of canalized thrombi. The view that the glomoid foci are inflammatory lesions secondary to necrosis of the media we believe to be untenable. First, we have never observed necrosis of the media, and second, the glomoid structure appears to be anything but inflammatory in its evolution. It is a morphologically mature structure from its very inception. A neoplastic origin cannot be excluded with certainty although biologically this is unlikely.

It seems to us that the clue to the origin of the glomoid structures is given by the following observations: They have never been observed in pulmonary hypertension secondary to mitral stenosis, emphysema, etc.

Secondly, in the overwhelming majority of cases, the lesions are associated with congenital cardiac defects. This would lead to the conclusion that they are congenital and anomalous structures. Among the few reported cases of "primary" pulmonary hypertension, one, significantly enough,[13] exhibited other extracardiac malformations. In our youngest case, the child of 7 months, the glomoid structure was morphologically a well-developed structure consisting of mature cellular capillary glomoid channels formed within a budding branch of the artery. The lumen of the affected vessel was completely filled by glomoid structure. The ultimate proof that the glomoid structures are congenital would be the demonstration of such alterations in the newly born. We venture to predict that eventually such an observation will be made.

In this interpretation, the pulmonary hypertension invariably attending this lesion is caused by the obstruction of innumerable finer intrapulmonary arterial channels. Anatomic evidence that this is so is apparent not only in the invariable association with sclerosis of major pulmonary arterial trunks, but also in the intense intimal hyperplasia that is manifest at the exit point of the efferent branch from its parent artery and throughout its course. The intense fibrosis, the hyalin transformation of the thickened intima, and the ultimate fibrosis and hyalinization of the glomoid body itself provide further support for this concept. Additional evidence is the omnipresent capillary sclerosis in the pulmonary alveolar walls, a lesion previously described in pulmonary hypertension.[17]

The 4 cases that we report nicely illustrate the time factor in the transformation of the lesions. Even in the youngest of the patients, after 7 months of postnatal life, the intimal alterations and fibrosis of the glomoid structures appear to be advanced, indicating that the degree of pulmonary hypertension was considerable, despite its brief duration.

Summary

Four cases of pulmonary hypertension are reported in which we believe the hypertension to be caused by obstruction of innumerable small branches of the pulmonary artery by glomoid lesions arising within the vessel lumens. In serial sections beyond the termination of the glomoid structures, the efferent portions of vessels exhibit some of the anatomic characteristics of veins. This is only apparent, however, because the vessel terminates in pulmonary capillaries and thus constitutes an arterial channel. Proximal to the glomoid lesions, the vessel is the seat of profound sclerosis, the intensity of which is directly related to the duration of the hypertension as measured by the age of the individual. Distal to the lesion, the vessel is essentially normal, since the intra-

vascular pressure has been neutralized. Evidence is submitted to support the belief that these glomoid structures are congenital in origin. The alterations in the 4 cases indicate progressive anatomic changes, expressive of a profound and protracted pulmonary hypertension apparently beginning at birth. Cases with glomoid lesions should not be included in the category of "primary" pulmonary hypertension.

References

1. Rutishauser, E., and Feuardent, R. Schnittrekonstruktion glomusartiger Bildungen (Anastomositis) der Lunge. *Schweiz. Ztschr. allg. Path.*, 1952, **15**, 641–644.
2. Gordon, A. J.; Donoso, E.; Kuhn, L. A.; Ravitch, M. M., and Himmelstein, A. Patent ductus arteriosus with reversal of flow. *New England J. Med.*, 1954, **251**, 923–927.
3. Heath, D., and Edwards, J. E. The pathology of hypertensive pulmonary vascular disease; a description of six grades of structural changes in the pulmonary arteries with special reference in congenital cardiac septal defects. *Circulation*, 1958, **18**, 533–547.
4. Cross, K. R., and Kobayashi, C. K. Primary pulmonary vascular sclerosis. Report of a case. *Am. J. Clin. Path.*, 1947, **17**, 155–162.
5. Gombert, H. Beiträge zur Pathologie der Vorhofsscheidewande des Herzens. (Cor triatriatum mit Verdoppelung des rechten Vorhofs. Endarteriopathia pulmonalis bei offenem Foramen ovale). *Beitr. path. Anat.*, 1933, **91**, 483–502.
6. Rossall, R. E., and Thompson, H. Formation of new vascular channels in the lungs of a patient with secondary pulmonary hypertension. *J. Path. & Bact.*, 1958, **76**, 593–598.
7. Bredt, H. Die primäre Erkrankung der Lungenschlagader in ihren verschiedenen Formen. (Arteriopathia pulmonalis idiogenica). *Virchows Arch. path. Anat.*, 1932, **284**, 126–153.
8. Harrison, C. V. The pathology of the pulmonary vessels in pulmonary hypertension. *Brit. J. Radiol.*, 1958, **31**, 217–226.
9. Wagenvoort, C. A. The morphology of certain vascular lesions in pulmonary hypertension. *J. Path. & Bact.*, 1959, **78**, 503–511.
10. Spencer, H. Primary pulmonary hypertension and related vascular changes in the lungs. *J. Path. & Bact.*, 1950, **62**, 75–84.
11. Rutishauser, E., and Blanc, W. Anastomoses artério-veineuses glomiques du poumon avec syndrome d'insuffisance droite et cyanose. *Schweiz. Ztschr. allg. Path.*, 1950, **13**, 61–65.
12. Kucsko, L. Über arteriovenöse Verbindungen in der menschlichen Lunge und ihre funktionelle Bedeutung. *Frankfurt. Ztschr. Path.*, 1953, **64**, 54–83.
13. Hufner, R. F., and McNicol, C. A. The pathologic physiology of microscopic pulmonary vascular shunts. *A.M.A. Arch. Path.*, 1958, **65**, 554–560.
14. Brewer, D. B. Fibrous occlusion and anastomosis of the pulmonary vessels in a case of pulmonary hypertension associated with patent ductus arteriosus. *J. Path. & Bact.*, 1955, **70**, 299–310.
15. McCormack, L. J. Glomoid hyperplasia of the pulmonary vasculature; a phenomenon in severe pulmonary hypertension. (Abstract) *Am. J. Path.*, 1959, **35**, 668.

16. NAEYE, R. L., and VENNART, G. P. The structure and significance of pulmonary plexiform structures. *Am. J. Path.*, 1960, **36**, 593–605.

17. MOSCHCOWITZ, E. Hypertension of the pulmonary circulation; its causes, dynamics and relation to other circulatory states. *Am. J. M. Sc.*, 1927, **174**, 388–406.

[*Illustrations follow*]

Legends for Figures

Except where indicated, photographs were prepared from sections stained by hematoxylin and eosin.

Fig. 1. Case 1. A hernia-like projection from the lumen of a small pulmonary artery which shows marked intimal thickening. The lumen of the projection is filled by a glomoid structure (a). × 110.

Fig. 2. Case 1. A succeeding stage to that shown in Figure 1. The glomoid structure has disappeared except at the periphery, and the lumen contains fibrin. × 110.

Fig. 3. Case 1. A succeeding stage to that shown in Figure 2. The glomoid structure (a) is now completely separated from the parent vessel. × 110.

Fig. 4. Case 1. A succeeding stage to that shown in Figure 3. The structure has now undergone transformation to a well-formed vessel having the appearance of a vein with well-developed media (a). × 110.

Fig. 5. Case 1. A succeeding stage to that shown in Figure 4. The normal-appearing vein-like structure (e) extends for a good distance into the pulmonary parenchyma and becomes the artery of a neighboring smaller bronchus. Eventually it becomes progressively smaller and enters pulmonary capillaries. × 110.

Fig. 6. Case 1. In arteries of larger caliber, the earliest stage is a penetration of the wall of the vessel by a small branch. At the mouth of the penetration the intima is thickened (a) and occasionally hyalinized. The branch enters a glomoid body (g) embedded in the muscular wall and adventitia. Weigert elastic tissue stain, van Gieson stain. × 110.

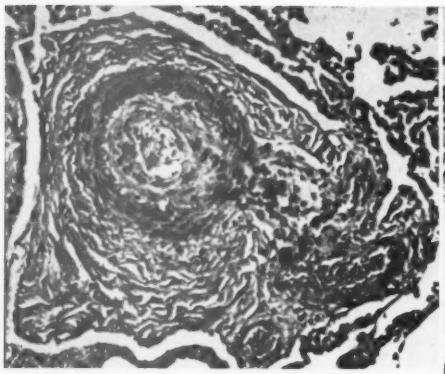

1

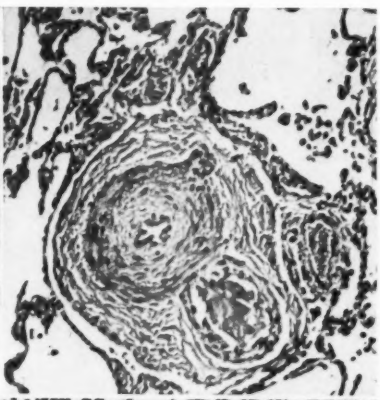

2

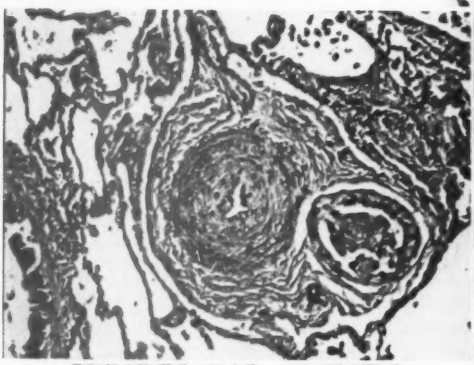

3

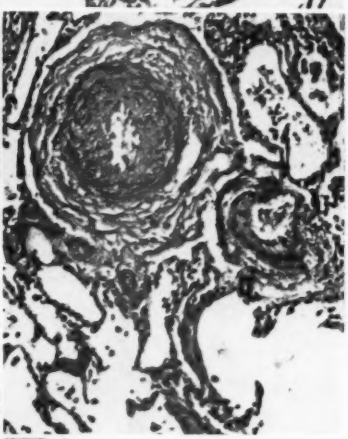

4

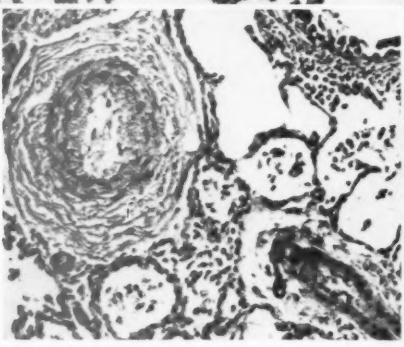

5

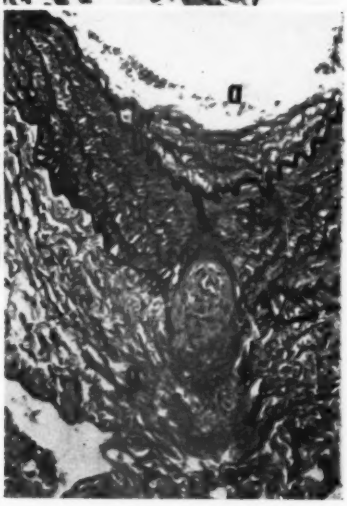

6

FIG. 7. Case 1. A succeeding stage to that shown in Figure 6. The glomoid body (g) proceeds further outward toward the pulmonary parenchyma. × 110.

FIG. 8. Case 1. A succeeding stage to that shown in Figure 7. The glomoid body has disappeared and is succeeded by a well-defined normal vein-like structure (g). × 110.

FIG. 9. Case 2. An opening of the branch from a parent vessel. The lumen is filled with thickened intima which has undergone hyalinization (a). If followed, this branch enters a semicircular cellular whorl containing tiny spaces which resemble capillaries but are smaller in diameter than red cells. This structure may disappear completely and merge into surrounding fibrous tissue. More often it is converted into a structure similar to that shown in Figure 10. × 220.

FIG. 10. Case 2. A well-formed cellular glomoid structure completely fills the lumen of a secondary arterial branch (g). Beyond it is a triangular space filled with erythrocytes (a). × 220.

FIG. 11. Case 2. A stage succeeding that shown in Figure 10. The glomoid structure acquires a lumen (a) which enters a long, normal-appearing vessel (e). The latter becomes the accompanying artery of a smaller neighboring bronchus. If followed, it eventually enters pulmonary capillaries. × 220.

7

8

11

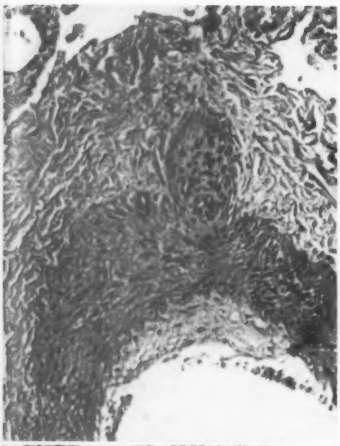

7

8

11

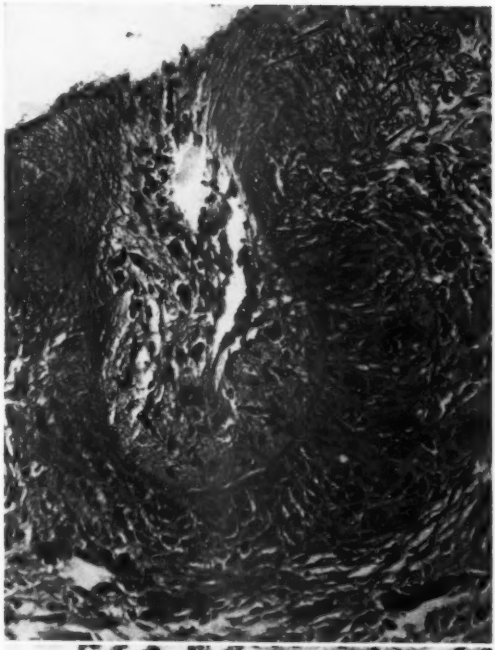

9

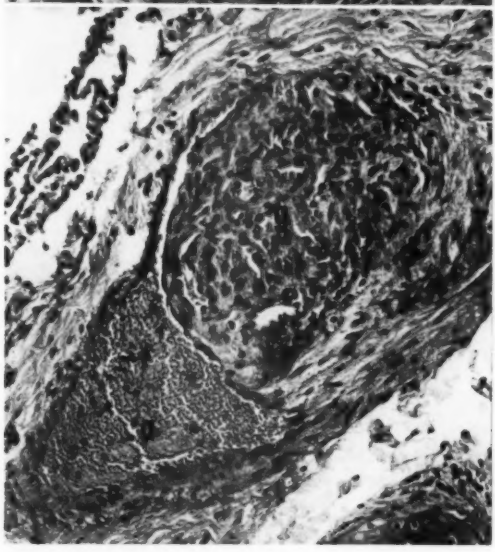

10

FIG. 12. Case 3. A branching arteriole (a) with a fibrous hyalinized and narrowed lumen terminates in a glomoid structure which completely occludes the lumen (g). × 110.

FIG. 13. Case 3. A glomoid structure (g) contains wide capillaries surrounded by fibrosis which is partially hyalinized. × 110.

FIG. 14. Case 4. Branching of an arteriole from the parent artery. The walls are much thickened by fibrosis and hyalinization (a) and the vessel terminates in a glomoid structure which is densely fibrous and partially hyalinized (g). × 110.

FIG. 15. Case 4. Another glomoid structure containing dilated capillaries separated from one another by marked fibrosis (g). × 110.

FIG. 16. Case 4. The same glomoid structure shown in Figure 15 (g) terminates in an efferent artery (e). × 110.

12

14

12

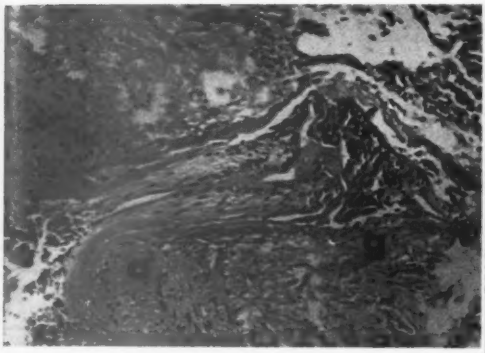

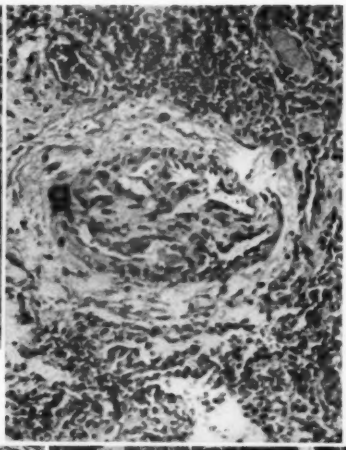

13

14

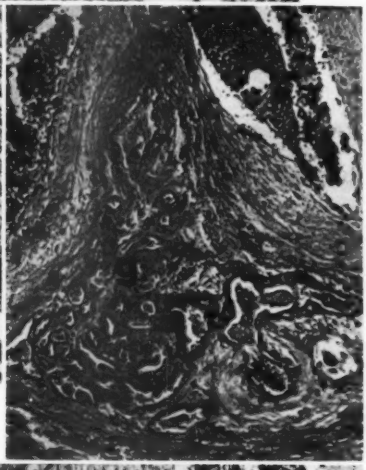

15

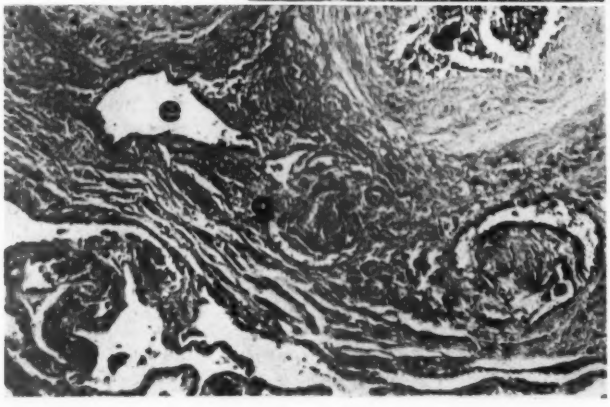

16

EXPERIMENTAL PULMONARY EMBOLISM WITH SERUM-INDUCED THROMBI AGED IN VIVO

DAVID G. FREIMAN, M.D.; STANFORD WESSLER, M.D., AND MORLEY LERTZMAN, M.D.

From the Department of Pathology and the Medical Research Department of the Yamins Research Laboratory, Beth Israel Hospital, and the Departments of Pathology and Medicine, Harvard Medical School, Boston, Mass.

In a previous communication, an adaptation of the technique of serum-induced thrombosis to the study of pulmonary embolism was described, and the behavior and fate of thrombi thus formed and promptly released into the circulation of the dog were reported.[1] It was apparent from these studies that a marked reduction in the volume of thrombo-emboli occurred within the first few days, presumably by lysis. It was also evident that the amount of embolic material persisting in the pulmonary arteries and proceeding to organization was related to the amount of freshly formed thrombus released.

To clarify further the role of the embolus itself in determining its fate in the lung, a modification of the technique of serum-induced thrombosis and pulmonary embolization was devised whereby autologous thrombi were permitted to remain in their peripheral veins of origin for 2 to 3 weeks prior to their release into the circulation of the dog. The present report describes these studies and compares the behavior and eventual fate of the aged thrombo-emboli with the observations on freshly formed emboli previously reported.

MATERIAL AND METHODS

The technique used for the production of thrombi in the dog was similar to that previously described.[1,2] Mongrel dogs, 15 to 20 kg. in weight, were anesthetized with sodium pentobarbital. A segment of each jugular vein was freed from the surrounding tissues, and its tributaries ligated. Thirty ml. of heterologous canine serum eluate[3] was then infused into a forepaw vein in 30 seconds. Within 60 seconds after completion of the infusion, clamps were placed on each jugular vein, isolating segments averaging 4 cm. in length. Following thrombus formation in these segments, each jugular vein was narrowed, but not occluded, by a silk ligature placed proximal to the clamps. The clamps were then removed and the thrombus contained within the isolated segment was permitted to move spontaneously to the area of narrowing where it was retained. Following this procedure, the wounds were closed and the animals returned to their cages for periods of 12 to 22 days.

At the end of this 12 to 22 day period, the dogs were re-anesthetized and the partially organized thrombus removed from one of the veins. Difficulty was frequently encountered in separating it from the vessel, and fragments of vein wall

Supported by Research Grant H-3777 from the National Institutes of Health, United States Public Health Service, and by a grant-in-aid from the American Heart Association.

Accepted for publication, February 28, 1961.

often remained attached to the thrombus. In some animals, also, variable amounts of the organized portion of the thrombus remained behind. Once removed, the aged thrombus was measured with a caliper and re-introduced into the jugular vein proximal to the site of narrowing. In those instances in which fracture of the thrombus occurred during the process of freeing it from the vein or during re-entry, the largest fragment, after being measured, was released to the lung and the smaller retained for microscopic examination. The thrombus in the contralateral vein was left undisturbed until the termination of each experiment.

Animals were sacrificed by the intravenous injection of sodium pentobarbital 5 minutes to 12 weeks after release of the embolus. Each dog received 1 mg. of heparin per kg. of body weight 5 minutes before death to prevent post-mortem clotting. Surgical asepsis was used throughout, and no antibiotic agents were administered.

At necropsy, the venous pathways from the areas of the jugular vein isolation to the heart were dissected *in situ*. The heart and lungs of each animal were then removed *en bloc* from the junction of the venae cavae to the ascending aorta without loss of blood. Blood was drained by gravity from the heart through a 40-μ sieve to recover loose thrombi, after which the right and left cardiac chambers were opened and examined. The pulmonary arteries were then dissected, and the size, location and gross appearance of all emboli found were noted. Each lobe was also examined for evidence of infarction and was subjected to multiple section. Recovered thrombi were fixed in 10 per cent formalin in isotonic saline for histologic examination. The distal portions of one or more lobes were similarly fixed and were examined microscopically for minute emboli in peripheral pulmonary arteries.

Studies on 27 control animals in which jugular vein thrombi were formed but not released to the lungs have been reported previously.[1] No thrombotic material resembling the partially organized emboli released in these experiments could be found after meticulous dissection of the pulmonary arteries of any of these animals.

Results

The data obtained in 36 dogs subjected to embolization with single, aged thrombo-emboli are summarized in Table I. In the 9 animals sacri-

Table I

RECOVERY OF PULMONARY EMBOLI FOLLOWING RELEASE OF A SINGLE AGED THROMBUS

Time of sacrifice after embolization	No. of dogs	No. of dogs in which embolus was recovered			No. in which embolus was not recovered
		In pulmonary arteries	In right ventricle	In great veins	
5 minutes	7	4	1	1	1
1 hour	2	2	0	0	0
14–28 days	14	13	0	0	1
31–40 days	6	6	0	0	0
41–43 days	3	3	0	0	0
64–84 days	4	3	0	0	1

ficed within 1 hour of embolization, thrombi identical with those released were recovered in 8, 6 from a pulmonary artery. The remaining thrombi were recovered, 5 minutes following release, at the junction of the left jugular and subclavian veins in one instance, and from the

right ventricular chamber in the other. In the ninth dog, the thrombus was not recovered, and was presumably lost or overlooked during dissection of the venous pathway. In each instance the recovered thrombus was intact, and was identified as that sent off by its size, by specific characteristics of shape and general appearance recorded at the time of embolization, by comparison of the microscopic appearance with that of the thrombus permitted to organize *in situ* in the control vein, and, in a few instances, by comparison with a fragment of the released thrombus which had been retained for microscopic study.

All emboli recovered within 1 hour of release were firm, pink to pale yellow, and nonadherent. On microscopic examination, each was composed of fibrillary or amorphous material consistent with old fibrin and red cell debris; traces of prior organization were usually evident near the surface (Fig. 1). Scattered foci of calcification and foreign body giant cells were occasionally present (Fig. 2). An incomplete outer zone of dense fibrosis and granulation tissue and adherent fragments of vein wall were noted in some instances (Fig. 3). All these features are consistent with those of a serum-induced thrombus permitted to organize for 2 to 3 weeks in a peripheral vein. No evidence of local organization in the pulmonary arteries could be identified.

The remaining 27 dogs were sacrificed at intervals from 14 to 84 days after embolization (Table I). Partially adherent thrombi were recovered in all but 2 instances, the latter after 28 and 64 days, respectively. Emboli recovered during the third week showed only a slight to moderate reduction in volume as compared to those recovered later, and in at least one instance no alteration could be detected. In subsequent weeks these emboli underwent progressive organization and reduction in volume. Only minute, adherent, organizing nubbins could be found in 3 of the 4 dogs examined 2 months after embolization, and in the remaining animal no trace of an embolus was evident.

Microscopic examination of the adherent emboli showed evidence of local organization superimposed on the changes previously described (Figs. 4 and 5). In several instances the appearance was similar to that of the serum-induced control thrombus permitted to remain undisturbed in the contralateral jugular vein. More commonly, however, the degree of organization of the embolus was less advanced than that of the control jugular vein thrombus. Deposits of hemosiderin and accumulations of lipid-containing macrophages were frequent. The latter, when partially incorporated into the intima of the pulmonary arterial wall (Fig. 6) resembled atheromatous plaques found in human pulmonary arteries. Similar lesions were also observed in the dogs subjected to massive embolization with fresh thrombi. Some of the organized residua also

tended to form ridges and bands across the lumen (Figs. 7 and 8), similar to those previously described,[1] and bearing a close resemblance to the "bridges" commonly observed in the lumens of human pulmonary arteries at necropsy.

In contrast to the behavior of fresh emboli which had a tendency to curl up in the right ventricle or to become enmeshed in the chordae of the tricuspid valve,[1] most of the aged, partially organized emboli had already reached the pulmonary arteries within 5 minutes following release. No evidence of the delay commonly noted with fresh emboli was observed after this time (Table I). Furthermore, although fracture of some of the emboli occurred at the time of removal from the vein of origin and reinsertion into the circulation, no spontaneous fracture of a partially organized embolus occurred in transit. No evidence of pulmonary infarction was observed.

Discussion

In the group of experiments previously reported,[1] a rapid reduction in the volume of single, freshly formed, serum-induced thrombo-emboli was readily apparent during the first few days after their appearance in the pulmonary arteries of the dog. Evidence of adherence and early organization was not observed prior to the fifth day. Embolic fragments were recovered in only 4 of the 9 animals examined between the fifth and 14th days, and in each such instance showed evidence of early organization. In those animals examined after 14 days, no traces of the original embolus could be found. The contraction in volume of multiple, freshly formed emboli during the first 2 weeks was even more striking, although variable amounts of residual thrombi were found in every instance at the end of this period as well as in succeeding weeks. The volume of recovered emboli continued to diminish with time, however, and small organized nubbins were all that remained after 6 weeks. In some of these animals no traces of the original massive embolization could be found.

On the basis of these data obtained with fresh emboli, it would appear that the thrombolytic mechanism, particularly effective during the first few days following embolization, plays a critical role in determining how much, if any, thrombotic material will persist sufficiently long to undergo organization. It is also evident that the processes of organization are capable of disposing of most of this residuum.

The results of the present experiments with aged thrombi further support and extend the scope of these concepts. When serum-induced thrombi were confined to their veins of origin for 2 to 3 weeks prior to release, the rate and extent of lysis during the first 2 weeks following embolization to the lung was significantly less than that observed with

fresh emboli. The reduction in volume of the aged embolus at the end of this 2-week period was, for the most part, slight. Even when such thrombo-emboli were examined 4 or more weeks after embolization, their removal from the pulmonary arteries had progressed very slowly. By the end of 6 weeks, however, the extent of organization was such that it was often impossible to determine, either grossly or microscopically, whether the observed residuum had originated as a massive fresh embolus or as a single, small, aged embolus.

The primary difference in the behavior of freshly formed as opposed to aged serum-induced emboli, therefore, lies in the differing rate and extent of thrombolysis occurring within the first 2 weeks following embolization. Since the thrombi produced in the 2 sets of experiments were initially formed in the same fashion and under similar experimental conditions, and since there is no reason to postulate any difference in the average thrombolytic capacity of the 2 groups of animals studied, this difference in rate of lysis, and in the results observed, must be in considerable measure attributable to the composition of the embolus at the time of release. The slow reduction in volume of these older thrombi during the first 2 weeks following embolization as compared with the dramatic disappearance of the freshly formed thrombi suggests that the fibrin content may be less susceptible to endogenous fibrinolytic activity. This is in accord with reported observations indicating that experimental thrombi permitted to age *in vivo* for 5 days will no longer undergo lysis upon exposure to infused thrombolytic agents.[3]

Those portions of an embolus which are not lysed undergo organization, and, in this regard, the removal of an intravascular thrombus has much in common with the disposal of an extravascular fibrinous exudate. Under both these circumstances, the rate and extent of organization might be expected to bear an inverse relation to the rate and extent of fibrinolysis, modified by such variables as the degree of contact with living tissue and local nutrition. Since the process of organization is not only more delayed in onset but slower in rate than that of lysis, the persistence for many weeks in the pulmonary arteries of such residua in the form of partially organized plugs and bands, or of endothelialized mural plaques containing foam cells and hemosiderin, can be readily explained. These experimental observations also provide support for the concept that similar residua frequently observed in human necropsy material are thrombotic in origin.

Summary

The fate of serum-induced autologous thrombi permitted to remain in their veins of origin for 2 to 3 weeks prior to their release as emboli was determined in a series of dogs by sacrificing the animals at intervals

UNIVERSITY of PENNSYLVANIA LIBRARIES

from 5 minutes to 12 weeks after embolization. The reduction in volume of the aged embolus during the first 2 weeks was slight. This was in marked contrast to the behavior of freshly formed thrombo-emboli as previously reported. By the end of 6 weeks, however, it was impossible to determine whether an observed residuum had originated as a massive fresh or as a small aged embolus.

The slower rate of thrombolysis of these aged emboli appears attributable to the composition of the embolus at the time of its release, and supports the view that the fibrin content may be less susceptible than freshly formed fibrin to endogenous fibrinolytic activity. Under these circumstances, a larger proportion of thrombotic material persists long enough to undergo organization.

References

1. Wessler, S.; Freiman, D. G.; Ballon, J. D.; Katz, J. H.; Wolff, R., and Wolf, E. Experimental pulmonary embolism with serum-induced thrombi. *Am. J. Path.*, 1961, 38, 89–101.
2. Wessler, S. Studies in intravascular coagulation. III. The pathogenesis of serum-induced venous thrombosis. *J. Clin. Invest.*, 1955, 34, 647–651.
3. Ambrus, J. L.; Ambrus, C. M.; Back, N.; Sokal, J. E., and Collins, G. L. Clinical and experimental studies on fibrinolytic enzymes. *Ann. New York Acad. Sc.*, 1957, 68, 97–137.

Mrs. Carol Ho and Mrs. Helen Silver provided valuable technical assistance.

Legends for Figures

Except where indicated, photographs were prepared from sections stained with hematoxylin and eosin.

Fig. 1. A thrombo-embolus aged for 2 weeks in the jugular vein and recovered from a pulmonary artery 5 minutes after embolization. The capillaries noted are the result of prior organization. Gomori trichrome stain. × 65.

Fig. 2. Focus of calcification and foreign body giant cells in an aged embolus recovered from a pulmonary artery. × 84.

Fig. 3. Peripheral zone of fibrosis on an aged embolus recovered 5 minutes after release. Gomori trichrome stain. × 65.

Fig. 4. An embolus at the bifurcation of a pulmonary artery in a dog sacrificed 14 days after release of a thrombus aged for 2 weeks in the jugular vein. *In situ* organization has occurred along the line of contact. × 10.

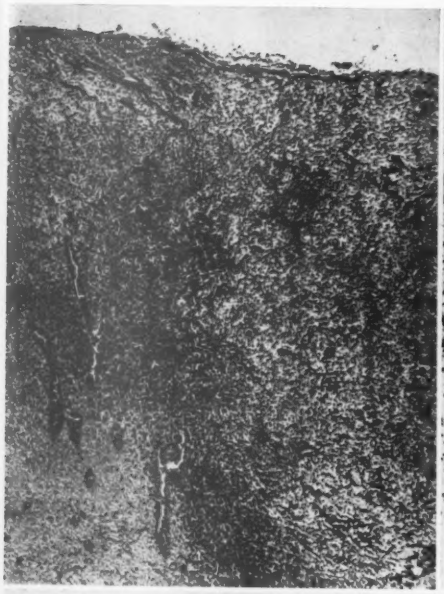

1

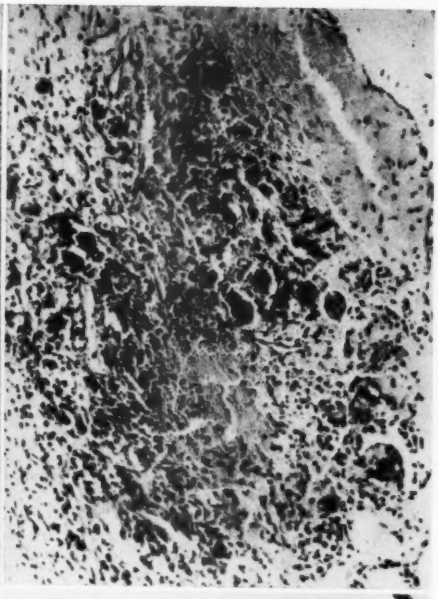

2

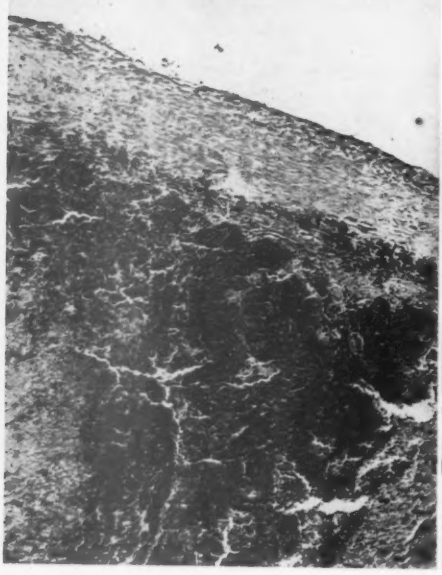

3

4

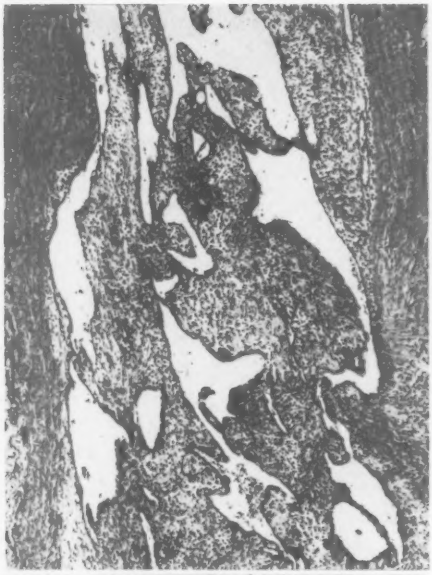

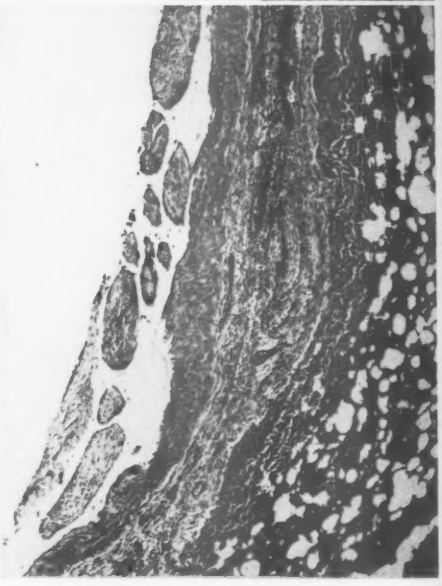

FIG. 5. An organizing embolus from a pulmonary artery of a dog sacrificed 14 days after release of an aged thrombus. The bandlike pattern of organization suggests an early stage of "bridging." × 43.

FIG. 6. A portion of the organizing embolus depicted in Figure 5. Numerous lipophages are present. Incorporation of part of the thrombus into the arterial intima mimics an atheromatous plaque. × 120.

FIG. 7. An embolus in a pulmonary artery of a dog sacrificed 43 days after release of an aged thrombus. Organization into strands suggests "bridging." × 45.

FIG. 8. Organized bands in a pulmonary artery of a dog sacrificed 70 days after release of an aged embolus. × 43.

BEHAVIOR OF ACID PHOSPHATASE IN THE RETICULO-ENDOTHELIAL SYSTEM OF GENETICALLY SUSCEPTIBLE AND RESISTANT MICE INFECTED WITH S. TYPHIMURIUM

DIETHELM BÖHME, M.D.; MAX WACHSTEIN, M.D., AND HOWARD A. SCHNEIDER, PH.D.

From the Departments of Pathology, New York Hospital-Cornell Medical Center, New York, and St. Catherine's Hospital, Brooklyn, and the Rockefeller Institute, New York, N.Y.

The reticuloendothelial system (RES) as originally defined by Kiyono and Aschoff has been generally considered as a major factor in the defense of the host against infection.[1] This generalization is based chiefly upon 3 observations[2]: first, reticuloendothelial cells are capable of phagocytosis; second, "blockade" of the RES has a detrimental effect upon the outcome of a variety of experimental infections; and third, antibodies are manufactured by cells derived from the RES. There is some evidence, however, that this over-all view may be an oversimplified one. For example, a recent study[3] has shown that the ability to clear intravenously injected carbon black had no predictive value in forecasting survivorship in mouse salmonellosis when tested in genetically resistant and susceptible mouse strains. Indeed, a rapid rise in clearing ability was prognostic of a fatal outcome of the infectious disease.

Clearing carbon black from the blood stream, it may be said, is but one phenomenologic aspect of reticuloendothelial function, and if doubt has been raised concerning its clear relationship to natural resistance to infection, there may be profit in turning to an examination of some other functional aspects of this system as it responds to infection. Histochemical staining methods and quantitative measurements have shown the Kupffer cell to be the site of considerable enzymatic activity.[4,5] It remains a moot question how far the enzymes hitherto demonstrated are instrumental in nonspecific resistance against infection.

In this study we have elected to examine the histochemical behavior of the enzyme, acid phosphatase, in the reticuloendothelial cells of liver and spleen of two genetically resistant and susceptible mouse stocks during the course of infection with *Salmonella typhimurium*.

MATERIAL AND METHODS

Animals. Two inbred mouse strains were used, the salmonellosis-susceptible BSVS and the resistant BRVR. The origins of these strains have been described elsewhere.[6]

These studies were supported by research grant B1565(C) from the National Institute for Neurological Diseases and Blindness, United States Public Health Service, and research grant A688C, United States Public Health Service.

Accepted for publication, March 6, 1961.

In the experiments reported here, only 2 to 3 month old males were used and housed in individual cages in a special air-conditioned room at 80° F., 50 per cent relative humidity, and with a 12-hour fluorescent light day. The mice had been reared and were continued on a commercial (Dietrich and Gambrill) pasteurized, pathogen-free stock diet and tap water *ad libitum*.

Infection. The animals were infected with *S. typhimurium* by the double strain inoculation procedure.[7] The Salmonella strains, RIA (avirulent) and SR-11 (virulent), have been described in detail elsewhere.[8] For the avirulent infection phase, 1,000 cells of a 16-hour culture of RIA in Penassay broth (Difco Laboratories) were suspended in a final volume of 0.25 cc. of normal, sterile saline and injected intraperitoneally. This was followed 2 days later by the virulent infection phase which consisted of 100,000 cells of a 16-hour culture of the SR-11 strain in Penassay broth, likewise suspended in 0.25 cc. of normal, sterile saline, injected intraperitoneally. The infective doses were determined both turbidimetrically and by plate count.

Acid Phosphatase. For acid phosphatase staining, liver and spleen were fixed immediately after removal in formol calcium overnight at 4° C. Sections were cut at 4 μ with a Sartorius freezing microtome and then stained following a modified Gomori procedure at pH 6.[9] Acid phosphatase-staining reticuloendothelial cells in liver and spleen were counted under oil objective magnification and the mean count per sample tissue determined from 10 random fields. A cell was considered positive if any staining reaction for phosphatase was detected under these standardized conditions. No attempt was made to estimate the intensity of the staining reaction. Sections from the same block were also stained at the same time with hematoxylin and eosin.

Statistical Evaluation. The mean frequencies of acid phosphatase-positive RE cells per microscopic field per tissue sampled were evaluated by a nonparametric ordinal test, the Mann-Whitney U test.[10] By this means it was possible to estimate the confidence to be attached to the verdict that the enzymic activity of one group of samples was greater or less than another group. The use of this nonparametric test thus avoided untested assumptions on the distribution, variance and scalar relations of the enzymic activity.

Experimental Plan

The experimental plan provided for two parallel sets of test animals and controls. The first set served to test the genetically predicted survivorship differences and included 20 BSVS and 19 BRVR mice, 2 to 3 months old, which were infected and observed for 30 days.

The second set, infected at the same time as the first, provided the samples for a time course study of the acid phosphatase activity in liver and spleen. Thirty-one BSVS mice, 2 to 3 months of age, were divided into 8 uninfected controls and 23 infected mice. On days 2, 3, 4, 5 and 8 after infection, 3 mice were killed and their livers and spleens removed and stained for acid phosphatase as described above. Eight animals of the infected group died before they could be tested. Of the uninfected controls, 5 were killed and tested before the start of the experiment and 3 at the end.

Similarly, 34 BRVR males, 2 to 3 months old, were divided into groups of 9 uninfected controls and 25 infected animals which were used for acid-phosphatase staining on post-infection days 2, 3, 4, 5, 8, 15, 21 and 30 in groups of 3. Two animals died before they could be tested. Of the uninfected controls, 6 were killed and tested before the start of the experiment and 3 at the end.

Results

The results of the survivorship experiment are presented in Table I and Text-figure 1. The predicted difference in survivorship was observed, for all the BSVS mice died while the BRVR mice survived to 79 per cent.

TABLE I

MORTALITY OF GENETICALLY SUSCEPTIBLE (BSVS) AND GENETICALLY RESISTANT (BRVR) MICE FOLLOWING INTRAPERITONEAL INFECTION * WITH *S. typhimurium*

Mouse strain	No. of mice	Cumulative deaths, on days										
		2	4	6	8	10	12	14	16	18	20	30
BSVS	20	0	1	2	5	11	16	20	20	20	20	20
BRVR	19	0	0	0	1	3	4	4	4	4	4	4

* The animals were infected first with 1,000 viable cells of the avirulent strain on day 0, followed 2 days later by 100,000 cells of the virulent strain SR-11 (day 2). The infective doses were given in a final volume of 0.25 ml. of normal sterile saline. Both the avirulent and virulent strains had been grown in Penassay broth for 16 hours before use. The infective dose was determined both turbidimetrically and by plate count.

Tables II and III demonstrate the results in the time course study of the relative number of reticuloendothelial cells in liver and spleen exhibiting a positive staining reaction for acid phosphatase. The number of staining cells in the liver, i.e. the Kupffer cells, showed a more clearly defined trend than those in the spleen. This agreed with observations made in the carbon pickup test.[11] It should be remarked that many more technical difficulties were encountered in making the spleen counts than in the liver. As a consequence, although both tissues are reported here, in

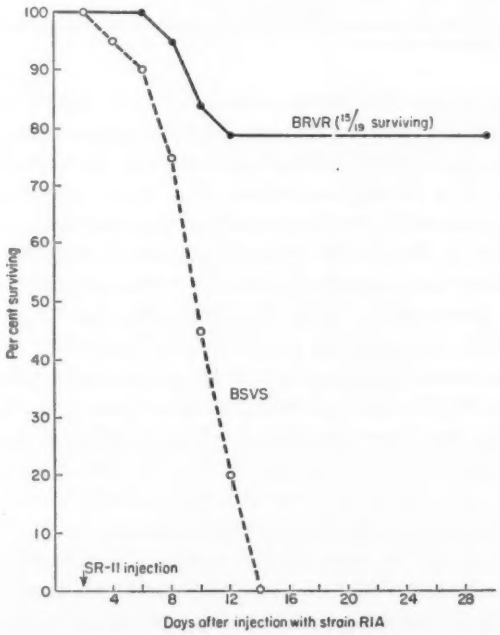

TEXT-FIGURE 1. Mortality following intraperitoneal injection of *S. typhimurium*.

what follows we have selected the liver as the index organ for analysis.

On this basis no significant changes with time were observed in liver acid phosphatase in either of the mouse strains when these were left as uninfected controls and estimated at the beginning and end of the

TABLE II

MEAN NUMBER OF ACID PHOSPHATASE-STAINING RE CELLS PER OIL IMMERSION FIELD IN THE LIVER AND SPLEEN OF GENETICALLY SUSCEPTIBLE (BSVS) AND RESISTANT (BRVR) MICE IN *S. typhimurium* INFECTION *

Day post infection with RIA	BSVS						BRVR					
	Liver			Spleen			Liver			Spleen		
2	20	9	14	16	15	19	4	8	6	30	16	36
3	13	16	11	30	19	44	8	15	11	34	50	35
4	12	13	14	20	31	16	6	10	10	29	43	33
5	6	3	5	18	16	19	14	12	6	33	25	37
8	9	6	6	29	12	22	12	11	11	25	25	28
15	Dead			Dead			24	12		25	20	
21	Dead			Dead			7	11	10	36	40	30
30	Dead			Dead			8	14	19	37	14	28
Uninfected controls:												
At start	6	4	5	18	22	14	5	5	5	20	55	30
	9	13		20	20		5	6	3	26	14	18
At end	7	5	6	35	33	40	4	4	5	30	29	30

* Same as in Table I.

experimental period. For these same uninfected control animals, statistical comparison between the two strains suggested that BSVS mice had a slightly greater acid phosphatase activity than did BRVR mice, but this was of a borderline nature ($P = 0.05$), and probably more animals would be needed to adopt or reject this estimate.

The increase in Kupffer cell acid phosphatase in response to infection with *S. typhimurium* is apparent from the results presented in Table II; the analysis presented in Table III shows this rise to be statistically significant. The rise occurred earlier in the susceptible BSVS, as evidenced by the unambiguous rise above the uninfected controls on day 2, at which time BRVR mice had not yet given a clear sign of their ultimate response. These data were obtained, it will be recalled, after 2 days of infection with avirulent RIA and just before the introduction of virulent SR-11. These elevated levels were maintained until the fifth day of the infection and were depressed on the eighth day.

The resistant BRVR mice showed a somewhat different response to infection. Compared with the uninfected controls, their Kupffer cell count had not risen on day 2, i.e., 2 days following infection with the

avirulent Salmonella strain RIA ($P > 0.05$). On day 3, i.e., 1 day after virulent infection with strain SR-11, the stainable Kupffer cell count had climbed to significant levels above the control animals ($P < 0.001$). Subsequently, this relationship held true through the remainder of the experiment. Interestingly, the magnitude of the rise of acid phosphatase activity was parallel in the two mouse strains on those days where a rise was evident in either. Statistical comparison revealed no significant differences.

Histologic examination of the hematoxylin and eosin-stained sections revealed identical features in the livers and spleens of the uninfected susceptible and resistant animals (Figs. 1 to 4). Following infection, on day 2, the first perinecrotic infiltrates made their appearance in the livers of the BSVS mice, accompanied by a marked increase in acid phosphatase-staining Kupffer cells (Figs. 5 and 6), while the livers of the BRVR mice still showed a normal appearance (Figs. 7 and 8).

On day 4, the livers of the susceptible mice were riddled with abscesses

TABLE III

STATISTICAL EVALUATION OF THE OBSERVED FREQUENCIES OF ACID PHOSPHATASE-POSITIVE KUPFFER CELLS IN THE LIVER OF BRVR AND BSVS MICE FOLLOWING INFECTION * WITH *S. typhimurium* (AS REPORTED IN TABLE II)

Comparison	Infection Day	P
Infected BSVS *versus* noninfected BSVS	2	< 0.02
	3	< 0.02
	4	< 0.02
	5	> 0.1
	8	> 0.3
Infected BRVR *versus* noninfected BRVR	2	> 0.05
	3	< 0.001
	4	< 0.01
	5	< 0.01
	8	< 0.001
	15	< 0.03
	21	< 0.001
	30	< 0.001

* As in Table I.

(Fig. 9) while the number of acid phosphatase-staining Kupffer cells was greatly increased as compared with day 2 (Fig. 10). The spleens were generally enlarged, but the number of staining reticuloendothelial cells appeared not to be conspicuously increased over that found on day

2. In contrast, the resistant BRVR mice displayed only slight changes in their livers (Fig. 11). On the fifth day, large abscesses were noted in both livers and spleens of the susceptible mice (Figs. 12 and 13). The number of stained Kupffer cells had now dropped markedly. At this time, marked changes were also found in the organs of all resistant animals. These included formation of thrombi in the hepatic and splenic veins and the appearance of large abscesses in the liver and spleen (Fig. 14). The number of acid phosphatase-staining Kupffer cells was found to be markedly increased (Fig. 15). As stated before, the number of acid phosphatase-staining cells in the white pulp of the spleen did not exhibit any spectacular alterations.

In spite of the striking histologic changes described above, most of the BRVR mice overcame their disease. On day 15, there were still conspicuous lesions present in their livers, while the number of acid phosphatase-staining Kupffer cells remained elevated (Fig. 16). Most of the lesions had disappeared on day 21, and none were found on day 30 (Fig. 18). The number of stained Kupffer cells was somewhat reduced, but was still elevated above the controls (Fig. 17). By day 21, no changes could be observed any longer in the spleens.

Discussion

We may begin our view of the results with the general observation that mouse salmonellosis is accompanied by a rise in the acid phosphatase activity in the reticuloendothelial cells of the liver. This confirms the reports of other investigators [12,13] for other instances of other infections. However, it seems appropriate to inquire next whether this functional response of the RES is meaningful in its relation to infection, or merely casual. To do this we must examine this association more closely, and in what follows we will confine our discussion to the model infection of mouse salmonellosis.

There are two unambiguous outcomes of an infectious disease: death or recovery. Fortunately, in the mouse salmonellosis model, these divergent outcomes can be arranged predictively by the use, as we have done, of resistant and susceptible host genotypes. What is implicit in the present attention paid to the RES is the postulation so frequently made that increased RES activity is associated with a favorable outcome in infectious disease: increased RES activity is equated with increased survivorship. But we have remarked earlier in this paper that there is ground for doubt that this is necessarily the case. One such reason for doubt was the observation that one aspect of RES function, a rise in carbon black clearance, was *not* correlated with survivorship in mouse salmonellosis.[8] Using the same disease and the same genetically

arranged differences in survivorship, we have here examined another aspect of RES function, acid phosphatase activity. Put as briefly as possible, it would appear that here, too, this particular activity of the RES has no positive predictive value for survivorship; the association can be regarded as an effect of infection without any favorable causal implications for the outcome of infection.

This view is based on the following considerations drawn from the present experiment. (1) Susceptible (BSVS) mice showed an earlier rise (by day 2) in acid phosphatase activity in the liver than did resistant (BRVR) following infection. (2) A fall in liver acid phosphatase activity in BSVS mice (day 5 and 8) from the previously elevated level was coincident with the onset of morbidity and death (Fig. 1); hence it is a concomitant effect rather than an antecedent cause. (3) The rise of liver acid phosphatase activity in BRVR mice, when it occurred, was no greater in magnitude than that observed in the BSVS mice, but was attended by an entirely different outcome, namely, survival. (4) The acid phosphatase activity in the liver of the infected but surviving BRVR mice remained elevated (day 30) above that of the uninfected controls at the end of the experiment. Again, this may be interpreted as an effect of the infection, for it is well known that survivors of mouse salmonellosis harbor latent Salmonellae.[14]

All these specifications, we believe, lend credence to the view that the RES is an anatomic locus, which, in its increase of acid phosphatase activity, exhibits a response to infection, but the response is not predictive of the outcome of the infection. It appears more likely, at the present stage of our understanding, to be a concomitant event of unspecified significance.

Summary

Susceptible (BSVS) and resistant (BRVR) mice were experimentally infected with *Salmonella typhimurium*. The double strain inoculation technique was used, in which both virulent and avirulent *S. typhimurium* are injected into the host. The BSVS mice died without exception, and the BRVR mice survived to 79 per cent. No deaths occurred during the experimental period in noninfected control mice.

Parallel to this survivorship test and, concurrently, measurement of the acid phosphatase activity of liver and spleen tissue was made at frequent intervals by the enumeration of cells stained by a modified Gomori technique. This proved technically uncertain in the instance of splenic tissue, but statistically satisfactory enumerations were possible in hepatic tissue where acid phosphatase activity was discerned in the Kupffer cells.

In noninfected control animals no quantitative differences appeared during the experimental period, and there were no significant differences between the BSVS and BRVR mice. Following infection, acid phosphatase activity increased in BSVS and BRVR mice to about the same extent, but at different times. The susceptible mice showed a rapid but short-lasting increase in the number of acid phosphatase-staining cells in the liver; this was followed by a drop to control levels coincident with morbidity. The resistant animals exhibited a delayed increase in the numbers of acid phosphatase-staining cells and continued to show an elevated level to the end of the 30-day experimental period.

Such increased enzymic activity in the liver RES thus proved to have no predictive value for the outcome of mouse salmonellosis. It is suggested that the enzymatic changes are more indicative of an indifferent effect of the infection than they are causally related to its outcome.

References

1. Aschoff, L. Lectures on Pathology. Paul B. Hoeber, Inc., New York, 1924, p. 1.
2. Böhme, D. H. The reticuloendothelial system and nonspecific resistance. *Ann. New York Acad. Sc.*, 1960, **88**, 172–183.
3. Böhme, D. H.; Schneider, H. A., and Lee, J. M. Some physiopathological parameters of natural resistance to infection in murine salmonellosis. *J. Exper. Med.*, 1959, **110**, 9–26.
4. Novikoff, A. B., and Essner, E. The liver cell—some new approaches to its study. *Am. J. Med.*, 1960, **29**, 102–131.
5. Biozzi, G. B.; Halpern, B. N.; Stiffel, C., and Mouton, D. Quantitative study of the metabolic activity of the Kupffer cells on a heat-denatured serum albumin labelled with ^{131}I. *Brit. J. Exper. Path.*, 1958, **39**, 510–518.
6. Webster, L. T. Inheritance of resistance of mice to enteric bacterial and neurotropic virus infection. *J. Exper. Med.*, 1937, **65**, 261–286.
7. Schneider, H. A. Nutrition of the host and natural resistance to infection. III. The conditions necessary for maximal effect of diet. *J. Exper. Med.*, 1948, **87**, 103–118.
8. Schneider, H. A., and Zinder, N. D. Nutrition of the host and natural resistance to infection. V. An improved assay employing genetic markers in the double strain inoculation test. *J. Exper. Med.*, 1956, **103**, 207–223.
9. Wachstein, M. and Meisel, E. Observations with Gomori's technique for acid phosphatase. (Abstract) *J. Histochem.*, 1958, **6**, 389–390.
10. Siegel, S. Nonparametric Statistics: for the Behavioral Sciences. McGraw-Hill Book Co., Inc., New York, 1956, p. 156.
11. Böhme, D. H., and Bouvier, C. A. Influence of infection upon the reticuloendothelial system, internal organs and distribution of circulating leucocytes of normal albino mice. *J. Infect. Dis.*, 1959, **105**, 222–237.
12. Barka, T. Personal communication.

13. THORBECKE, G. J.; OLD, L. J.; BENACERRAF, B., and CLARKE, D. A. RE function and phosphatase activity in mouse liver. (Abstract) *Fed. Proc.*, 1960, 19, 134.

14. HOBSON, D. Chronic bacterial carriage in survivors of experimental mouse typhoid. *J. Path. & Bact.*, 1957, 73, 399–410.

[*Illustrations follow*]

Legends for Figures

All photographs were prepared at a magnification of 75 times. Except where indicated, the sections were stained with hematoxylin and eosin.

Fig. 1. BRVR mouse, uninfected control. Liver.

Fig. 2. BRVR mouse, uninfected control. Liver. Acid phosphatase, modified Gomori technique.

Fig. 3. BSVS mouse, uninfected control. Liver.

Fig. 4. BSVS mouse, uninfected control. Liver. Acid phosphatase, modified Gomori technique.

Fig. 5. BSVS mouse. Day 2. An inflammatory infiltration related to a focus of liver necrosis.

Fig. 6. BSVS mouse. Day 2. Increase in active Kupffer cells in the liver. Acid phosphatase, modified Gomori technique.

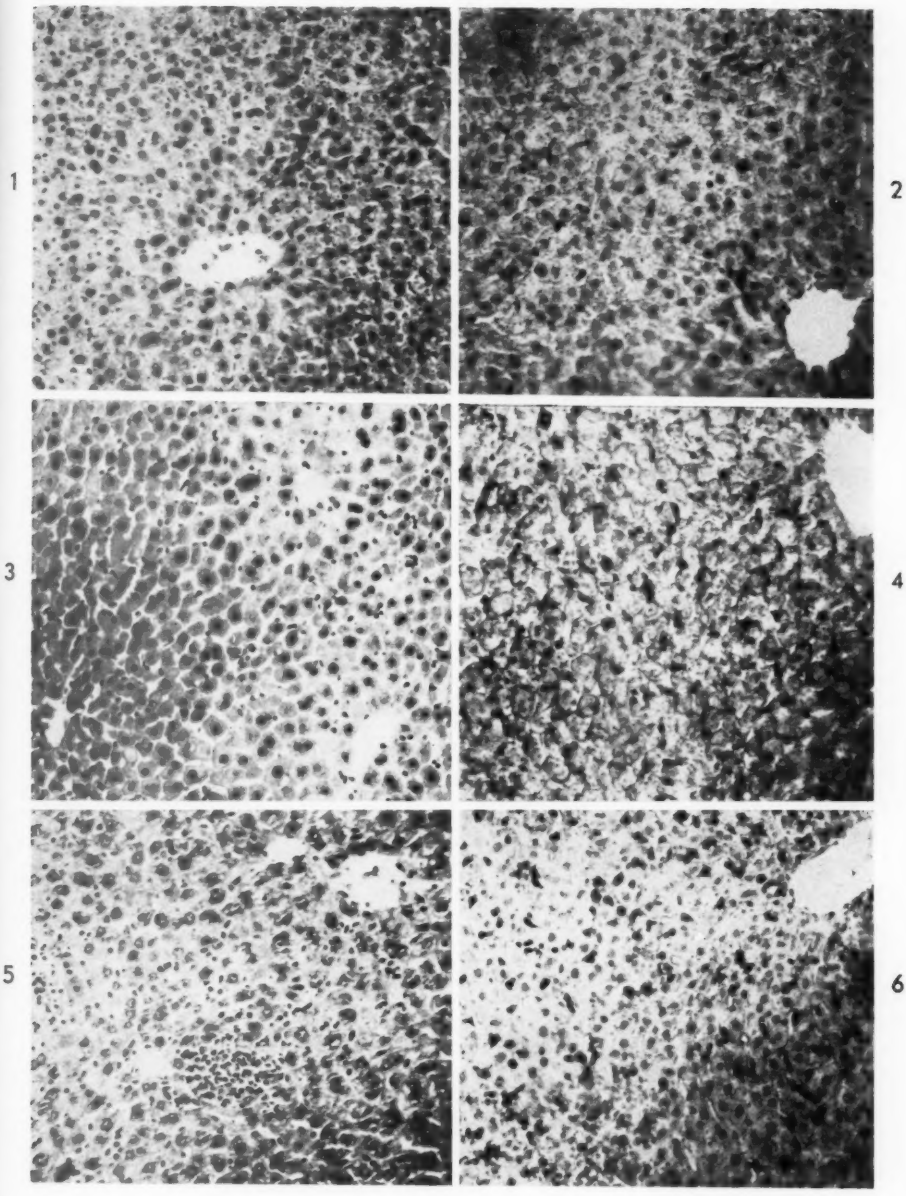
1
2
3
4
5
6

FIG. 7. BRVR mouse. Day 2. Minimal alterations in the liver.

FIG. 8. BRVR mouse. Day 2. Number of Kupffer cells still at control level (note slight nonspecific nuclear staining). Acid phosphatase, modified Gomori technique.

FIG. 9. BSVS mouse. Day 4. One of many minute liver abscesses.

FIG. 10. BSVS mouse. Day 4. Increase in active Kupffer cells. Acid phosphatase, modified Gomori technique.

FIG. 11. BRVR mouse. Day 4. The number of Kupffer cells is normal. Acid phosphatase, modified Gomori technique.

FIG. 12. BSVS mouse. Day 5. A focus of liver necrosis.

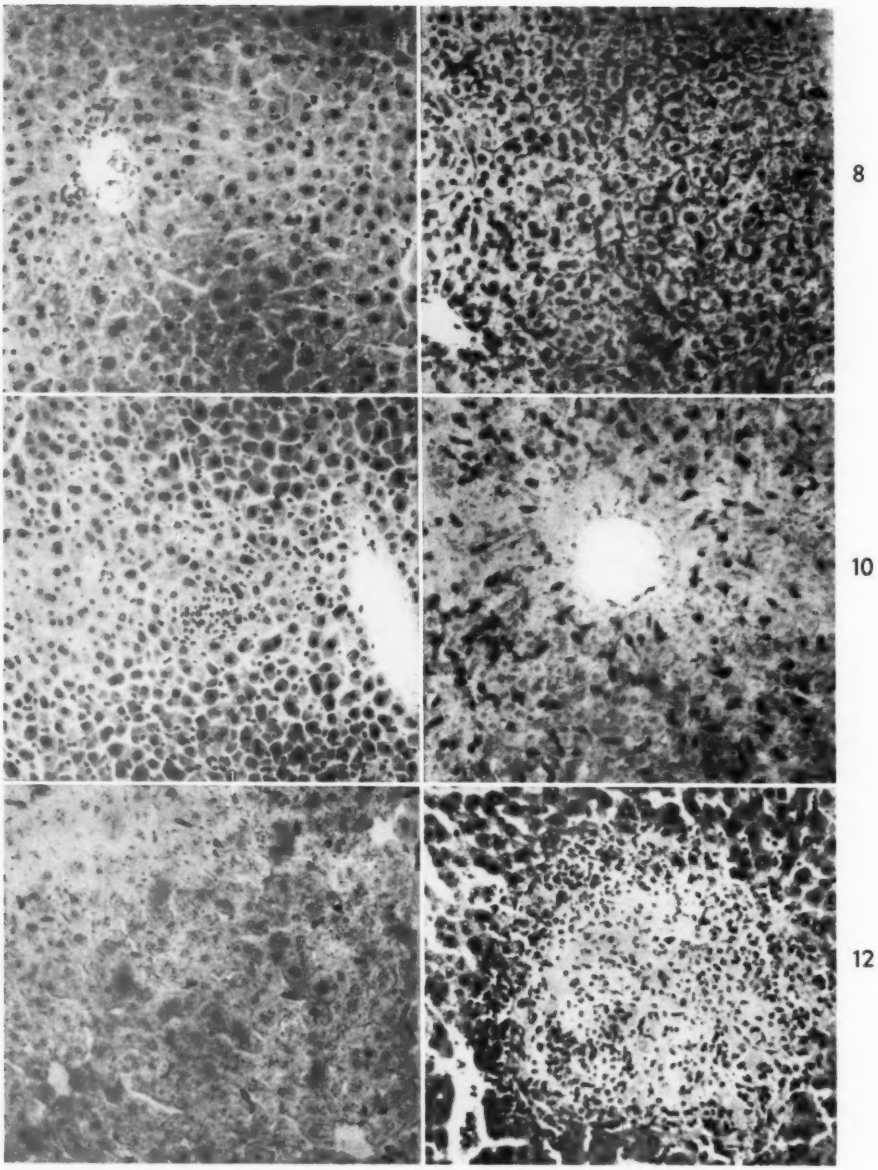
7
8
9
10
11
12

FIG. 13. BSVS mouse. Day 5. A large liver abscess.

FIG. 14. BRVR mouse. Day 8. A large area of liver necrosis.

FIG. 15. BRVR mouse. Day 8. Increase of active Kupffer cells in the liver. (Note slight nonspecific nuclear staining of liver cells.) Acid phosphatase, modified Gomori technique.

FIG. 16. BRVR mouse. Day 15. Number of active Kupffer cells still increased. Acid phosphatase, modified Gomori technique.

FIG. 17. BRVR mouse. Day 21. Number of active Kupffer cells still elevated above controls, though somewhat reduced from earlier stages. Acid phosphatase, modified Gomori technique.

FIG. 18. BRVR mouse. Day 30. Liver free of changes.

13

15

17

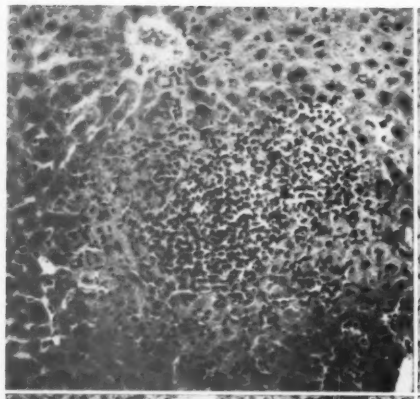

13

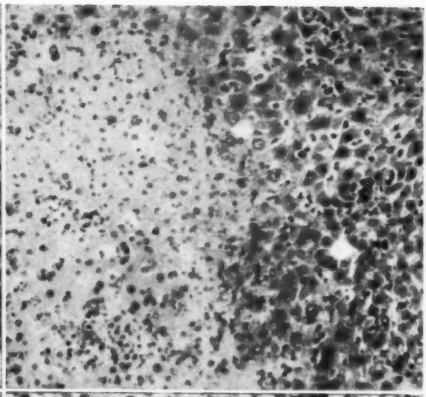

14

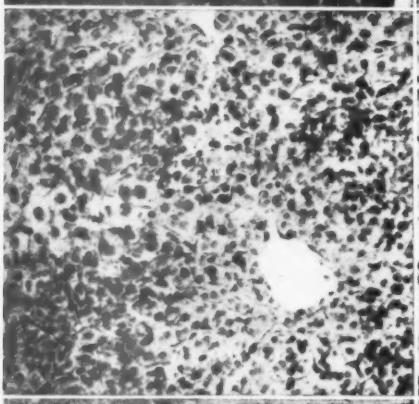

15

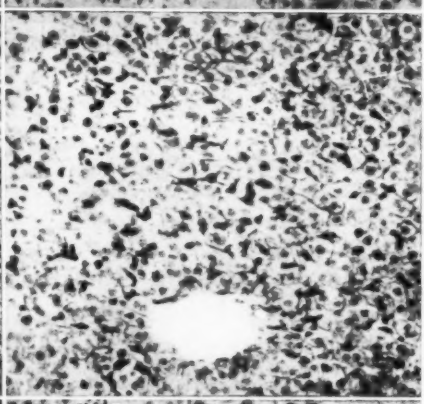

16

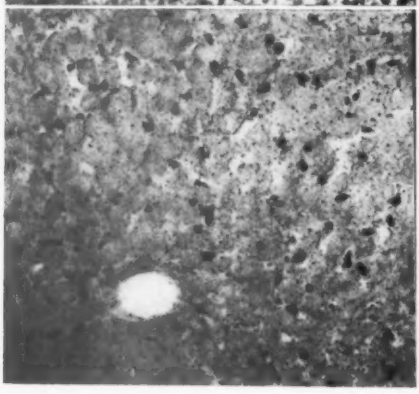

17

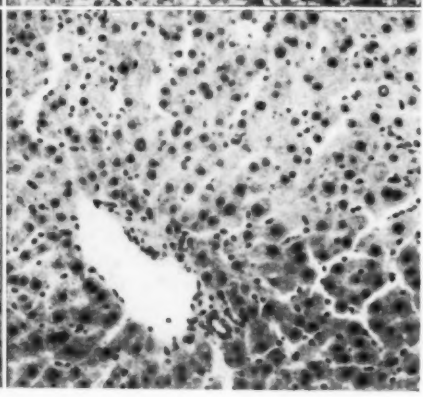

18

FROZEN SPLEEN REIMPLANTED AND CHALLENGED WITH BARTONELLA

WILLIAM H. CROSBY, COLONEL, MC, AND NAOMI R. BENJAMIN, B.S.

From the Department of Hematology, Walter Reed Army Institute of Research, Walter Reed Army Medical Center, Washington, D.C.

Following splenectomy in many mammals, bits of splenic tissue or the entire spleen may be reimplanted in the animal's body. Here they undergo almost complete necrosis and then are reconstituted to form splenculi with a microscopic structure almost indistinguishable from that of the original organ.[1,2] After it had been learned that these excised bits of spleen could be frozen and thawed without destroying the ability to become reconstituted,[3] it was desired to pursue the problem further, to learn if the reconstituted spleens possessed any of the functions peculiar to the spleen.

It is known that animals which are susceptible to infection by *Haemobartonella muris* do not usually develop clinical evidence of the disease when the spleen is present.[4] After splenectomy the organism produces a severe hemolytic anemia characterized by the presence of the organism in the circulating red cells. The hemolytic process is acute, severe, and the animals often die. It was the purpose of this experiment to ascertain whether implants which had been frozen and thawed would react to the *H. muris* infection in the same manner as the intact spleen.

MATERIAL AND METHODS

The experiment employed 3 litters of white rats of the WRCF strain. At the age of 2 weeks (weight about 20 gm.) the members of 2 litters had splenectomies, and the spleens were reimplanted. The third litter did not have splenectomy. Splenectomy was performed through a left abdominal incision under ether anesthesia. The wound was closed with silk. After its removal, the spleen was cut into several pieces which were dropped into the peritoneal cavity through a stab wound in the right abdominal wall. Before implantation, some of the splenic fragments were frozen; some were not. Those specimens to be frozen were first placed in a test tube and incubated for 40 minutes in 10 ml. of a mixture of 30 per cent glycerol and 70 per cent normal saline. To freeze the tissue, the test tube (11 by 150 mm.) was placed in acetone and dry ice and left there at least 10 minutes, when it was placed in water at 37° C. The thawed fragments were immediately placed in the peritoneum. The nonfrozen tissue was also incubated in the glycerol solution at room temperature. All implantations were autologous.

Four months later all of the animals (weight 300 to 350 gm.) were inoculated with *H. muris* by intraperitoneal injection of 0.5 ml. of a 2 per cent suspension of red cells from a splenectomized rat known to be infected and with a high rate of visible parasitization of his red cells. Thereafter, blood smears of the inoculated animals were

Accepted for publication, March 1, 1961.

examined at intervals until the animals died. Each animal was examined at necropsy, with particular attention to the site of splenectomy and the site of implantation. The urinary bladder was opened for evidence of hemoglobinuria; black urine indicated the presence of the hemolytic anemia which occurs in bartonellosis. At the time of inoculation a group of control rats of the same strain and of comparable weight and age with intact spleens were also given injections of the infectious material.

Results

Twenty-one rats had splenectomy, and the spleens were reimplanted (Table I). The implanted spleen tissue survived and reconstituted itself in 14 rats. In 5 animals no splenic tissue was found at necropsy. In 15 animals the spleen had been frozen and thawed before reimplantation;

Table I

RESULTS OF INTRAPERITONEAL IMPLANTATION OF SPLENIC TISSUE *

Rat no.		Frozen or not	Death after inoculation (days)	Site of implant	Splenic bed
Litter 12	98	F	5		+
	99	F	5	Abdominal wall	
	100	F	5		
	101	F	5	Intestine	
	102	F	8	Pancreas	
	103	F	8	Omentum	
	104	N	5	Omentum	
	105	N	6	Abdominal wall	
Litter 13	106	N	5	Subcutaneous tissue	
	107	N	5	Mesentery	
	108	N	5	Stomach	
	109	N	5	Abdominal wall	
	110	F	5		+
	111	F	5		
	112	F	5	Mesentery	+
	113	F	6		
	114	F	5	Mesentery	
	115	F	0		
	116	F	5		
	117	F	8	Colon	
	118	F	5	Intestine	

* Implantations were made 4 months earlier. Some implants had been frozen, others not. All animals (except no. 115) died of bartonella anemia.

in 8 of the 15 the implanted spleen survived. In 6 of the animals the spleen had not been frozen; in all of these the spleen survived. Splenculi were found in the splenic bed in 3 rats. These splenculi could have represented remnants of the original spleen broken off during the operation, or accessory spleens, or the implant which migrated from the site of implantation before becoming fixed. In only one of these 3 animals was there a splenculus at the site of implantation in addition to the one in the splenic bed.

Following inoculation with *H. muris*, the red cells in blood smears contained no inclusions until the fourth or fifth day. The 11 control animals without splenectomy also developed inclusion bodies on the fifth day, and one of them died on that day. The rest were re-examined on the eighth day and no inclusion bodies were found. After 3 months these animals were still surviving and in evident good health. After the appearance of red-cell inclusion bodies, the splenectomized rats usually died within a day, but several of them survived for 3 days. Death was associated with evidence of hemolytic disease, extreme pallor of tissues and hemoglobinuria manifest in the bladder at necropsy. The splenculi were usually small, 5 to 10 mm., and often lobulated or nodular. None was on a pedicle. The blood supply evidently was provided by multiple small vessels (Fig. 1). The implanted spleens were found embedded on various abdominal organs: stomach, intestine, pancreas, omentum, liver and parietal muscles (Table I).

The microscopic anatomy of the reconstituted spleens closely resembled that of the normal rat spleen, with cords of red pulp between the malpighian corpuscles. Characteristic splenic sinusoids and central arteries were also present, but there appeared to be no trabecular structure. In the animals dead with bartonellosis the red pulp was preponderant and filled with phagocytic cells containing innumerable erythrocytes. The sinusoids were inconspicuous. Except for the trabeculae and the thinness of its capsule, the spleen in the control rat without splenectomy that died with bartonellosis was indistinguishable from the splenculi in the splenectomized animals (Figs. 2 to 4).

In some sections splenic tissue appeared to be growing beyond the splencular capsule and extending into structures upon which the splenculus had implanted itself (Figs. 5 and 6). Several of the rats were pregnant at death, and in two cases the blood of the pups almost at term was examined. In one instance the mother died on the fifth day, and the pups' blood was negative for inclusion bodies; in the other case the mother died on the eighth day, and the pups' blood contained inclusions.

Discussion

Autologous splenic tissue which had been frozen, thawed, and replaced in the peritoneal cavity of rats was viable and capable of implanting and reconstituting itself. It was impossible to distinguish between successful implants which had been frozen and those which had not. They differed from the intact spleen in that the trabecular structure was not apparent and the blood supply was received, not through a hilar ramification but through numerous vessels at the periphery of the implant. The appearance of some implants suggested that they were growing, the splenic

tissue penetrating its capsule and extending itself into structures such as muscle or omentum, upon which engraftment had occurred. It is suspected that these excrescences become nodules and that this pattern of growth could account for the nodular appearance of some of the implants.

In these experiments the splenic tissue was dropped loose into the peritoneal cavity, and the successful implants attached themselves to the peritoneal organs. They were found on the omentum, the mesentery, the pancreas, the liver, the intestine and the abdominal wall. They had penetrated the peritoneum, received blood supply and had become covered by serosa (Figs. 7 and 8). The implants were not blandly symbiotic at the site of attachment but were capable of causing some degree of local accommodation (Fig. 5). In this regard they resembled endometrial implants.

The animals were inoculated with *H. muris* to determine whether the implants were capable of functioning as splenic tissue. In at least one clinical case, splenic implants demonstrated splenic function.[5] During splenectomy for hereditary spherocytosis, a woman's spleen was ruptured and splenic pulp spilled into her abdomen. Immediately after the operation her hemolytic disorder was relieved but later recurred, and abdominal exploration revealed many splenculi implanted in the peritoneal cavity. The implants had resumed the splenic function of destroying prematurely the spherocytic red cells.

In our rats a comparison of intact spleen with frozen-thawed splenic implants, after death of the animals from bartonella anemia, demonstrated a similarity of splenic reaction (Figs. 2 and 3). The pattern of intense erythrophagocytosis indicated that the implanted spleen had reacted to the challenge of Bartonella infection in the same fashion as the intact spleen.

The reaction of the implants and of the host to infection with *H. muris* was surprising. Years ago this sort of experiment was performed by Perla and Marmorston-Gottesman,[6] under somewhat different circumstances and with definitely different results. Their rats were of the Wistar strain, known to be infected with *H. muris*. Splenectomy resulted in a severe, often lethal hemolytic reaction. In one series of experiments these investigators performed a partial splenectomy, cutting off a tip of the spleen and implanting it under the abdominal skin. When, after 4 weeks, the remainder of the spleen was removed, the animals died of Bartonella anemia, but if the second stage of splenectomy was delayed until 7 weeks, the animals survived. The splenic transplant was sufficient to protect them against the disease.

The failure of the implants to protect our rats directed attention to

the several differences between our experiment and that of Perla and Marmorston-Gottesman. (1) The WRCF strain of rats is derived from the Wistar strain, but has been free of *H. muris* infection for many generations. During this time "racial tolerance" to the disease may have disappeared. All of our control animals with intact spleens developed bartonellosis and one of them died; one pregnant rat transmitted the infection to her pups with intact spleens *in utero*. (2) If antibodies against *H. muris* are a part of resistance to the disease (and this point is not clear [4]), our rats were without the benefit of the chronic subclinical infection which was present in Perla's rats. (3) Strains of the *H. muris* organism may vary in virulence. (4) Our inoculum may have been excessive.

It is not possible to say why the splenic implants did not provide protection against Bartonella anemia. It is, however, significant that the implants reacted to the disease in the same manner as the intact spleen of the one animal that died. The defense mechanism was overwhelmed, but the splenic tissue reacted with intense erythrophagocytosis.

Summary

1. In a group of rats, autogenous splenic tissue which had been frozen, thawed, and replaced in the peritoneal cavity remained capable of implanting itself beneath the serosa. The reconstituted splenculi had a microscopic structure closely resembling that of a normal spleen.

2. Splenectomized rats with implanted splenculi were inoculated with *Haemobartonella muris*, and all promptly died of Bartonella anemia. In a control group of animals with intact spleens, all but one survived the infection.

3. The reimplanted spleens reacted to the hemolytic challenge in the same manner as did the intact spleen in one control rat that died. There was engorgement of the red pulp and intense erythrophagocytosis.

4. Some of the implanted spleens appeared to be growing through the capsule and extending splenic tissue into adjacent structures.

References

1. Marine, D., and Manley, O. T. Homeotransplantation and autotransplantation of the spleen in rabbits. III. Further data on growth, permanence, effect of age, and partial or complete removal of the spleen. *J. Exper. Med.*, 1920, **32**, 113–133.

2. Perla, D. The regeneration of autoplastic splenic transplants. *Am. J. Path.*, 1936, **12**, 665–676.

3. Rothberg, H., and Crosby, W. H. Preservation of splenic tissue at low temperature. (Abstract) *Clin. Res.*, 1957, **5**, 152.

4. Weinman, D. Infectious anemias due to Bartonella and related red cell parasites (review). *Tr. Am. Philos. Soc.*, 1944, **33**, 243–350.

5. STOBIE, G. H. Splenosis. *Canad. M.A.J.*, 1947, **56**, 374–377.
6. PERLA, D., and MARMORSTON-GOTTESMAN, J. Studies on *Bartonella muris* anemia of albino rats. III. The protective effect of autoplastic splenic transplants on the *Bartonella muris* anemia of splenectomized rats. *J. Exper. Med.*, 1930, **52**, 131–143.

LEGENDS FOR FIGURES

Photomicrographs were prepared from sections stained with hematoxylin and eosin.

FIG. 1. Rat 10. Frozen-thawed splenic implant, 4 weeks after implantation. Centrally and at bottom left are necrotic remnants of the implanted tissue. The newly reconstituted areas demonstrate characteristic splenic architecture except for the blood supply provided by numerous small vessels which can be seen in the surrounding fibrous tissue. × 25.

FIG. 2. Control rat 1. The intact spleen of a normal rat that died of Bartonella anemia. The malpighian corpuscle stands in dark contrast against the pale, congested red pulp. On the left, perpendicular to the surface, is a splenic trabecula. × 86.

FIG. 3. Rat 114. Implant of frozen splenic tissue in a rat fatally infected with *H. muris*. A similarity to the intact spleen (Fig. 2) is apparent. The sinusoids are easily seen, but there is no trabecular structure manifest. × 86.

FIG. 4. Rat 114. Detail of the red pulp in a splenic implant, showing the reaction to Bartonella. Phagocytic cells packed with erythrocytes have been mistaken for sinusoids.[6] A sinusoid cut longitudinally is in the center of this illustration. × 173.

All photomicrographs were made by Miss Sally Craig, Medical Audiovisual Department, Walter Reed Army Institute of Research.

1

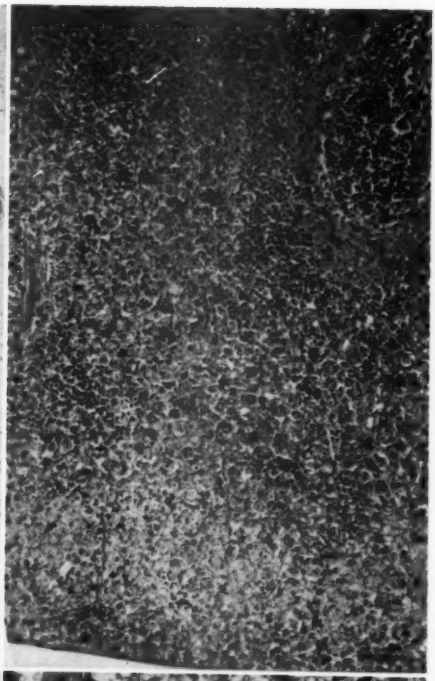

2

3

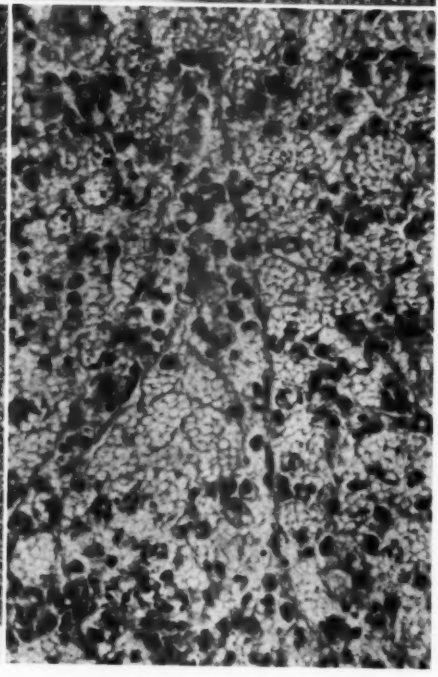

4

Fig. 5. Rat 109. A splenic implant showing its attachment to abdominal wall muscle. Muscle fibers can be seen between the two splenic lobules. The capsule of the spleen is infiltrated with small cells which appear also between muscle fibers adjacent to the spleen. × 45.

FIG. 6. Rat 117. A frozen implant showing a pseudo-hilus formed by 4 nodules. The splenic capsule at the tips of the 2 nodules on the right has all but disappeared. On the lower nodule the infiltrating cells have concentrated in a pattern resembling a malpighian corpuscle. Above, there appears to be some red pulp outside the infiltrated capsule. This may be the manner by which small splenic implants become larger and nodular. × 52.

FIG. 7. Rat 101. A splenic implant on the small intestine. The serosa is reflected over the implant. × 86.

FIG. 8. Rat 117. A splenic implant on the surface of the colon. The implant was evidently embedded in the omentum. × 45.

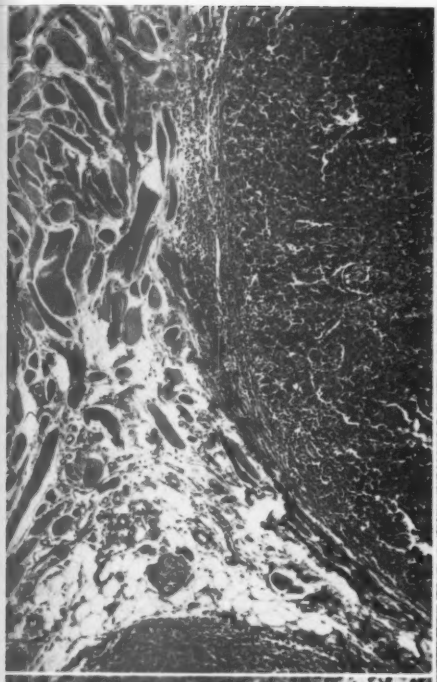

5

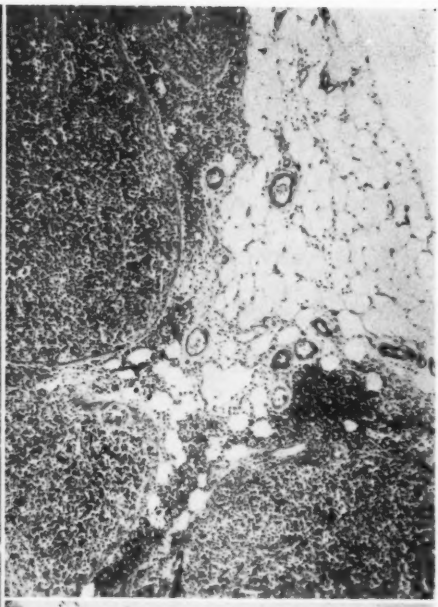

6

7

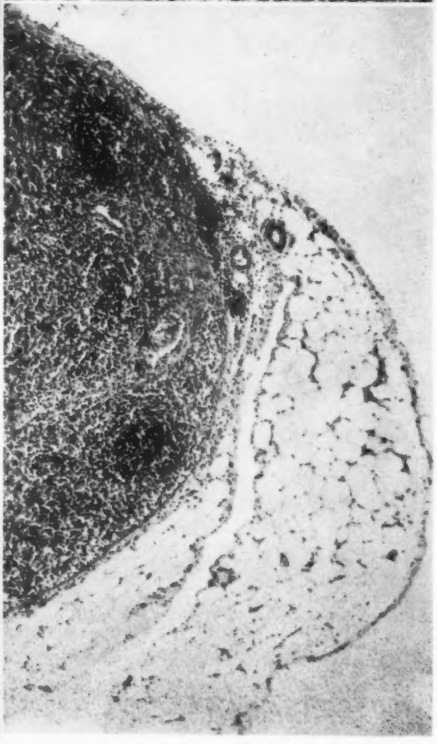

8